Purification of C-phycocyanin from *Spirulina* – adsorption pretreatment options

Eric Joseph Roberts Payne

In fulfilment of the requirements for the degree of Master of Science

Supervisors: Associate Professor Marijke Fagan-Endres; Professor Sue Harrison

Department of Chemical Engineering
Faculty of Engineering and the Built Environment
University of Cape Town

February 2023

Plagiarism Declaration

1. I know that plagiarism is wrong. Plagiarism is to use another's work and to pretend that it is one's own.
2. I have used the Harvard system for citation and referencing. Each significant contribution to, and quotation in, this report from the work, or works, of other people has been attributed, and has been cited and referenced.
3. This report is my own unaided work, except for assistance received from the teaching staff.
4. I have not allowed, and will not allow, anyone to copy my work with the intention of passing it off as his or her own work.
5. This thesis/dissertation has been submitted to the Turnitin module (or equivalent similarity and originality checking software) and I confirm that my supervisor has seen my report and any concerns revealed by such have been resolved with my supervisor.

Signed by candidate

Signature

Abstract

C-phycocyanin (C-PC) is an attractive blue pigment obtained from the cyanobacterium *Spirulina* and certain other species of microalgae. In recent years, C-PC has been used as a naturally derived colourant in cosmetic and food products due to the toxic effects of synthetic pigments. Cultivation of microalgae, like *Spirulina*, is well established, but there is scope to find new and more efficient ways of recovering the products they possess, including C-PC.

There are many techniques which can be used to purify C-PC from *Spirulina*, where the choice of which is dependent on the desired C-PC application. Different applications require different degrees of C-PC purity, where this is measured as a ratio of the absorbance of C-PC in a sample relative to the total absorbance protein. Work was done at the Centre for Bioprocess Engineering Research (CeBER) to develop a process using aqueous two-phase separation (ATPS) and ammonium sulfate precipitation to generate C-PC for cosmetic use, which has a minimum purity requirement of 1.5. A patent was obtained before further work was conducted on this process to optimise certain aspects of it. Following on from this research, it was recommended that an adsorption pretreatment be incorporated into the process prior to the ATPS and precipitation to improve the C-PC purity entering these stages. This adsorption pretreatment was proposed to use chitosan and activated charcoal due to the potential they have shown in C-PC purification processes. They are both easy to use and are known to be efficient as adsorbents – chitosan due to its two distinct hydroxyl and carbonyl functional groups, and activated charcoal because of its high surface area. The goal of this research project was to test the pretreatment and understand what impacts it has on the ability of the overall process to generate cosmetic-grade C-PC reliably and efficiently.

Leaching tests of the Carbocraft *Spirulina* used in this research project yielded an optimal period of 17 to 24 hours for the C-PC extraction from the *Spirulina* and showed that a cell disruption step was not necessary for this specific powder. Testing the adsorbents individually indicated that chitosan can selectively remove unwanted proteins while activated charcoal tends to adsorb indiscriminately. However, a significant improvement in purity is observed when they are used in combination. An attempt was made to optimise the concentrations of chitosan and activated charcoal as well as the adsorption pH and contact time through a central composite design. However, this does not provide any clear indication of optimal values, due to the high degree of experimental error and narrow range of purities. Running an adsorption prior to a polyethylene glycol (PEG) and citrate ATPS generated C-PC purities of approximately 1.5. However, the ATPS required a significant dilution to be effective and the C-PC recovery of this step was lower than 40%, making it potentially inefficient to scale up and impractical economically due to the high C-PC loss.

A different process configuration was thus suggested, excluding ATPS but using ammonium sulfate precipitation followed by microfiltration and ultrafiltration. These two steps are included to reduce the levels of unwanted microorganisms and salts for cosmetic-grade C-PC. When feeding a crude extract with its concentration reduced with buffer by 50%, this purification train was able to consistently generate purities greater than 1.5. Additionally, by conducting activated charcoal adsorption in a packed column, the C-PC recovery of this stage of the process was improved and the low recovery as a consequence of using powdered activated charcoal in suspension and dead-end centrifugation can be avoided. C-PC powder was obtained by freeze drying samples which had been purified using the proposed process. These powdered samples were tested and found to have E-values (measure of colour intensity) competitive with commercially available products. The process was also shown to be robust and can handle variations in *Spirulina* feed. Ultimately, this confirmed that an

adsorption step coupled with other standard purification techniques can be used to reliably generate cosmetic-grade C-PC with recoveries of 80% and above.

Acknowledgements

I have thanked everyone mentioned in these acknowledgements many times over the past two years, but one can never say thank you enough and so this seems like a good opportunity to show my gratitude once and for all.

The first big thank you is to my supervisor Associate Professor Marijke Fagan-Endres for being such a calm and understanding presence and for always seeming to know how all the different bits of the project fitted together (plus for getting all my edits back to me so quickly – I really appreciate it Marijke!).

CeBER wouldn't exist without my co-supervisor Professor Sue Harrison and so I am grateful to her for getting the C-phycocyanin project started (and funded more importantly). Equally, Dr Thanos Kotsiopoulos deserves much appreciation for spending all his time keeping things at CeBER together.

More thanks are required for other members of the CeBER staff. To Sharon and Tich for always helping me inside the lab and to Ruegshana and Sue J for always helping me outside it.

It would be remiss of me not to thank Dr Melinda Griffiths (and baby Jessica) for coming into the lab when she did. I learnt so much from just watching her go about her work and one day I hope to be even half as organised and efficient as she is.

I was lucky over the last two years to have housemates who provided a happy home to come back to every day and so I am thankful to them for their support and equal love of cats. My family, although slightly further away, probably deserve some thanks as well – so here it is. Naturally, I wouldn't be here without them and I feel very fortunate that I was given a family I actually enjoy speaking to and spending time with.

On a more serious note, I am grateful to The Technology and Human Resources for Industry Programme for providing me with the funding that enabled me to conduct this research.

Finally (and possibly most importantly), a huge thanks to the members of both the Chem-Eng Cup Organising Committee and the CeBER Lunch Squad (even those who were not as dedicated or serious about timekeeping). Without all of them, being on campus and in the lab would not have been nearly as fun. They really made these past two years some of the most enjoyable of my life and the memories and laughs they have given me will remain long after my knowledge of C-phycocyanin purification has faded.

Table of Contents

List of Figures

List of Tables

Acronyms and Abbreviations

AC	Activated charcoal
APC	Allophycocyanin
ATPS	Aqueous two-phase separation
BET	Brunauer-Emmett-Teller
BT	Brenntag
C	Central point
CC	Carbocraft
CeBER	Centre for Bioprocess Engineering Research
CFU	Colony forming units
C-PC	C-phycocyanin
CS	Chitosan
D	DARCO
DW	Dry weight
EAC	Extruded activated charcoal
GAC	Granular activated charcoal
GCN	Green Create Nutra
HCW	Health Connection Wholefoods
MS	Mean squared error
MW	Molecular weight
NC	Nature's Choice
OD	Optical density
PAC	Powdered activated charcoal
PBS	Potassium buffered saline
PE	Phycoerythrin
PEG	Polyethylene glycol
R	Rotocarb
RSP	Raw Spirulina Powder
RTD	Residence time distribution
S	Sigma
UCT	University of Cape Town

1 Introduction

1.1 Project Context

In recent years, there has been a concerted effort to move away from synthetically derived products and to rather use more sustainable, naturally occurring alternatives. Artificial colourants are an example of such products and can have significant detrimental impacts on the health of both humans and the environment (Kaur et al., 2009). There has consequently been a drive to find biological sources of pigments for use in the food and cosmetics industries. Certain algal species are amongst the most common of these sources, due to the pigments they possess as part of their light harvesting mechanism and because they can be easily and economically cultivated (Kuddus et al., 2013).

Particular water-soluble pigments classed as phycobiliproteins – known as phycoerythrin, C-phycocyanin and allophycocyanin – are able to form phycobilisomes, assisting the cells with the harvesting of light energy (Eriksen, 2008). C-phycocyanin (C-PC), specifically, displays an attractive, bright blue colour once it has been extracted and thus is sought after for applications in which this a desirable property. C-PC is present in many different species of microalgae but is most commonly obtained from the harvesting of *Spirulina*, a cyanobacterium. There are many different approaches and techniques which can be used to obtain C-PC from the *Spirulina* cells, where the choice of which to use is often dependent on the intended applications. Thus research is continuously being conducted to find the most suitable and efficient methods to purify C-PC for a given product specification.

1.2 Background on CeBER Patented Process and Subsequent Work

The design of a C-PC extraction and purification process to produce C-PC powder from *Spirulina* for the cosmetic industry is the goal of specific research being done by the Centre for Bioprocess Engineering (CeBER) at the University of Cape Town (UCT). A patent was obtained by CeBER for a method of generating cosmetic-grade C-PC, which consisted of coupling an aqueous two-phase separation (ATPS) with multiple precipitation stages to purify a crude C-PC extract (Harrison et al., 2020). This crude extract is obtained by disrupting the *Spirulina* cells and leaching them in citrate buffer before removing the cell debris by centrifugation. The patented ATPS typically makes use of polyethylene glycol (PEG) and maltodextrin as the two phases to separate, with the C-PC reporting to the maltodextrin-rich phase. Ammonium sulfate is subsequently used to precipitate the C-PC out of solution. The ATPS and precipitation purification steps were designed to increase the purity of the C-PC and reduce the microbial contamination to levels sufficient to be classified as cosmetic-grade.

In addition to the work completed to generate this patent, further research was done in an attempt to optimise the process and enable it to operate more efficiently (Hockey, 2022). This included testing different concentrations of the various chemical components used in the ATPS and varying the molecular weight of the PEG. The option of including an additional ATPS stage – making use of PEG and citrate – was also investigated, where this would be coupled with the standard PEG-maltodextrin ATPS as described in the patent.

This work by Hockey (2022) found that higher purities were achieved after the inclusion of the second ATPS stage. However, despite this improvement, the process was found to still be unable to consistently meet the requirements for cosmetic-grade C-PC. It was recommended

by Hockey (2022) that a pretreatment step be included to purify the crude extract before any ATPS or precipitation is done. Adsorption, using chitosan and/or activated charcoal, was proposed as a viable option for this pretreatment based on results presented in literature. Studies by Liao et al. (2011), Fekrat et al. (2019) and Safaei et al. (2019) all used chitosan and activated charcoal as part of their C-PC purification processes, where they were found to make a positive contribution to the product generated by improving the C-PC purity. Therefore, by improving the purity of the crude extract to the process, including an adsorption pretreatment step, it is hoped to improve the output of the entire process sufficiently to ensure that the final product consistently meets the specifications required for cosmetic-grade C-PC.

This research project therefore focuses on investigating the performance of the activated charcoal and chitosan adsorption pretreatment of a crude extract from dried *Spirulina* powder. The adsorption performance will be assessed in terms of its ability to improve the purity of C-PC in the crude extract, as well as by considering how well it can be incorporated with the other stages of the patented process.

1.3 Scope and Constraints of Research

The scope of this project is predominantly limited to the performance of an adsorption pretreatment using chitosan and/or activated charcoal and its impact on the CeBER C-PC purification process as a whole. No other purification techniques were investigated as an alternative to adsorption for pretreatment of the crude extract, and no additional chemicals were considered for their effectiveness as potential adsorbents. The exact properties of the adsorbents used were not determined within the experimental work and the only properties presented in the report were those specified by the suppliers. Furthermore, no specific work was performed to determine the exact mechanism of adsorption between activated charcoal or chitosan and the components present in the solution to be purified, including C-PC.

For the duration of this research project, work was done concurrently by Dr Melinda Griffiths and Mr Uzair Kadir at CeBER, focusing on other aspects of the C-PC purification process. Certain unpublished results from their work have not been repeated in this study but have at times been used to inform particular decisions made in this project. When this has occurred, the input of their research has been clearly noted.

1.4 Structure of Dissertation

This chapter (Chapter 1) serves as the introduction to the dissertation and provides a brief context around natural pigments such as C-PC, and summarises the work that has already been done on its purification. It also clarifies the scope of the research and underlines the structure of the report to follow.

Chapter 2 consists of an investigation into available literature and helps to guide the direction of the research. The literature review introduces the topic of microalgae in general before focusing on *Spirulina* and its associated properties and applications. Chapter 2 then discusses the uses of C-PC as well the available techniques for purifying it, before going into more detail about the CeBER patented process and potential benefits to including an adsorption step.

The research methodology is covered in Chapter 3 where the experimental approach is presented, and the materials and methods used in this project are discussed.

Chapter 4 explicitly defines the problem statement the study hopes to address, as well as the overall objectives of the project. In addition, key questions have been listed with the hope of guiding the research towards being able to meet the objectives which have been set out.

Chapter 5 is the first of the results chapters and initially considers the leaching stage of the purification, trying to understand the minimum period needed to perform it as well as the impact of the cell disruption step.

Chapter 6 looks at the adsorption as an isolated step by considering the impact of using chitosan and activated charcoal individually as well as in combination. Additionally, a central composite design was used to try and determine optimal values of these adsorbent concentrations, as well as the contact time and pH.

The impact of coupling the adsorption with a PEG-citrate ATPS was investigated in Chapter 7 to understand how the adsorption impacts other stages of the process.

Further results are presented in Chapter 8, where the focus switched to testing the performance of a proposed process – consisting of leaching, adsorption, precipitation, filtration and freeze drying. Adjustments to this process were then considered, where these comprised altering the order of unit operations, including additional steps and changing the configuration of the adsorption stage. The robustness of the process was then investigated by testing different sources of *Spirulina* powder to identify what impact this has on the final product.

Finally, Chapter 9 provides a conclusion of the research done throughout the course of the project. Recommendations are also provided, both in terms of the viability of the process on a commercial scale, as well as suggestions for future work.

2 Literature Review

2.1 Background on *Spirulina*

2.1.1 Microalgae industrial use

Microalgae are one of the oldest life forms on the planet, existing in the ocean for the last 3 billion years. In recent times, they have been increasingly used in industrial processes as a source of naturally produced higher-value components and as alternatives to synthetic equivalents, due to the associated health benefits (Silva et al., 2020). Additional advantages are the wide distribution of countless different microalgal species, their adaptability to a variety of environmental conditions and their ability to accumulate large quantities of biomass by harvesting solar energy through photosynthesis (Guedes et al., 2011; Begum et al., 2016). Microalgae are further favoured for use in industrial applications because they combine the properties of plants, such as simple nutritional requirements, with the faster growth rates seen in other microorganisms. This allows for the generation of novel bioproducts like vitamins and pigments, which can be used in a variety of different industries – such as those for food, cosmetics and pharmaceuticals (Guedes, Amaro & Malcata, 2011). The products isolated from the different species of microalgae are preferred for use in these sorts of industries because they are generally less toxic or carcinogenic than the alternatives generated synthetically (Begum et al., 2016).

2.1.2 Spirulina

One of the most commonly investigated and cultivated microalgae in industry is the filamentous cyanobacterium *Spirulina (Arthrospira) platensis*. It is found predominantly in marine ecosystems, specifically in Africa and Asia (Ragusa et al., 2021). *Spirulina* is one of the few photoautotrophic microbes which is able to be grown in open ponds due to its ability to outcompete potential contaminating organisms (Kuddus et al., 2013; Eriksen, 2008). It is also easily harvested from these ponds through filtration because of its filamentous structure (Griffiths et al., 2016). The popularity of *Spirulina* is seen in its global market value of $348 million in 2018, with this industry predicted to grow further at an annual rate of 10.5% (Silva et al., 2020).

Spirulina is the source of a significant number of bioactive molecules such as proteins, unsaturated fatty acids, vitamins, minerals and pigments (Patel & Goyal, 2013). It has been deemed safe for human use and thus has supposedly been consumed by different cultural groups across the globe over the past few centuries, while also being a common ingredient in nutraceutical formulations . The major reasons for the attraction of *Spirulina* supplements are because of its reportedly antioxidant, anticancer, anti-inflammatory and antidiabetic properties (Patel & Goyal, 2013; Silva et al., 2020). The herbal, vitamin and mineral nutraceuticals containing *Spirulina* can be purchased in tablet, capsule, flaked or powdered form – further emphasising the demand for these microalgal products.

The two most common methods for growing *Spirulina* for use in industrial applications are open cultivation, as mentioned previously, and photobioreactors. Open cultivation takes place in natural waters like lakes or lagoons or in artificially constructed raceway ponds and is the traditional method for the growth of microalgae, due to the easier construction and operation required (Silva et al., 2020; Soni et al., 2017). However, the use of photobioreactors is increasing, due to the lower chance of contamination and more controlled environmental

conditions. Specifically with regards to *Spirulina*, the photobioreactor is favoured because of the reduced risk of contamination as well as increased biomass productivities (Silva et al., 2020). There are numerous factors which impact the efficiency of *Spirulina* growth, and thus the use of the photobioreactor better allows for these parameters to be controlled, some of which include temperature, pH, light wavelength and salinity (Begum et al., 2016). However, these benefits need to be weighed up against the increase in required operating costs when growing *Spirulina* and other microalgae in photobioreactors.

2.2 Background on C-phycocyanin

2.2.1 Intracellular products available from *Spirulina*

Growth conditions – such as temperature and pH as well as light intensity and wavelength – influence the relative composition of the various intracellular products which can be isolated from *Spirulina*, where the biological pigments have some of the most varied applications. As with the microalgae itself, these pigments can be used in medical research, cosmetics and the food industry, often as a substitute for artificial colourants, due to the advantages associated with naturally generated products. Commonly used synthetic dyes are classified as irritants or allergens and often have toxic or carcinogenic effects, while they are often also derived from non-renewable sources (Kaur et al., 2009). Therefore, the benefits associated with natural colourants have resulted in an increased interest in the research into microalgal pigments, as seen in the significantly higher number (approximately 80% increase) of publications in this area of study in the last 10 years (Silva et al., 2020). The three major classes of photosynthetic pigments present in microalgae are phycobilins, chlorophylls and carotenoids, where the phycobilins are water-soluble and the latter two are fat-soluble (Begum et al., 2016). One type of phycobilin is C-phycocyanin, a blue, light-harvesting pigment that is found in *Spirulina* in concentrations of up to 20% of the dry cellular weight, as well as in eukaryotic algae such as cryptophytes and rhodophytes (Eriksen, 2008; Chaiklahan, Chirasuwan & Bunnag, 2012; Papadaki et al., 2017).

2.2.2 Structure of C-phycocyanin and other phycobiliproteins

The other classes of phycobilins are allophycocyanin, which is predominantly isolated from cyanobacteria, and phycoerythrin, which is largely found in red algae (Telegina et al., 2018). These phycobilin groups are assembled into more complex structures known as phycobilisomes, which are attached to the outer surface of thylakoid membranes present in microalgae and form part of the cell's photosynthetic electron transport chain as they lie adjacent to the photosynthetic reaction centre of photosystem II (Moraes et al., 2011; Kaur et al., 2009). The phycobilisomes are composed of a core as well as different rods formed by the phycobiliproteins, which are linked together by polypeptides. Each of the phycobiliproteins contain chromophores of various types and number, where they are classified by their respective structures as phycocyanobilin, phycoerythrobilin, phycoviolobilin and phycourobilin (Wang et al., 2001). The pigment-protein complex is therefore created by the chromophore bonding to the protein unit. These phycobiliproteins share similar structures created by a common subunit organisation where the α and β subunits form an αβ heterodimer. The monomers in the phycobiliprotein assembly pathway can aggregate together to produce disc-shaped $(\alpha\beta)_3$ trimers which can create an $(\alpha\beta)_6$ hexamer, which is the functional unit of phycocyanin if two of the trimers bond together (Wang et al., 2001). Although the size of these subunits varies between different C-phycocyanin-producing organisms – and occasionally within the organism itself – it has been reported that each has a molecular weight of between 17.5 and 20 kDa (Wan et al., 2021). Therefore, the sizes of the C-phycocyanin trimers and

hexamers can range in molecular weight from approximately 113 to 225 kDa, respectively (Sørensen, Hantke & Eriksen, 2013).

Within C-phycocyanin specifically, these α and β subunits are relatively homologous, where the α-chain has one phycocyanobilin attached at cysteine 84 and the β-chain has two attached at cysteines 84 and 155 (Eriksen, 2008; Wang et al., 2001). These phycocyanins which have only phycocyanobilin chromophores attached are the most commonly found type and are known as C-phycocyanin (C-PC) (Eriksen, 2008). Within the phycobilisomes, the rods are predominantly composed of numerous C-phycocyanin hexamers but can occasionally also include phycoerythrin hexamers in the rod tip in certain species of microalgae. The core of the phycobilisomes, which is connected to the thylakoid membrane, contain distinct allophycocyanin rods and linker polypeptides and the light energy absorbed by the phycobilisomes is therefore transferred from the phycoerythrin in the tip, through the C-phycocyanin, to this allophycocyanin core (Wang et al., 2001; Kaur et al., 2009). A visual representation of a phycobilisome can be seen in Figure 1, where each of the phycobiliproteins forming the structure are considered. Along with their role in the light harvesting of the cell, phycobiliproteins are also used for intracellular nitrogen storage. They are some of the most abundant proteins present in cyanobacteria like *Spirulina* but are not essential to the functioning of the cell. Therefore they are selectively degraded and used in other cellular operations when there is a shortage of nitrogen (Eriksen, 2008).

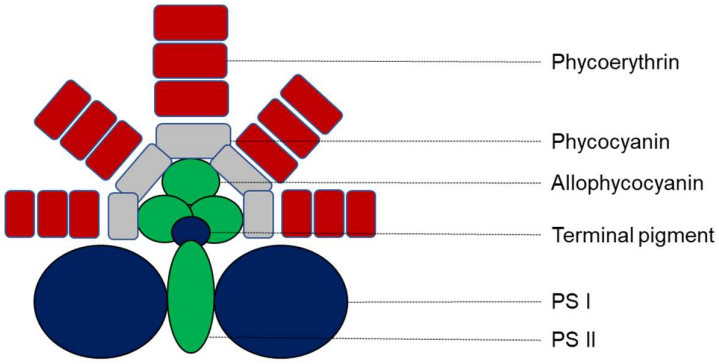

Figure 1: Structure of phycobiliproteins making up the phycobilisome, adapted from Kaur et al., (2009).

2.2.3 Commercial uses of C-phycocyanin

It has been reported that many of the nutritional benefits associated with the consumption of *Spirulina* can be credited to the presence of C-PC in the algae (Patel & Goyal, 2013). This aspect of C-PC, along with the previously mentioned harmful impacts of synthetic colourants, has resulted in an increase in the use of C-PC as a blue pigment in various food items, some of which include blue chewing gum, soft drinks and certain dairy products. There has also been an increase in the use of C-PC within the cosmetics industry, seen in products such as lipsticks, eyeliners and other makeup items (Kaur et al., 2009).

However, the main industrial application of C-PC and the other phycobiliproteins, involves their suitability as fluorescent markers in certain medical research. When phycobilisomes are extracted into an aqueous buffer, they disintegrate into their phycobiliprotein constituents. In doing this, these phycobiliproteins, including C-PC, then lose their natural ability to accept excitation light energy and become highly fluorescent (Eriksen, 2008). It is these fluorescent

properties which allow them to be used extensively in immunological assays and as markers in gel electrophoresis, isoelectric focusing and gel exclusion chromatography (Kuddus et al., 2013).

2.2.4 Characterisation of C-phycocyanin product quality

Quantification of C-phycocyanin purity

The discussion in literature around the quality of a C-PC product focuses predominantly on the purity of the sample. The purity is an important property to report for a C-PC recovery process as it determines in which applications the final product can be used. Due to the wide variation in the applications of C-PC, it is unsurprising that different levels of product purity are required within each of the separate industries. The reported purity is defined as the ratio of the absorbance, or optical density (OD), of a C-PC sample at a wavelength of 620 nm to the absorbance at a wavelength of 280 nm as seen in Equation 2.1.

$$Purity_{C-PC} = \frac{OD_{620}}{OD_{280}} \qquad 2.1$$

This is used as the indication of the sample purity because C-PC has a maximum absorbance at 620 nm, while the absorbance of the total concentration of proteins is 280 nm and therefore the ratio of the two values demonstrates how well the C-PC has been separated from the other contaminating proteins (Wang et al., 2012). The highest purity of C-PC is required for the use in analytical applications and it has been reported that a minimum value of 4.0 is needed (Patil et al., 2006). C-PC with a purity of 3.9 has been considered sufficient to be used as reactive grade, while food grade C-PC has been required to have a purity of at least 0.7 (Patil et al., 2006). A C-PC purity of approximately 1.5 is needed for the sample to be considered sufficient for use in cosmetic products, as many of the cosmetic benefits found through the use of *Spirulina* can be attributed to the presence of the C-PC (Chaiklahan, Chirasuwan & Bunnag, 2012; Ragusa et al., 2021).

Quantification of C-phycocyanin concentration

The concentration of C-PC is another useful product quality to measure as it is independent of the purity. It is important with respect to an end product, but also is beneficial in the evaluation of a C-PC purification process, as it provides an indication of the recovery of the pigment at each stage of the downstream process.

However, unlike with the purity, there is not simply one method which has been consistently used in literature to determine the concentration of C-PC in a sample. Numerous equations have been developed to calculate the concentration of C-PC, based on the absorbance of the sample at certain wavelengths. Some of these equations are based upon one another, but each has its own rationale behind why it is supposedly able to most accurately represent the concentration of C-PC in a solution.

The most commonly used equation in literature to quantify C-PC in a sample was developed by Bennett and Bogorad (1973), who investigated the chromatic adaption of the cyanobacterium *Fremyella diplosiphon*. As part of this study, it was necessary to quantify the relative concentrations of the three phycobiliproteins present in *F. diplosiphon* – namely C-phycoerythrin (PE), C-PC and allophycocyanin (APC). This was done by solving three

simultaneous equations, where each related the optical density at a specific wavelength to the extinction coefficients, ε, and concentrations, C, of the three phycobiliproteins.

$$OD_{\lambda} = \varepsilon_{PE,\lambda} \cdot C_{PE} + \varepsilon_{C-PC,\lambda} \cdot C_{C-PC} + \varepsilon_{APC,\lambda} \cdot C_{APC} \quad 2.2$$

Equation 2.2 demonstrates this, where the three wavelengths, λ, considered were 562 nm, 615 nm and 652 nm as the reported absorption maxima of C-phycoerythrin, C-PC and allophycocyanin respectively (Bennett & Bogorad, 1973).

After measuring the extinction coefficients for each of the phycobiliproteins at the three different wavelengths, it was possible to rearrange these equations in terms of concentration. The final relationship for the concentrations of the three phycobiliproteins in $mg.mL^{-1}$ subsequently determined by Bennett and Bogorad (1973) can be seen in Equations 2.3-2.5.

$$C_{C-PC}[\mathrm{mg.\,m}L^{-1}] = \frac{OD_{615} - 0.474 \cdot OD_{652}}{5.34} \quad 2.3$$

$$C_{APC}[\mathrm{mg.\,m}L^{-1}] = \frac{OD_{652} - 0.208 \cdot OD_{652}}{5.09} \quad 2.4$$

$$C_{PE}[\mathrm{mg.\,m}L^{-1}] = \frac{OD_{652} - 2.41 \cdot C_{C-PC} - 0.849 \cdot C_{APC}}{9.62} \quad 2.5$$

Using Equation 2.3 to quantify the amount of C-PC in a solution has been extensively applied in subsequent investigations concerning the extraction and purification of C-PC from various types of microalgae. The prevalence of this equation can be easily seen by considering the number of citations of this original paper by Bennett and Bogorad (1973), where it has received over 1000 citations since being published, with the majority of these occurring in the last 15 years as C-PC has gained more recognition as an alternative to synthetic colourants (Web of Science, 2023). However, many of the publications that have referenced this equation when quantifying the concentration of C-PC have modified it in certain ways. One of the most common modifications is to adjust the specific wavelengths which were used by Bennett and Bogorad (1973) to better represent the exact absorption maxima of the phycobiliproteins, namely C-PC and allophycocyanin. An example of this is seen below where the maximum absorbance of C-PC was chosen to be 620 nm (Moraes et al., 2011).

$$C_{C-PC}[\mathrm{mg.\,m}L^{-1}] = \frac{OD_{620} - 0.474 \cdot OD_{652}}{5.34} \quad 2.6$$

Other similar relationships have also been presented in literature, again where the basis for the concentration of C-PC is that of Bennett and Bogorad (1973), where these can be seen in Equations 2.7 and 2.8 (Fekrat et al., 2019; Yacobi et al., 2015).

$$C_{C-PC}[\mathrm{mg.\,m}L^{-1}] = \frac{OD_{618} - 0.474 \cdot OD_{652}}{5.34} \quad 2.7$$

$$C_{C-PC}[\text{mg.mL}^{-1}] = \frac{OD_{617} - 0.474 \cdot OD_{652}}{5.34} \quad 2.8$$

The equations presented by Moraes et al. (2011), Fekrat et al. (2019) and Yacobi et al. (2015) vary only slightly from each other and from the original one determined by Bennett and Bogorad (1973), and they therefore generate similar results for the concentration of C-PC in solution. However, it is important to note that these more recent equations have adjusted the wavelength of maximum absorbance for C-PC without adjusting the coefficients of the equation. This is despite the fact that in the original method used by Bennett and Bogorad (1973) to develop this equation, they used the specific wavelengths 562 nm, 615 nm and 652 nm to measure the extinction coefficients and from there determine the coefficients seen in Equations 2.3 to 2.5. Therefore, using these same coefficients in the equation, but adjusting the wavelengths, does not have a basis in logic and could lead to errors in the determination of the concentration of C-PC in solution.

Yoshikawa and Belay (2008) used the approach of Bennett and Bogorad (1973), but measured their own set of extinction coefficients for a sample extracted from *S. platensis*. They then again solved simultaneous equations using extinction coefficients at the three wavelengths of maximum absorbance of phycoerythrin, C-PC and allophycocyanin respectively. These extinction coefficients were measured at what they considered to be the absorption maxima for C-PC and allophycocyanin of 620 nm and 650 nm respectively. Using these extinction coefficients, equations were developed for the concentrations of both C-PC and allophycocyanin, in Equations 2.9 and 2.10 with the concentration in units of mg.mL^{-1}.

$$C_{C-PC}[\text{mg.mL}^{-1}] = 0.162 \cdot OD_{620} - 0.098 \cdot OD_{650} \quad 2.9$$

$$C_{APC}[\text{mg.mL}^{-1}] = 0.180 \cdot OD_{650} - 0.042 \cdot OD_{620} \quad 2.10$$

Equations 2.9 and 2.10 can be rearranged so that they are of the same form as the original one reported by Bennett and Bogorad (1973) in order for them to be more easily compared.

$$C_{C-PC}[\text{mg.mL}^{-1}] = \frac{OD_{620} - 0.605 \cdot OD_{650}}{6.17} \quad 2.11$$

$$C_{APC}[\text{mg.mL}^{-1}] = \frac{OD_{650} - 0.234 \cdot OD_{620}}{5.56} \quad 2.12$$

These equations were calibrated by taking a standard sample of both phycobiliproteins and diluting these to various levels. The absorbances of the samples were measured before Equations 2.9 and 2.10 were used to determine the concentrations of C-PC and allophycocyanin respectively, where these calculated values were compared to the known diluted concentrations. The result of this calibration showed that the C-PC equation was able to predict the concentration in the sample with an accuracy of between 96.4% and 99.5%, while the corresponding accuracy for allophycocyanin was between 98.0% and 101.5% (Yoshikawa & Belay, 2008).

A paper by Tandeau de Marsac and Houmard (1988) investigated chromatic adaptation of cyanobacteria, and used the method of solving simultaneous equations first discussed by Bennett and Bogorad (1973) to develop an equation to determine C-PC concentration in solution. Similarly to Yoshikawa and Belay (2008), they did not use the extinction coefficients measured by Bennett and Bogorad (1973) and instead included extinction coefficients reported by Bryant et al. (1979), which were based on averages of data available in literature. These average literature extinction coefficients were obtained from *Anabaena* sp., *Synechocystis* sp., *Synechococcus* sp. and *Porphyridium cruentum* (Bryant et al., 1976*;* Cohen-Bazire et al., 1977; Glazer and Hixson, 1975). Their final expression can be seen in Equation 2.13.

$$C_{C-PC}[\mathrm{mg.\,m}L^{-1}] = \frac{OD_{620} - 0.7 \cdot OD_{650}}{7.38} \quad 2.13$$

It is argued in the paper by Tandeau de Marsac and Houmard (1988) that Equation 2.13 can be successfully applied to all cyanobacterial strains, as it is dependent on the relative proportions of the different phycobiliproteins and not on their absolute concentrations.

As with Equations 2.6 to 2.8, a C-PC quantification equation developed by Lauceri et al. (2018) is based on the initial one developed by Bennett and Bogorad (1973). However, this equation does not simply adjust the absorbance wavelengths, and has a specific rationale for why the equation needs to be further adapted to increase the accuracy of determining the concentration of C-PC. The purpose of the study was to investigate the impact of chlorophyll *a* on the spectrophotometric quantification of phycobiliproteins from the cyanobacteria *Microcystis aeruginosa*. The initial equation developed by Bennett and Bogorad (1973) (Equation 2.3) was adjusted by considering the contribution of chlorophyll *a* on the total absorbance of the cyanobacterial sample at both 620 nm and 652 nm. They also considered the impact of the phycobiliproteins, C-PC and allophycocyanin, on the absorbance of the sample at 675 nm, the maximum absorbance of chlorophyll *a*. The final equation for the concentration of C-PC is given by Equation 2.14 (Lauceri et al., 2018).

$$C_{C-PC}[\mathrm{mg.\,m}L^{-1}] = \frac{(1.012 \cdot OD_{620} - 0.215 \cdot OD_{675}) - 0.474 \cdot (1.038 \cdot OD_{652} - 0.256 \cdot OD_{675})}{5.34} \quad 2.14$$

Equation 2.14 was developed by determining the ratio of absorbances at the optimal C-PC and allophycocyanin wavelengths, of 620 nm and 652 nm respectively, to the absorbance at 675 nm for both the phycobiliproteins and chlorophyll *a*. These ratios were determined separately for a pure sample of the phycobiliproteins, uncontaminated by chlorophyll *a*, and for a sample of chlorophyll *a* without the presence of the phycobiliproteins. Ultimately, it was found that this adjusted equation reduced the error in calculating the C-PC concentration when compared to the initial Bennett and Bogorad (1973) equation. This error was determined by considering the difference between the calculated C-PC and allophycocyanin concentrations of a sample, including the presence of chlorophyll *a* to the concentrations calculated for a pure sample containing only the phycobiliproteins (Lauceri et al., 2018).

Following on from these sets of equations, there is another set of methods which have been used in literature to determine C-PC concentration, that is not based on the initial work done by Bennett and Bogorad (1973). Two approaches were reported by Beer and Eshel (1985), where the initial relationship discussed (seen in Equation 2.15) reportedly makes use of specific absorbance values taken from both O Carra et al. (1964) and O Carra (1965), but there is no discussion around the choice of wavelengths.

$$C_{C-PC}[\text{mg. m}L^{-1}] = 0.15 \cdot (OD_{618} - OD_{730}) \quad 2.15$$

The second equation developed by Beer and Eshel (1985) is based on Equation 2.15, but tries to correct for a baseline slant in the optical density readings. It does this by considering the troughs at wavelengths of 592 nm and 645 nm visible on the full absorbance spectrum, as these troughs exist adjacent to the peaks caused by phycoerythrin and C-PC. Equation 2.16 therefore apparently corrects for the slant of the baseline and minimises the error associated with the other components present in the cyanobacteria. However, despite a description of the logic of including these additional wavelengths, there was no clear explanation of how the coefficient of 0.51 was determined.

$$C_{C-PC}[\text{mg. m}L^{-1}] = 0.15 \cdot ((OD_{618} - OD_{645}) - 0.51 \cdot (OD_{592} - OD_{645})) \quad 2.16$$

Beer and Eshel (1985) compared the C-PC concentrations obtained from Equations 2.15 and 2.16 as well as Equation 2.7, using a crude extract obtained from *Gracilaria* sp., a genus of red algae, to determine their respective accuracies in predicting the concentration of C-PC. Initially, Beer and Eshel (1985) compared the various equations on extracts which had been prepared using different centrifugation forces, between 5000 g and 30000 g, to understand if there was any impact on the absorbance readings – and subsequent determination of C-PC concentration – caused by interfering particulate components. It was reported that Equations 2.7 and 2.15 overestimated the concentration of C-PC, seen in the decreasing values as the centrifugation force increased. By contrast, using Equation 2.16 resulted in the calculation of similar concentrations at the different speeds. Additionally, when different amounts of contaminating substances were increased through the addition of *Ulva* sp., the concentration of C-PC determined through Equation 2.16 (which corrected for the baseline slant) remained constant. On the contrary, Equations 2.7 and 2.15 again overestimated the concentration of C-PC in solution, as the values determined using the respective equations increased as the proportion of extract obtained from *Ulva* sp. increased. Moreover, Beer and Eshel (1985) considered Equation 2.17, reported by Kursar et al. (1983), to understand if that would also overestimate the concentration of C-PC. They concluded that it was found to overestimate the concentration of C-PC.

$$C_{C-PC}[\text{mg. m}L^{-1}] = 0.1511 \cdot OD_{614} - 0.0991 \cdot OD_{651} \quad 2.17$$

Quantification of C-phycocyanin product E-value

A property that is often used to advertise and characterise commercial C-PC products is the E-value. Despite it not being discussed extensively in literature, as opposed to purity, the E-value is often the property used to market C-PC, particularly for food and cosmetic products. The E-value is defined as the absorbance at 620 nm, OD_{620}, of a 1% solution of C-PC powder dissolved in deionised water. This means that the E-value is independent of the purity, as it does not take into account the amount of other contaminating proteins and is simply a representation of the amount of C-PC in the final sample. It is reported as E18 or E30 for example, where a higher E-value generally indicates greater value commercially.

Quantification of microbial contamination

The amount of microbial contamination is another factor to consider when trying to understand the suitability of a C-PC product for commercial applications. There are no widely discussed

standards on the maximum allowable levels of bacterial loading, but it has been reported in commercial products that food grade C-PC needs to be within the maximum plate count of 1000 colony forming units (CFU) per gram of C-PC product (Sensient, 2021). Therefore, the purposes of designing and operating an effective C-PC extraction and purification train are not only to increase the purity and concentration of the product to the desired level, but also to ensure that the bacterial loading, as measured by the plate count of colony forming units, is sufficiently low.

2.3 C-phycocyanin extraction and purification

As has been discussed, C-PC is utilised in a variety of different industries, where the quality of the product required is highly dependent on the intended use. Therefore, the choice of which techniques to include in a C-PC purification process depends on the desired product application. There are various methods which can be used to obtain and purify C-PC from *Spirulina*, where each approach has inherent associated advantages and disadvantages. Different combinations of techniques result in different final purities of C-PC but also greatly vary in cost. Further, it is possible for a C-PC recovery process to fail to produce a high purity or yield of C-PC, due to poor choices in the cell disruption method, order and combination of purification steps or by conducting these processes at unsuitable conditions (Safaei et al., 2019). Therefore, when attempting to select the optimal configuration of extraction technologies, it is important to consider what the desired C-PC application will be, what purity is required and consequently how valuable the product will be commercially.

2.3.1 C-phycocyanin extraction

Traditionally, the first step in any C-PC extraction process is the disruption of the microalgal cells, whether they are present as wet or dry biomass. This is because C-PC is an intracellular product and thus needs to be released from the cells. Due to the strong cell walls of cyanobacteria like *Spirulina* and high amounts of contaminants, this extraction can often be difficult to achieve and so the choice of technique used needs to be made carefully (İlter et al., 2018; Kumar et al., 2014). Examples of cell disruption methods are bead milling, homogenisation, sonication, enzymatic treatment through lysozymes, and freeze-thaw cycles. All of these methods result in the C-PC present in the *Spirulina* cells leaching into a buffer solution (Kuddus et al., 2013; İlter et al., 2018).

A study was conducted by İlter et al. (2018), where the various extraction methods were tested for different types of *Spirulina* biomass. It was found that using an ultrasound extraction technique on frozen *Spirulina* cells and leaching them in a calcium chloride solution resulted in the maximum amount of C-PC being obtained. However, it was also discussed that the classical extraction method of homogenisation produced C-PC with the most vivid blue colour, implying that it led a more selective extraction. Therefore, the choice on which cell disruption technique to use, as well as the choice of the form of biomass, is dependent on the targets of the C-PC purification process (İlter et al., 2018).

The current extraction process utilised by CeBER, as discussed in Chapter 1.2, has an initial bead milling step before leaching the C-PC into a citrate buffer – where this buffer was chosen because of its lower environmental impact than the phosphate equivalent (Harrison et al., 2020). To note, it has been seen that with dry *Spirulina* powder, there is not always the need for a disruption step and that simply leaching the powder in a potassium phosphate buffer for a period of time allows for a sufficient amount of the C-PC present in the biomass to be extracted. This is possibly due to adequate disruption having already occurred during the harvesting or drying process (Liao et al., 2011; Fekrat et al., 2019).

2.3.2 C-phycocyanin purification

Different purification techniques

As with the numerous options which can be used to perform the initial extraction of the C-PC from the *Spirulina* cells, there are many different techniques that can be used to improve the quality of the C-PC product so that it meets the purity requirements for whatever application is desired. The most commonly used of these methods are multistep chromatography, ultrafiltration , aqueous two-phase separation (ATPS), and ammonium sulfate precipitation. C-PC purification processes frequently use multiple stages of each of these techniques and they are often used in combination with one another.

Chromatography

The principle of chromatography as a means of purifying proteins, specifically C-PC in this case, is to utilise differences in physical and chemical properties between the components as a means to separate them. This is done by feeding the solution into a column and purifying desired proteins as a result of selective interactions between this mobile phase and the stationary phase present in the column. Chromatographic methods – whether hydrophobic, ion-exchange or size-exclusion – greatly increase the purification costs because of the expensive packing materials needed for this stationary phase, especially when attempting to scale up the process to generate higher volumes of product, while also requiring significant periods of time to perform (Liao et al., 2011; Patil and Raghavarao, 2007). However, chromatography techniques are able to generate high purity samples, with purities of greater than 5 being reported in processes which include ion-exchange chromatography (Patil et al., 2006; Yan et al., 2011). For this reason, these methods are traditionally used to obtain analytical or reactive grade C-PC due to the strict purity requirements and higher commercial value of the products, implying that the additional expense of the purification process is justified by the revenue that can be obtained.

Ultrafiltration

As has been mentioned, C-PC exists predominantly in the form of trimers and hexamers with fairly large molecular weights. This means that it is possible to use ultrafiltration to selectively retain the larger C-PC molecules and allow other smaller proteins and other contaminants to pass through, depending on the exact size of the membrane used. This has a few benefits in terms of C-PC purification. Naturally, if other proteins are removed, the purity measurement of C-PC will be increased due to the lower absorbance reading at 280 nm. Additionally, ultrafiltration is an effective method of concentrating the C-PC product, thereby reducing the volume sent through to subsequent downstream steps such as drying, allowing them to operate more efficiently (Schwartz, 2003). Ultrafiltration also allows for diafiltration, in which salts – remaining in the sample from previous upstream steps such as ATPS or precipitation – can be removed or buffer exchange can take place if the C-PC needs to be stored in a different type of preparation buffer (Doran, 2013). Finally, if ultrafiltration is coupled with a form of microfiltration, then the bacterial load of the sample can in theory be completely reduced. This can be achieved by using a microfilter with pore sizes of around 0.2 μm, as this will prevent any unwanted microorganisms from passing into the desired solution but is still large enough to allow C-PC to permeate through the membrane. Several examples of the successful use of ultrafiltration in C-PC purification processes can be found in literature. It was shown by Rito-Palomares et al. (2001) that ultrafiltration was able to increase C-PC purity between 2.4 and 3.1, while purity was increased from 0.54 to 1.11 by Chaiklahan et al. (2011) using this same method. Additionally, another study measured an increase in C-PC purity from

0.74 to 1.16 (Nisticò et al., 2022). The ultrafiltration purification step can be incorporated alongside several other unit operations such as chromatography, ATPS and precipitation, although, depending on where exactly it takes place in the downstream process, different molecular weight membranes can be used. There is a wide range of these membrane sizes; certain examples that have been used and reported in literature are 12 to 14 kDa, 30 kDa, 50 kDa and 20 kDa comprised of different materials such as polyethersulfone and other types of polymers (Park et al., 2022; Rito-Palomares et al., 2001; Chaiklahan et al., 2011; Nisticò et al., 2022).

ATPS

As its name describes, ATPS is a purification technique that utilises two aqueous phases into which molecules and other components are able to preferentially partition. Therefore, by correctly selecting the two liquid phases to separate, it is possible for C-PC to favourably move into one phase, with unwanted proteins moving into the other, successfully increasing the purity of the C-PC solution obtained. The supposed benefit of using an ATPS to produce C-PC is its ability to be efficiently and economically implemented in large scale extraction processes while simultaneously maintaining high yield and C-PC purity in a manner which does not impact the protein's activity (Patil and Raghavarao, 2007; Chethana et al., 2015). Another advantage of an ATPS is that the process of selectively partitioning the desired C-PC in one phase and the contaminants in the other phase results in an increase in the concentration of the C-PC product obtained (Patil & Raghavarao, 2007). This decreases the sample volume which needs to undergo further purification, reducing the size requirements and costs of the subsequent downstream processing steps.

The majority of ATPS processes for the purification of C-PC use polyethylene glycol (PEG) for the C-PC-recovering phase, with the undesired proteins selectively partitioning into a salt phase. Various salts – such as sodium phosphate, potassium phosphate, magnesium sulfate, sodium sulfate, ammonium sulfate and sodium citrate – have been tested for their effectiveness in purifying C-PC from a crude extract, where it was found that the phosphate salts, in particular potassium phosphate, showed the most promising results in terms of C-PC purity and yield (Patil & Raghavarao, 2007).

Precipitation

Ammonium sulfate precipitation is often used in the recovery of C-PC because it is a cheap and reliable technology and results in C-PC being readily precipitated (Kamble et al., 2013). Precipitation of a protein out of solution into a solid form occurs as a result of a change in the composition of the solvent, such as the pH or salt concentration. Therefore, by carefully selecting the amount of ammonium sulfate present in a solution, C-PC can be preferentially precipitated – with other proteins remaining in solution – and hence its purity can be increased in an easy and efficient manner. Kamble et al. (2013) were able to increase the purity of C-PC from an initial value of 0.161 to a purity of 0.628 by using an ammonium sulfate precipitation with a saturation concentration of 50%. Another study was done by Kumar et al. (2014) where a precipitation at 65% saturation was able to improve the C-PC purity from 0.75 to 1.5, showing the benefit of including this step in the purification process. However, it must be noted that there are some potential drawbacks associated with utilising the ammonium sulfate precipitation as part of a C-PC purification process. It has been discussed in literature sources that precipitation using ammonium sulfate does require long processing times and can potentially lead to the denaturation of the protein, reducing the quality of C-PC in the product (Liao et al., 2011).

Patented CeBER process

As discussed previously, the goal of this research project is to improve an extraction and purification process developed in CeBER that targets the production of cosmetic-grade C-PC. Cosmetic grade has a lower purity requirement than analytical or reactive grade, and correspondingly has a lower selling price. Because of this, chromatographic purification techniques are too expensive, and cheaper purification methods need to be used. It is for this reason that the CeBER patented purification process consists of ATPS and precipitation stages, with the aim of producing cosmetic-grade C-PC (Harrison et al., 2020).

The majority of ATPS used in the purification of C-PC, as was mentioned in Chapter 2.3.2, comprises of PEG and a salt as the two phases to separate. However, the issue with these PEG-salt ATPS systems is that due to the ability of PEG to bind stably to C-PC, there is the formation of PEG-protein complexes. This makes it difficult to recover the C-PC from the PEG and often requires the use of an additional ultrafiltration step to conduct this separation (Harrison et al., 2020); Liao et al., 2011). This has led to investigations into alternative ATPS processes in an attempt to still make use of the benefits they provided, while avoiding the problems associated with the PEG-salt system. Significant work was done in CeBER to test an ATPS C-PC purification process that makes use of PEG and a carbohydrate-containing phase as the two phases to separate. Using this technique, which CeBER has successfully patented, allows the C-PC to be partitioned into the carbohydrate-containing phase, increasing its purity and concentration while simultaneously avoiding the difficulties in recovering it from the PEG phase, as is the case with traditional ATPS processes (Harrison et al., 2020).

There are many different options for the specific carbohydrate used in the carbohydrate-containing phase, where it can be selected from a wide group consisting of the following compounds: maltodextrin, ficoll, dextran, starch, glucose, fructose, galactose, mannose, sucrose, cellobiose, lactose, lactulose, maltose, maltulose, arabinose, ribose, xylose and trehalose (Harrison et al., 2020). Out of these, maltodextrin is the most commonly used in the process, as its combination with PEG 10000 resulted in the highest recoveries of C-PC. Although maltodextrin also forms complexes with C-PC, they are weakly bonded and therefore the C-PC can be easily recovered from the maltodextrin in a subsequent purification step (Harrison et al., 2020).

The patented process makes use of multiple stages of ammonium sulfate precipitation subsequent to the ATPS, where the combination of the precipitation and ATPS are used to reach the required purity grade of C-PC. The use of both of these techniques as part of the C-PC purification process is important, because the ATPS on its own does not sufficiently reduce the contamination of other microbial contaminants, and performing the ammonium sulfate precipitation as the sole recovery process does not result in a C-PC product with sufficient purity to meet cosmetic-grade as is required (Harrison et al., 2020). The specific process described by Harrison et al. (2020) in the patent utilises three stages of ammonium sulfate precipitation once the ATPS has been performed and the C-PC has been separated from other substances in the extract. Each stage takes place with a slightly different ammonium sulfate concentration, varying from about 14% by mass to approximately 36%, and is fed either as an aqueous solution or as a solid, with optimal performance being achieved at specific concentrations within this range. Between each stage, the precipitated C-PC is removed from the clear supernatant liquid before the pellet is resuspended in water and again treated with the ammonium sulfate solution. A visual representation of the full process can be seen in Figure 2, with the stages forming part of the CeBER patent being represented by the dashed lines. The results of this multi-stage purification demonstrate how the purity of the C-PC being

produced significantly increases after each precipitation with the microbial loading, described by the number of colony forming units, decreasing after each stage (Harrison et al., 2020).

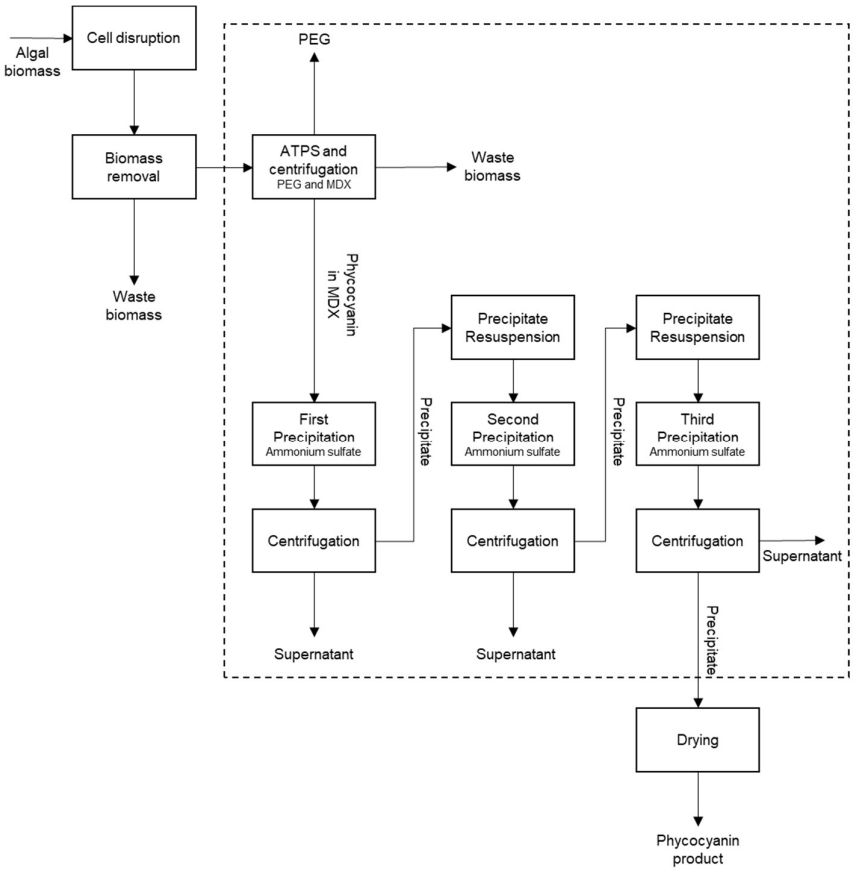

Figure 2: Schematic of full C-PC purification process including CeBER patented stages, adapted from Harrison et al., (2020).

Further work on patent

Although the patented process showed promise in generating cosmetic-grade C-PC, there was the opportunity to improve its performance through further research. For this reason, Hockey (2022) focused on various aspects of the ATPS step of the CeBER patented process. Initially the work focused on testing the PEG-maltodextrin ATPS by investigating different starting concentrations of both components, and determining the effect this had on the purity and recovery of C-PC. Subsequently, Hockey (2022) looked at adjusting the molecular weight of the PEG between 6000 and 20000 $g.mol^{-1}$ to see what impact this had on the performance of the purification stage. It was found that when compared to the original process on which the patent was based, a lower weight fraction of maltodextrin and a higher weight fraction of PEG were preferred. Additionally, the initial molecular weight of PEG 10000 was still seen to lead to the best performance in terms of C-PC recovery and purity. However, despite the improvements achieved as a result of this investigation into the PEG-maltodextrin ATPS, it was discovered that the increase in purity of C-PC – reported as the purification factor – was still significantly lower than studies conducted in literature on PEG-salt ATPS systems (Hockey, 2022).

Therefore, Hockey (2022) took the approach of designing a two-stage ATPS step, which consisted of an initial PEG-salt stage – which, as has been discussed, is the predominant form of ATPS traditionally used in C-PC purification – with the C-PC favouring the top PEG phase and this phase then being sent through to a PEG-maltodextrin ATPS. This new configuration of the process can be seen in Figure 3 and would, in theory, make use of the benefit of an increase in C-PC purity achieved through the PEG-salt ATPS but enable the C-PC to be more easily recovered from maltodextrin through precipitation and avoid the issues with trying to break up the complex formed between PEG and C-PC (Hockey, 2022). Therefore, Hockey (2022) conducted a similar investigation as for the one-stage ATPS where initially different molecular weights of PEG were tested for a PEG-citrate ATPS. Following on from this, the concentrations of PEG and citrate for the first stage of the ATPS were optimised before the same was done for the concentrations of PEG and maltodextrin for the second ATPS stage. It was determined that PEG 4000 was the optimal molecular weight in terms of maximising C-PC purity and recovery over both stages of the ATPS, and that for the PEG-citrate system, lower PEG 4000 and higher citrate concentrations were favoured; while the general trend for the PEG 4000 and maltodextrin ATPS was that it worked more efficiently at lower concentrations of both components (Hockey, 2022).

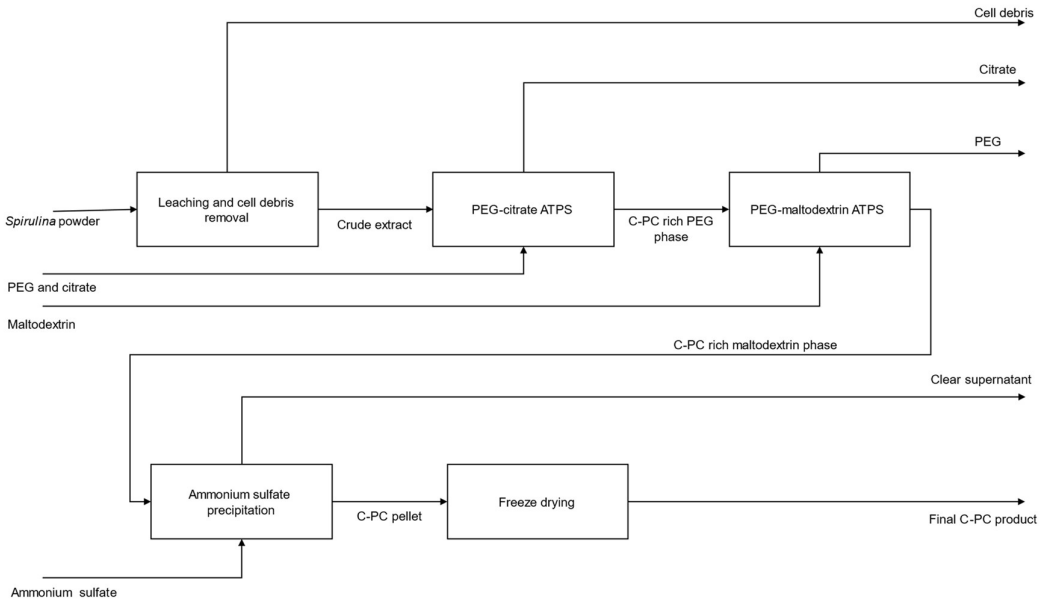

Figure 3: Block flow diagram for adjustment to CeBER C-PC purification process proposed by Hockey (2022).

The research done by Hockey (2022) was focused entirely on the ATPS stage of the process. However, a recommendation of their work was that adsorption should be considered as an additional pretreatment step in the process, to be included after the cell debris removal and before the ATPS takes place (where these are shown in Figure 3). This was suggested as it could be used to potentially enhance the product generated by the patented purification process, ensuring that cosmetic-grade product is consistently achieved.

Adsorption

Adsorption using either or both chitosan and activated charcoal is a purification technique that has been shown to be effective in the C-PC literature, and has the benefit that it is inexpensive

to operate. In order to best incorporate these adsorbents into the process, it is important to better understand their respective properties as well as their current use in C-PC purification. However, it is also necessary to first provide some background on the process and mechanism of adsorption itself. Adsorption is a process which results in a molecule being transferred from a bulk fluid on to the surface of a solid. If the adsorbent material and solution to be treated are maintained in contact for a sufficient period of time, then an adsorbent equilibrium can be reached. When this occurs, the rate of material desorbing from occupied sites on the adsorbent is equivalent to the rate of new molecules adsorbing on to the adsorbent's unoccupied site (Chiou, 2002). However, if the period of adsorption is shorter and equilibrium is not reached, then only certain quantities of material will be adsorbed. Additionally, when conducting adsorption processes, another issue to be cognisant of is the selectivity of the adsorbent to the material to be removed. Certain adsorbents have the ability to be highly selective where only specific molecules are removed improving the efficiency of the separation and allowing other components to remain in solution (Saini & Shankar, 2019). However, other adsorbents are not as selective and have the tendency to remove multiple different types of molecules. In this case, there are multiple components competing for the adsorbent active sites and resulting in a less efficient separation. However, the selectivity of adsorbents can be improved by modifying certain of their structural properties (Saini & Shankar, 2019).

Activated charcoal

Structure

Activated carbon, also known as activated charcoal, is carbon which has been processed to have an extremely fine structure and high internal and external surface area, resulting in it possessing strong adsorptive properties. It is most commonly available in either a powdered or granular form and is often used in industrial processes – such as water treatment, air pollution, gas storage and catalysis – due to its ease of design and operation and its selectivity towards certain substances (Tadda et al., 2018; Belhachemi, 2021). This selectivity allows it to be used as an adsorbent to remove low concentrations of both synthetic and natural contaminants from desired aqueous product streams. This adsorption process takes place as a result of the hydrophobic electrostatic interactions between the dissolved adsorbate and the activated charcoal adsorbent, resulting in the contaminant being retained on the surface of the activated charcoal. Other interactions such as ion exchange and hydrogen bonding can also be involved (Mansour et al., 2018; Demirbas, 2009). Adsorption as a process is favoured because of its generally high removal efficiency even at low concentrations of the impurity, possible adsorbent regeneration, applicability to both continuous and batch processes, as well as being simple to operate (Demirbas, 2009). However, it must be noted that the cost of regeneration and subsequent reuse of the adsorbent can at times be prohibitively high (Mansour et al., 2018; Quesada et al., 2020). The main physical characteristic of activated charcoal products is their porous structure, and it is this which enables its successful use as an adsorbent in industrial processes (Menéndez-Díaz & Martín-Gullón, 2006). The porous structure is formed by pores of different sizes, where these can be classified into three groups. The smallest pores – which have a width of less than 2 nm – are known as micropores, mesopores have widths in the range of 2 nm to 50 nm, and macropores are pores larger than 50 nm (Menéndez-Díaz & Martín-Gullón, 2006). A representation of an example of this pore distribution can be seen in Figure 4.

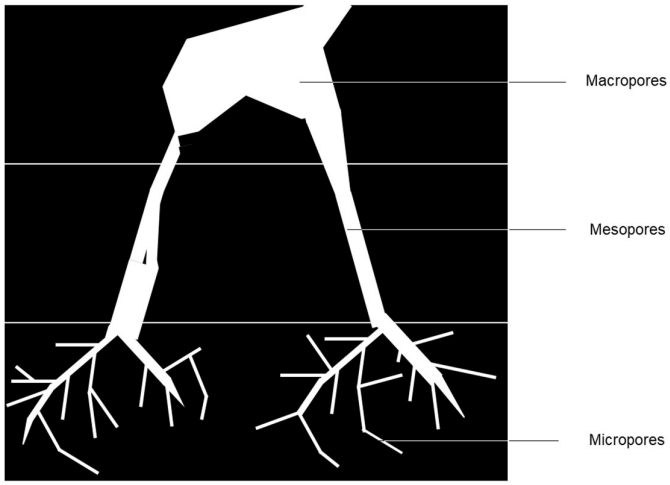

Figure 4: Representation of pore distribution within activated charcoal, adapted from Menéndez-Díaz and Martín-Gullón (2006).

It has been reported that up to 95% of the total surface area of an activated charcoal particle is made up of the micropore volume (Belhachemi, 2021). In addition to the pores forming the basis of the activated charcoal, there may be functional groups which form as a result of heteroatoms that bond themselves to carbon atoms on the edge of the activated charcoal structure and give rise to carbon adsorbents with different chemical properties.

Potential raw materials and activation techniques

The presence of specific functional groups and the exact pore distribution of the carbon adsorbent are predominantly a function of both the original feedstock and activation process used (Zabi et al., 2021). Because activated charcoal is a form of non-graphitic carbon, it can in theory be formed from any type of solid carbonaceous material. For this reason, there are many different potential raw materials which can be activated – examples being coals, wood, peat and lignocellulosic biomass (Menéndez-Díaz and Martín-Gullón, 2006; Schobert, 2013). Out of these, the most widely used sources of activated charcoal are often the agricultural by-products, due to their renewability, cheapness and abundance (Tadda et al., 2018; Belhachemi, 2021). As mentioned, the properties of the resulting activated charcoal product are often dependent on the properties of the feedstock, and often activated charcoal generated from different raw materials but which have undergone identical processing steps have distinct characteristics (Schobert, 2013). Therefore, it is possible to tailor the selection of certain raw materials depending on the desired function. Activated charcoal is generated from these feedstocks most commonly using either physical or chemical activation, although it must be noted that both approaches include chemical reactions in some form and so the use of these terms can potentially be misleading (Schobert, 2013). Generally, the choice between which of these two methods to use when attempting to produce activated charcoal is predominantly dependent on the final desired application of the adsorbent (Belhachemi, 2021).

Physical activation, also referred to as thermal activation, generally consists of two distinct consecutive steps (Mansour et al., 2018). The first step is the thermal carbonisation of the feedstock at medium or high temperatures to generate a carbon-rich char, which can then undergo the second step of activation where the char is partially gasified using an oxidising agent in a direct fired furnace (Menéndez-Díaz and Martín-Gullón, 2006; Schobert, 2013). Depending on the nature of the raw material, certain pretreatment steps are also sometimes required to prepare the carbon material prior to thermal activation. Crushing and sieving of the

feedstock is necessary to achieve the desired particle size, while a washing step is often required to remove dirt and mineral matter from the raw material (Menéndez-Díaz & Martín-Gullón, 2006). The purpose and importance of the carbonisation of the feedstock is to develop the micropore structure of the activated charcoal by decomposing the starting material. This results in the formation of a gaseous fraction – consisting of hydrogen and light hydrocarbons – as well as the solid, carbon-rich fraction (Menéndez-Díaz & Martín-Gullón, 2006). If the rate of heating is high during the carbonisation step, the solid fraction will have well-developed mesopores and macropores as well as a low density and hardness. On the other hand, a low rate of heating results in a solid char with high hardness and density (Menéndez-Díaz and Martín-Gullón, 2006; Belhachemi 2021). However, even after the carbonisation process, the full development of the pore structure still needs to be achieved through an activation step (Schobert, 2013). This activation is attained by partially oxidising the solid with a gas – either oxygen, steam or carbon dioxide – to remove part of the internal mass of the solid within the developing micropores and in so doing creating a material with a well-developed microporous structure (Menéndez-Díaz & Martín-Gullón, 2006). Oxygen is hardly used as the oxidising gas, because the high enthalpies of reaction result in runaway reactions occurring, and thus makes the temperature extremely difficult to control (Schobert, 2013). When using steam to activate the char, a wide range of temperatures – up to a maximum of 1000°C – can be utilised to ensure that the reaction takes place at the internal active site of the particle rather than only on its surface. This is important, because it allows internal porosity to develop inside the solid char and implies that steam is a good oxidising agent in the generation of an effective activated charcoal product (Menéndez-Díaz & Martín-Gullón, 2006). For the same temperature and pressure, activation using carbon dioxide is slower than what could be achieved with steam, and there is a greater potential for the reaction to take place on the surface of the particle, denying the opportunity for porosity to be developed. The final porosity of the charcoal activated by carbon dioxide is also often narrower; thus, the choice between using steam or carbon dioxide is often mostly dependent on the ultimate application of the product – with smaller micropores more appropriate for adsorption of gases and larger micropores being more suited to liquid phase adsorption (Menéndez-Díaz & Martín-Gullón, 2006).

Chemical activation, as opposed to physical activation, requires only one step by reacting the carbon feedstock with a chemical dehydrating reagent – most commonly zinc chloride, phosphoric acid or potassium hydroxide – where each results in a different pore distribution in the adsorbent (Schobert, 2013). Generally, whether or not chemical activation is feasible is dependent on the recovery of the reagent – consisting of an initial leaching step followed by drying of the washed carbon adsorbent – so that it can be reused in subsequent processes (Menéndez-Díaz & Martín-Gullón, 2006). Zinc chloride activation was the method most commonly used historically to generate activated charcoal because it results in an activated charcoal with a small distribution of microporosity (Schobert, 2013). This is especially true for lignocellulose feedstocks containing high quantities of volatiles such as wood. However, due to issues around low recovery and residual zinc in the adsorbent product, as well as increased regulations regarding plant emissions, zinc chloride is no longer the desired chemical reagent for the process (Menéndez-Díaz & Martín-Gullón, 2006). As with zinc chloride, activation using phosphoric acid is more effective for wood and other feedstocks with a high volatile concentration, but it is important to note that the quality of the final adsorbent is dependent on the specific raw material used as well as the conditions of treatment and amount of acid fed to the process (Belhachemi, 2021). Similarly to physical activation, often the first step is to grind and classify the feedstock so that the raw material is in a form which can be more easily activated. Once this has taken place, the phosphoric acid is mixed into the process and heat treatment takes place in an inert atmosphere, initially at 100°C to 200°C, after which the temperature is raised to between 400°C and 500°C. Finally, the product is washed so that the

phosphoric acid can be recovered in order to be reused, while the activated charcoal is then dried (Menéndez-Díaz & Martín-Gullón, 2006). Carbon adsorbents generated in this manner have the advantage over those formed using thermal activation because of their lower density and better developed mesopore structure. In contrast to the other chemical activation processes, using potassium hydroxide as the reagent is better suited when the feedstock contains fewer volatiles and a higher carbon content, for example in the different types of coal (Menéndez-Díaz and Martín-Gullón, 2006; Belhachemi, 2021). However, the process of developing the activated charcoal from the raw material remains similar, where the potassium hydroxide is mixed with the feedstock before heat treatment takes place at two temperatures – although the second temperature is higher than what was used for phosphoric acid at around 800°C – and the product is again washed to recover the chemical reagent (Menéndez-Díaz & Martín-Gullón, 2006). Ultimately, the use of potassium hydroxide in the chemical activation process results in a carbon product with a high adsorption capacity and a narrow micropore structure with no mesopores.

Forms of activated charcoal

The various properties of activated charcoal, such as its ability to selectively adsorb substances, results in it being applied to several different industries, for instance as a step in the process of recovering C-PC. Activated charcoal is reported to improve the extraction of C-PC because of its high surface area, its low cost and easy use, as well as the fact that it does not impact the biological activity of the protein (Liao et al., 2011). However, it is important to note that depending on the specific process and type of raw material used to generate the activated charcoal, the final product can be obtained in several different forms, where each has its own inherent characteristics and properties – where some may be more applicable for C-PC extraction than others. Some of the more common types of activated charcoal which are used in industrial processes are granular activated charcoal (GAC), powdered activated charcoal (PAC) and extruded activated charcoal (EAC), which is created by binding powdered charcoal together in the form of pellets (Potwora, 2016). One of the most crucial differences in the available types of activated charcoal are the sizes of the particles, because it is often this particle size that determines in which application the activated charcoal will be utilised. Because the uses of activated charcoal are so varied, it is difficult to generalise which types are best suited for each, but traditionally GAC and EAC are used in fixed-bed adsorption columns and in-line leaching tanks as their larger particle sizes reduce the level of the pressure drop across the length of the column (Potwora, 2016). PAC, on the other hand, with traditional particle sizes less than 100 µm, is mixed into the sample being treated before being separated out once the unwanted impurities have been adsorbed (Menéndez-Díaz & Martín-Gullón, 2006).

The most considerable issue with using PAC is the fact that it is not possible for the adsorbent to be reused or regenerated, and that it must therefore be discarded after removing the undesired impurities. Despite this, the greater surface area provided by PAC when compared to GAC implies that it may be the most effective form of activated charcoal to be used in the proposed pretreatment stage for purifying C-PC. However, within the classification of PAC there is still a great deal of variation in the available particle sizes, and so this is something that also needs to be taken into account. Because the adsorption of undesired impurities takes place on the surface of the activated charcoal particles, it is understandable that the larger the surface area of the particles, the quicker the adsorption process will occur. For this reason, smaller particles of activated charcoal – which have a greater surface area – will lead to a more efficient adsorption process in terms of removing the contaminants from an aqueous solution (Deniz, 2013; Jafari et al., 2017). The size of an activated charcoal particle is often defined as mesh size, which is the number of openings in a screen with an area of one squared

inch. Therefore, a greater mesh size implies that the openings are narrower and that only the smaller particles will be able to pass through the mesh sieve.

Other properties

It needs to be noted, however, that particle size is not the only important characteristic of activated charcoal, and that other properties – such as the specific surface area, pore-size distribution, pore volume and surface functional groups – also impact its effectiveness as an adsorbent (Yin et al., 2007; Mansour et al., 2018). The specific surface area – which is related to the size of the particles but also takes into account the area created by the porous structure within the activated charcoal – naturally has a large influence on how easily impurities can be removed from the solution. This specific surface area is often defined as the Brunauer-Emmett-Teller (BET) surface area, and is measured by considering the adsorption isotherms of N_2 at 77 K and CO_2 at 273 K. These isotherms describe the interactions at equilibrium where the two distinct phases have been in contact for a sufficient period of time to ensure that the concentration of the adsorbed gas on the surface of the activated charcoal is the same as in the bulk solution assuming monolayer adsorption (Mansour et al., 2018). The use of the two isotherms is complementary, as the CO_2 isotherm measures pores in the micropore size range, while the N_2 isotherm measures the area of the larger pores (Menéndez-Díaz and Martín-Gullón, 2006; Belhachemi, 2021)

Understandably, the pores present in the activated charcoal sample have a big impact on the magnitude of the BET surface area which can be measured. However, this magnitude is not the only property of the porous structure which has a bearing on how effectively the activated charcoal performs as an adsorbent. The nature of the pores is also crucial in understanding how the undesired impurities in the process will be adsorbed onto the surface of the charcoal. This porous structure is defined by the presence and relative distribution of micropores, mesopores and macropores, as well as their respective volumes. The majority of adsorption takes place at the sites provided by the micropores, and it is these micropores that contribute to the high surface area of activated charcoal particles. However, the macropores and mesopores serve an important role by providing the passages for these micropores to be reached by the adsorbed impurities, and activated charcoal samples with too narrow sizes of micropores and mesopores could potentially result in the adsorption sites not being accessible (Schobert, 2013; Menéndez-Díaz and Martín-Gullón, 2006; Mansour et al., 2018). These properties of the activated charcoal clearly have a significant influence on its effectiveness at removing different components and can therefore determine what processes the various activated charcoal samples are best suited to.

As previously discussed, another important property of the activated charcoal which impacts its performance as an adsorbent is the presence of different surface functional groups. The activated charcoal surface can be represented as a network of hexagonal planes of carbon atoms where the planes are cross-linked by bridging groups (Belhachemi, 2021). Heteroatoms, such as oxygen and hydrogen, can be incorporated into this network by bonding to the periphery of the planes, and it is these heteroatoms that create the functional groups on the surface of the activated charcoal and are potentially able to react with the adsorbate in the solution (Yin, Aroua & Daud, 2007). Examples of possible functional groups include carboxyl, phenol and lactone, which give the carbon an acidic character, as well as basic functional groups like pyrone, chromene and carbonyl (Belhachemi, 2021). The surface of activated charcoal is predominantly hydrophobic in nature, but if it contains oxygenated functional groups it can become less hydrophobic – which potentially results in water molecules being favoured at the adsorption sites rather than the impurity to be removed (Mansour et al., 2018). The specific adsorption of activated charcoal towards specific components can be improved

through an impregnation process where the functional group present on the surface of the activated charcoal can be selected to favour the removal of specific unwanted impurities (Henning & Schäfer, 1993).

However, despite the numerous benefits associated with using activated charcoal as an adsorbent, there are some potential drawbacks. One of these, which has already been discussed, is the lack of reusability of powdered activated charcoal and the fact that it needs to be disposed once it has adsorbed the contaminants and has been separated from the C-PC in the solution. This naturally increases the costs associated with including it in the process, and so it is often seen as advantageous to use it in combination with another type of natural polymer. These polymers can have high affinities for certain pollutants and also have large adsorption capacities, reducing the quantity of activated charcoal required (Quesada et al., 2020).

Chitosan

Chitosan is one such polymer and has been used in conjunction with activated charcoal in several industrial processes. It has been used to encapsulate and immobilise activated charcoal to increase the durability and to produce an adsorbent which has a wide adsorption spectrum towards pollutants (Quesada et al., 2020). Chitosan has also been used, along with activated charcoal, in various studies as an additional adsorbent in C-PC recovery processes where this adsorption step is able to increase the purity of the C-PC sample.

Chitin precursor

Chitosan is predominantly sourced through the deacetylation of chitin, one of the most abundant naturally occurring polysaccharides, because it forms the primary basis of fungal cell walls and the exoskeleton of arthropods, serving as a reinforcement in functions where strength is required (Dutta et al., 2002; Antonino et al., 2017; Jayakumar et al., 2010). Chitin is a derivative of cellulose, where the hydroxyl group attached to the second carbon is replaced by an acetamide group, with the resulting chitin therefore consisting of the β-(1,4) linking of 2-acetamido-2-deoxy-D-glucose monomers (Zhang et al., 2020). This structure of a chitin monomer is clearly represented in Figure 5. Chitin exists in three forms, which are each defined according to the orientation of the chitin linear polymer chain. The most common and resilient of these chains is α-chitin where the polysaccharide chains are orientated in an anti-parallel manner, and it is this specific polymer which forms the basis of the shells and skeletons of crustaceans and other arthropods (Arnold et al., 2020; Zhang et al., 2000). The other two forms are less common but are still naturally occurring, where β-chitin – which consists of parallel polymer chains – is found in the gladius of squids and the γ-form is found in insect cocoons and consists of a combination of both parallel and antiparallel chitin chains (Zhang et al., 2020). Large amounts of chitin-containing crustacean shell wastes are disposed into either landfills or the ocean every year and so there is a great deal of incentive to utilise this waste stream in other processes and to generate useful products such as chitosan (Arnold et al., 2020).

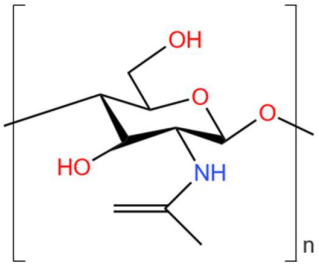

Figure 5: Visual representation of chitin structure, adapted from Zhang et al. (2000).

On an industrial scale, chitin is predominantly obtained from the unwanted remnants of prawn, shrimp, crab and lobster processing plants, however these waste products also contain considerable quantities of protein, calcium and magnesium carbonate (Antonino et al., 2017). Therefore, it is necessary to treat these wastes to extract and isolate the chitin from the rest of the components present. This is traditionally done through chemical means, where the ground crustacean shells are demineralised using a strong acid, such as HCl, and the protein is removed after adding a strong base like NaOH (Antonino et al., 2017; Arnold et al., 2020). The chitin produced has a low molecular weight because these harsh chemicals attack the crystal structure of the chitin and degrade the polymer chains. It must be noted however, that this process results in the generation of potentially toxic by-products and does not allow the recovery of the valuable minerals and amino acids present in the initial waste stream (Arnold et al., 2020). However, biotechnological routes for generating chitin from the crustacean processing waste are also available. The most common of these consists of the demineralisation of the waste through lactic acid bacteria fermentation and the use of proteases for deproteinisation. Through this approach, both the mineral and protein content of the chitin can be reduced significantly – by up to 99% and 95%, respectively – while also preventing the formation of the environmentally harmful by-products created by chemical extraction (Arnold et al., 2020). However, due to the various potential sources of chitin and the several different methods of extracting it, the commercial chitin products available are often not uniform in terms of quality (Barikani et al., 2014).

The benefit of extracting the chitin from these traditionally unwanted process streams is not only to reduce the amount of waste generated. Chitin also has certain properties which can prove useful for certain industrial applications, such as wastewater remediation, food production, pulp and paper treatment, cosmetics and in biomedical processes (Barikani et al., 2014). There are certain general properties and characteristics of chitin which allow it to be effective in these applications. One valuable property in many of these industries is chitin's antibacterial and antifungal ability, particularly when it is in the form of an oligosaccharide. Additionally, chitin is also seen as biocompatible, biodegradable and nontoxic and it is these properties which specifically allow it to be used in biomedical applications (Barikani et al., 2014; Islam et al., 2017; Yahyaei et al., 2018). Chitin is also reported to have good adsorptive properties and is therefore considered as a possible alternative to synthetically produced polymers (Islam, Bhuiyan & Islam, 2017). However, despite these advantages presented with respect to the potential uses of chitin, it must be noted that its poor solubility in both aqueous and organic solvents and low reactivity often limit its application in industry (Jayakumar et al., 2010b; Barikani et al., 2014; Mohamed, 2021). Therefore, chitin is predominantly extracted to be used as a precursor for the production of chitosan due to chitosan's greater chemical activity and adsorption ability (Gyliene, Rekertas & Šalkauskas, 2002). This greater activity is mainly as a result of the deacetylation which takes place in the reaction from chitin to chitosan (Islam, Bhuiyan & Islam, 2017).

Formation of chitosan

Generating chitosan from a chitin precursor can be done in several ways, where the key step is the removal of the acetyl group (C_2H_3O), present as part of the acetamide group in each of the chitin monomers. An example of a chitosan monomer, once deacetylation has taken place, can be seen in Figure 6.

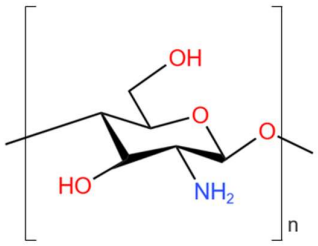

Figure 6: Visual representation of chitosan structure, adapted from Zhang et al. (2000).

One of the principal characteristics of chitosan is the degree to which the chitin has been deacetylated – where this degree is defined as the ratio of the amino groups (NH_2) present to the total sum of amino and acetamido groups (Sivashankari & Prabaharan, 2017). The degree of deacetylation varies depending on the exact precursor and mechanism involved, however, the process is considered to have generated chitosan if the degree of deacetylation is greater than 75%, with most commercial chitosan reaching a maximum of 95% (Gyliene et al., 2002; Guibal, 2004). The resulting chitosan consists of monomers which contain only the amine group, rather than the full acetoamide, and this amine in conjunction with the hydroxyl groups already present play a significant role in the effectiveness of chitosan as a biopolymer. Generally, the degree of deacetylation of a chitosan sample can be determined through either infrared spectroscopy or nuclear magnetic resonance (Mohamed, 2021).

As with the preparation of the chitin from the raw material feedstock, there are a few different approaches which can be used to further process this chitin in the goal of producing chitosan. The most common method of generating chitosan is through the hydrolysis and subsequent deacetylation of the acetamide groups present in chitin, using a concentrated strong base – such as NaOH or KOH – at temperatures greater than 100°C (Antonino et al., 2017; Min et al., 2004). The ultimate result of the deacetylation process is highly dependent on several factors – such as the exact concentration of base, temperature, the time of reaction, the source and initial concentration of chitin as well as its molecular weight and particle size (Sivashankari and Prabaharan, 2017; Vunain et al., 2017). A longer reaction time results in a greater degree of deacetylation and consequently a chitosan with a higher proportion of amino groups, however, an increase in the time of reaction also degrades the polymer chains and reduces the molecular weight of the final product (Sivashankari & Prabaharan, 2017). For this reason, flash treatment of the chitin over short periods and higher temperatures has been performed in an attempt to decrease the degradation rate, where this approach resulted in a higher maximum achievable degree of deacetylation (Focher et al., 1990). Despite some of the success in achieving deacetylation, this alkali method of treating chitin to form chitosan suffers from some inherent disadvantages. The most obvious issue with this process is the high quantities of NaOH or KOH required, however, it also consumes a significant amount of energy, and the final chitosan product often has a wide range of molecular weights and degrees of deacetylation (Sivashankari & Prabaharan, 2017).

Because of these disadvantages, enzymatic reactions have also been investigated as an alternative method of deacetylation. These chitin deacetylase enzymes can be isolated from species of fungi and insects such as *Mucor rouxii*, *Aspergillus nidulans*, *Absidia coerulea* and *Colletotrichum lindemuthianum* (Antonino et al., 2017). Chitin deacetylase has been found to have a narrow specificity for chitin substrates, reducing the range of potential products which can be generated and providing greater control over the process (Martinou et al., 1995; Sivashankari and Prabaharan, 2017). However, the enzyme is often not as effective at deacetylating less soluble chitin substrates, and so in these cases it is necessary for the crystalline chitin to undergo some form of pretreatment so that the acetyl groups are more accessible (Martinou, Kafetzopoulos & Bouriotis, 1995). This pretreatment often takes the form of reacting the chitin with HCl or a $CaCl_2$ and methanol solvent, which can considerably increase the maximum level of chitin deacetylation that can be achieved (Beaney et al., 2007). Despite being less environmentally harmful than the traditional method of deacetylation, this potential need for pretreatment is a drawback of using enzymes to generate chitosan. Another possible disadvantage with this approach is the cost of obtaining the chitin deacetylase – naturally an essential aspect of the enzymatic deacetylation process. Ultimately, the success of enzymatic deacetylation is dependent on the structure of the chitin, the available surface area, the properties of the enzyme and the mechanism of interaction between the enzyme and the substrate (Sivashankari & Prabaharan, 2017).

Properties of chitosan

As previously discussed, the existence of both hydroxyl and amino reactive functional groups in chitosan – where the presence of the amine is what differentiates it from chitin – allows it to be used in a wide variety of applications. Similarly to chitin, chitosan has been found to be easily biodegradable, nontoxic and biocompatible, while also displaying antioxidant and antiviral activity. Therefore, chitosan is often utilised in biomedical processes as well as other industries such as cosmetics, paper and pulp and wastewater remediation (Vunain, Mishra & Mamba, 2017). Despite the high degree of overlap with industries in which chitin has been used, chitosan is favoured because of its greater solubility in different types of solutions as a result of the presence of the amino group (Honarkar & Barikani, 2009). This functional group enables chitosan to undergo sets of reactions typical of amines, such as *N*-acylation and Schiff reactions, providing chitosan with greater versatility than chitin (Dutta et al., 2002; Vunain et al., 2017). The more versatile nature of chitosan also gives it a porous structure and allows it to be processed into different forms – such as gels, scaffolds, nanoparticles, beads, nanofibers and membranes (Vunain et al., 2017; Honarkar and Barikani, 2009). Despite the physiochemical and biological advantages associated with using chitosan over other biopolymers, there are certain limitations seen in its reactivity and processability. However, it is also easily modified, using either chemical or physical interactions, and in this manner these limitations can often be overcome (Vunain, Mishra & Mamba, 2017). Chitosan has poor solubility in most solvents at both neutral and high pH as a result of its hydrogen bonding network, rigidness and brittleness. Therefore, the goal of modification is to generate chitosan derivatives which are more soluble. This is possible due to the nature of the hydroxyl and amino functional groups, as this allows for the attachment of other functional groups and ligands to aid in solubility. Several different methods of chemical modification have been investigated, including blending chitosan with synthetic polymers, cross-linking radiation, enzymatic grafting and hydrophobisation (Vunain, Mishra & Mamba, 2017).

Although chitosan displays a wide range of properties and can be used in numerous different processes, its lack of uniformity means that certain types of chitosan are better suited to certain applications than others. For this reason, it is often important to characterise each specific chitosan sample to better understand how best it can be utilised. Chitosan is often

defined based on its degree of deacetylation, as this has the biggest impact on its chemical, physical and biological properties as a result of the amine groups produced being more reactive (Guibal, 2004; Martinou et al., 1995). However, it is also important to consider other characteristics of the chitosan product such as its molecular weight (MW) and crystallinity, as these also have an impact on its performance and the applications in which it can be used. Naturally, these factors are highly dependent on the initial source of the chitin, the chitin extraction method and the process of deacetylation. The acceptable range of molecular weights for commercial utilisation of chitosan is generally between 10^4 and 10^6 $g.mol^{-1}$, which is an important consideration, as the various forms of chitosan are more suited to different applications. Chitosan with a low molecular weight has certain limits on which processes it remains effective, due to its lower viscosity. However, low molecular weight chitosan is able to more easily penetrate the cell membrane of unwanted microorganisms and prevent the transcription of RNA and therefore the growth of the organisms, displaying the potential antimicrobial effect of smaller chitosan polymers (Islam et al., 2017; Vunain et al., 2017). On the other hand, derivatives modified from a high molecular weight chitosan were found to have a higher capability of enantioseparation than those modified from low molecular weight samples (Zhang et al., 2020). In terms of physical structure, lower MW chitosan is more rigid and has a greater level of conformation than higher molecular weight polymers. Other properties which have been found to be dependent on molecular weight are chitosan's binding capacity, chain flexibility, thermal stability and membrane pore size (Tsai & Chen, 2017). This indicates that the benefit of using either a low or high molecular weight chitosan is often dependent on the specific process involved and which properties of chitosan are required. However, if a specific molecular weight is needed for a particular application, there are potential methods of molecular weight modification, where these generally reduce the MW of the chitosan. The goal of MW modification is to reduce the molecular weight distribution range and manipulate it to be as close as possible to the desired value, while still maintaining the structure of the chitosan (Tsai & Chen, 2017). This modification can take the form of chemical, mechanical or high-energy degradation or by enzymatic hydrolysis. The success of the modification is highly dependent on factors such as temperature, concentration and time of reaction, however, it is also important to note that the degree of deacetylation of the initial chitosan sample also impacts the performance of MW modification, and that a higher degree of deacetylation makes it easier to reduce the molecular weight of the sample (Tsai & Chen, 2017).

This is an example of how the degree of deacetylation of the chitosan has a large influence on its overall properties. As has already been discussed, the higher the degree of deacetylation of the chitosan sample, the greater proportion of free amino groups present. It has also been explained that these amino groups are more reactive and, therefore, chitosan polymers with a higher degree of deacetylation are favoured for use as adsorbents (Guibal, 2004). For example, the adsorption of certain impurities, such as dyes, was found to be more efficient when using chitosan with a higher degree of deacetylation (Moura et al., 2016). Additionally, chitosan polymers with a greater degree of deacetylation have improved mechanical properties as a result of their more ordered molecular structure and higher level of crystallinity. This is due to the higher proportion of amino groups present, leading to hydrogen bonding between the molecules, which also implies that higher deacetylated chitosan degrades less easily. The degree of deacetylation has also been found to have an effect on chitosan's biodegradability and biocompatibility as well as its antioxidant and adsorption capabilities (Sivashankari & Prabaharan, 2017).

Forms of chitosan

On top of the potential differences in chitosan products seen in the degree of deacetylation and molecular weight, the physical form of the chitosan can also vary. It can be present in the form of a powder, beads, hydrogels, hollow fibres, flakes and films. It has been reported that out of these, chitosan powder and films were found to be the most suitable for the adsorption of impurities from an aqueous solution (Moura et al., 2016). As with activated charcoal, the powdered form of chitosan is able to better adsorb impurities because of its greater available surface area. However, the use of chitosan in powdered form implies that the adsorbent cannot be regenerated and must be disposed of once the impurities have been adsorbed onto its surface, and therefore this disadvantage needs to be considered when using powdered chitosan (Moura et al., 2016). Chitosan is particularly suited to being used as an adsorbent due to the number of hydroxyl groups which increase its hydrophilicity, the reactive nature of these hydroxyl groups, as well as the amino groups present and the flexible nature of the polymer structure (Miretzky & Cirelli, 2009). This ability as an adsorbent is what makes it such a potentially attractive component to include in a C-PC recovery process from *Spirulina*.

Studies using chitosan and activated charcoal in C-phycocyanin purification

The properties of chitosan which have been discussed in great detail – as a result of it containing both amino and hydroxyl functional groups serving as active sites – allow it to adsorb undesired proteins present in a crude C-PC extract, such as allophycocyanin which is often difficult to remove from C-PC, while enabling the C-PC to pass through, thereby improving its purity (Fekrat et al., 2019; Ng et al., 2019). The use of chitosan allows the purity to be improved in a relatively short duration, due to the low processing times required, while maintaining a sufficient product yield. In addition, the mild process conditions required for chitosan adsorption do not easily denature the desired protein and therefore the C-PC activity is maintained (Liao et al., 2011). The benefit of using chitosan – in conjunction with activated charcoal as an additional adsorbent – has been shown in several studies which either used these adsorbents as part of a larger C-PC purification process or specifically investigated the performance of this adsorption pretreatment step.

Several investigations have been conducted where chitosan and activated charcoal were included in a C-PC recovery process and were found to improve the purity of the C-PC. A study was performed by Lee et al. (2016) in an attempt to enhance the growth of *Spirulina* by varying the intensity and wavelength of the light used during the cultivation process. This study, however, also considered the purification of the C-PC grown in this manner and thus extraction methods were needed to generate a high enough purity C-PC product. One of the steps was to pass the crude C-PC extract through a column containing both 4% w/v of granulated activated charcoal (20 to 40 mesh size) and 0.3% w/v of chitosan at a pH of 7.2, and it was determined that the purity was improved from 2.4 to 3.1 while being able to obtain a C-PC concentration of 0.903 $mg.mL^{-1}$ (Lee et al., 2016). A similar research study was conducted by Patil et al. (2006), where various recovery methods were used in the C-PC purification train, including the use of an activated charcoal and chitosan adsorption step, thereby providing further insight into the potential of these substances as an option for pretreatment. The result of the investigation was an improvement in C-PC purity from 1.18 to 2.58 when a crude extract was passed through an adsorption column bed containing activated charcoal. When chitosan was mixed at a concentration of 2% v/v into the crude extract before passing through the column, this purity was even further improved to 3.96 (Patil et al., 2006). Another research study by Wang et al. (2012), this time focusing on the various aspects of the performance of an ATPS process, utilised chitosan to treat a crude C-PC extract. This investigation did not include activated charcoal but the improvement in C-PC purity from 0.89

to 1.57 as a result of adsorption with a 1% w/v solution of chitosan again emphasises its potential as a pretreatment option (Wang et al., 2012).

Rather than simply utilising activated charcoal or chitosan in the purification process, other studies have investigated the performance of this potential pretreatment in more detail, where different process variables – such as adsorbent concentration, pH or time – were optimised to produce the highest quality C-PC product. The first study of this sort was conducted by Safaei et al. (2019) and focused on the potential anticancer properties of C-PC. However, in order to evaluate these properties, it was necessary to obtain a pure C-PC product and thus the performance of the extraction process needed to be optimised. This included adsorption using both chitosan and activated charcoal at various concentrations, allowing conclusions to be drawn about the optimal values of each. The results suggested that the most efficient concentration of chitosan was 0.2% w/w, as this was the most efficient in terms of removing unwanted impurities. This enabled the purity of the C-PC generated to be improved from the control value of 1.2 to a final purity of 1.5, with a concentration of 0.125 $mg.mL^{-1}$. The equivalent optimal value of activated charcoal was reported as being 12% w/w, as this resulted in the maximum values of both concentration and purity of the C-PC, where the final concentration was measured to be 0.05 $mg.mL^{-1}$ and the purity was improved from 1.2 to 2.2. Higher concentrations of the activated charcoal, on the other hand, resulted in a lower quality C-phycocyanin product due to reduced purity and concentration achieved (Safaei et al., 2019). Another research study that has been published aimed to investigate the specific performance of C-PC purification achieved through an ion-exchange chromatography step (Liao et al., 2011). However, as with the study by Safaei et al. (2019), the performance of the chitosan and activated charcoal adsorption was optimised by varying the concentrations of each component as well as the pH of the system (Liao et al., 2011). The optimal conditions were therefore found to be a concentration of 0.29% w/w of 40 kDa chitosan with an activated charcoal concentration of 8% w/w and a pH of 6.9. These conditions allowed the purity of the C-PC to be improved from its initial value of 0.93 in the crude extract to 1.52 after chitosan adsorption and 2.78 after the addition of activated charcoal, while also resulting in yields of 95.8% and 85% after each step respectively (Liao et al., 2011).

The final example of a study of this sort was conducted by Fekrat et al. (2019), where again the chitosan and activated charcoal concentrations were varied to determine their impact on the purity and concentration of the C-phycocyanin product obtained after adsorption. Low molecular weight (50 to 190 kDa) chitosan was used for this adsorption step along with 100 to 400 mesh size activated charcoal. Different stirring times of the adsorption were also investigated to fully understand the effectiveness of the extraction technique, and whether or not this aspect of it could be further optimised. The theoretical highest purity and concentration values at the end of the different experimental runs were determined to be a chitosan concentration of 0.24% w/v and activated charcoal concentration of 8.4% w/v with an adsorption stirring time of 10.2 min. At these conditions, the purity was increased from its initial value of 0.44 when measured on the crude C-PC extract, to 3.14 at this optimal combination, while the concentration of C-phycocyanin exiting the adsorption stage was measured to be 0.27 $mg.mL^{-1}$ (Fekrat et al., 2019). The stirring time of 10.2 min led to a maximum purity because shorter stirring times were proposed to be insufficient to allow the chitosan and activated charcoal adsorbents to properly adsorb the impurities, while longer stirring times resulted in the C-PC being adsorbed rather than the undesired proteins. In these experiments, the chitosan was added after being dissolved in 1% acetic acid, and therefore, when the concentrations of chitosan were high, the acetic acid concentration also increased. This reduced the pH of the solution and lowered the purity of the C-PC product due to C-PC likely becoming denatured (Fekrat et al., 2019). When chitosan was added at concentrations lower than the optimal value of 0.24% w/v, it was found that these were less efficient at adsorbing

all the impurities present, and therefore the purity was not increased to the same extent. Naturally, a similar phenomenon occurred when the activated charcoal was brought into the solution at low concentrations. When the activated charcoal concentration was high, on the other hand, the reduction in purity achieved – when compared to the optimal concentration of 8.4% w/v – could be attributed to the additional amount of activated charcoal adsorbing the C-PC and removing it from the solution rather than the impurities (Fekrat et al., 2019). The various optimal values which have been reported in these papers provide an excellent starting point for any further investigations into the effectiveness of both chitosan and activated charcoal and thus these results are extremely useful in trying to understand this aspect of the possible C-PC extraction process.

The microbial loading of the C-PC is one of the most important characteristics of the final product, as has already been discussed, but none of the previous literature investigating adsorption using chitosan and activated charcoal have considered this aspect of the process. The nature of the *Spirulina* biomass is that it often already contains microbial contaminants from its native environment and thus part of already existing C-PC purification processes is to reduce this loading to a suitable number. It is not clear if these microbial contaminants would also be adsorbed by the chitosan and activated charcoal along with the undesired proteins, or if they would remain in the solution along with the C-PC product and would in fact use the adsorbents as a feedstock for growth. Both components could increase the potential for contamination due to them being excellent sources of carbon to sustain microbial growth. Ultimately, both activated charcoal and chitosan are potentially useful adsorbents to be used in a process to increase the purity of C-PC extracted from *Spirulina*. The literature discussed suggests that the use of chitosan and activated charcoal in an adsorption step does result in an increase in the purity of C-PC achieved. This would lead to a more efficient process, as the desired purity for cosmetic-grade C-PC can be achieved in a manner which appears to be easier and cheaper to perform. However, despite this significant evidence in favour of their use, there is still the need for further experimental research to be done to have a complete understanding of all aspects of the adsorption step and the results which can be achieved – especially in the context of trying to improve the output of the already existing C-PC purification process.

2.4 Literature Review Summary

As has been shown in this literature review, there is a significant potential – for economic as well as environmental reasons – associated with using biological sources to generate valuable products. The cyanobacterium *Spirulina* is an excellent example of these types of naturally occurring resources which can be used to obtain products of higher value. *Spirulina* is favoured because, as with many other species of microalgae, it can be cultivated relatively easily and has many reported health benefits, such as having antioxidant, anticancer and anti-diabetic properties. Because of this, *Spirulina* can be utilised in its current form in nutraceutical formulations, but it is also a potential source of products like pigments and other proteins as well as vitamins and minerals. C-PC is one of these pigments and shows many of the same health advantages as *Spirulina* and has a bright blue colour when extracted. Therefore, it can be used in many different applications like medical research and as a component in both food and cosmetic products.

The most commonly accepted method of quantifying the quality of a C-PC product is by measuring its purity, where this is simply a ratio of the absorbance reading at 620 nm (the absorbance maximum of C-PC) to the absorbance at 280 nm (the absorbance for general proteins). However, C-PC products often also need to meet other specifications such as a

defined E-value and a maximum allowable level of microbial contamination. The purity of a C-PC sample is often the main determinant for which applications it can be used, where food products generally only need to meet a purity of 0.7 and cosmetic-grade C-PC has a purity of at least 1.5. In order to be used in medical research, the purity of C-PC must be above 4 but the choice of which purification techniques are used is often what has the biggest impact on the C-PC purities achieved.

Generally, C-PC purification can be performed using techniques such as chromatography, ATPS, precipitation, filtration and adsorption. Chromatography is highly effective at producing C-PC with purities sufficient to be used in medical research, but this improved performance requires additional capital and operating costs, especially when being conducted on a large scale. Filtration is able to improve the purity of C-PC through careful choice in membrane size and has the additional advantage of being able to eliminate unwanted microorganisms and perform a buffer exchange to remove any salts still present in the product. ATPS and precipitation are not as effective as chromatography in terms of maximising the purity of C-PC but are simpler and cheaper to perform and can be more easily scaled up. The CeBER patented process aims to generate cosmetic-grade C-PC, and it is for this reason that ATPS and precipitation were chosen as the purification techniques to include.

The patent uses PEG and maltodextrin in the ATPS and ammonium sulfate as the chemical to precipitate C-PC out of solution. Further research was done by Hockey (2022) with the goal of investigating aspects of this patented process in order to improve its performance. This work focused on the ATPS – particularly the optimal composition of the various components and the idea of coupling a PEG-citrate ATPS with the PEG-maltodextrin system already present. This investigation increased the purity of the C-PC generated, but because it only focused on the ATPS and was not able to consistently generate cosmetic-grade C-PC, there were still other opportunities to further improve the outputs of the process. One of these was to include a pretreatment purification step after cell debris removal and before the ATPS, in an attempt to increase the purity of the C-PC entering the downstream part of the process, and hence making those purification steps more efficient.

Based on literature findings, adsorption using activated charcoal and chitosan showed a great deal of promise as this pretreatment. Both components are known to be effective adsorbent materials – chitosan because of its possession of two different functional groups, and activated charcoal because of its large surface area and highly porous physical structure. In addition, this step is relatively cheap and simple to perform, and both of these components have been used previously in C-PC purification processes and were shown to increase the purity of the C-PC which can be produced. However, more research needs to be conducted on this adsorption step to better understand its operation as well as its impact on the other purification steps present in the CeBER process, namely the ATPS and precipitation.

3 Defining the Research Project

3.1 Problem statement and objectives

The process which has been patented by CeBER has the goal of producing cosmetic-grade C-phycocyanin from *Spirulina*. However, as with any other process, there is the scope to investigate alternative configurations with the aim of improving the reliability and effectiveness of the C-PC purification. It is for this reason that an opportunity exists to incorporate a pretreatment into the overall downstream process once the initial cell debris removal step has taken place. This pretreatment will take the form of adsorption utilising both or either of chitosan and activated carbon, with the aim of removing the impurities present and thereby improving the purity of the crude C-PC extract entering the subsequent purification steps. The overarching goal is to guarantee the final C-PC product can consistently meet the requirements for cosmetic-grade C-PC in an operationally easy and efficient manner.

3.1.1 Research problem objectives

The objectives of this research project are therefore to investigate the performance of a C-PC extraction and purification process, which includes a proposed pretreatment consisting of a chitosan and activated charcoal adsorption step. The overall performance will be assessed in terms of C-PC purity, concentration and recovery, as well as the bacterial contamination. The impact of the adsorption pretreatment on the operation and key outputs of the subsequent ATPS and precipitation stages will be determined by testing if the final purity consistently meets the 1.5 desired for cosmetic-grade C-PC. In addition, it will also be concluded if the E-value of the final product is commercially competitive and if the contamination is reduced to less than 1000 $CFU.g^{-1}$, in line with the requirements of C-PC for cosmetic applications.

3.2 Key research questions

The key questions to address the research problem objectives are as follows:

- Do the adsorbents, chitosan and activated carbon, selectively adsorb unwanted proteins and in doing so remove impurities from the extract while allowing the C-PC to pass through?
- What are the optimal adsorbent concentrations in terms of maximising both the purity and recovery of the C-PC from the crude extract?
- What are the other optimal adsorption conditions, such as pH and contact time?
- Do activated carbon and chitosan achieve better results when they are used in combination or is a more efficient process obtained when only one of the adsorbents is used, and if so, which?
- What impact does the adsorption have on the subsequent downstream purification steps of the CeBER process?
- Can the success of the adsorption step lead to more efficient alternative process configurations by adjusting or eliminating any of the currently used subsequent purification stages?

4 Approach to Project and Methodology

4.1 Research methodology

As has been extensively discussed, the goal of this project is to improve a C-phycocyanin purification process by incorporating an adsorption pretreatment step using activated charcoal and chitosan. The first step in this research project was to complete a review into pertinent literature to understand the different aspects of the existing process and the reasons for the proposed benefit of including the chitosan and activated charcoal. Additionally, studies which considered C-PC purification using activated charcoal and chitosan were identified to better appreciate how to incorporate this step most effectively into the process.

The next step was to focus on generating results through experimental work in the laboratory. This consisted of different sets of runs, where each was evaluated in terms of performance by taking spectrophotometric absorbance measurements to determine C-PC purity and recovery. Results of certain experiments were used to navigate the decisions around what further sets of data were needed and what work in the laboratory would be required to obtain them.

4.2 Experimental approach

The full approach taken for generating data in the laboratory can be summarised into a few distinct blocks of experimental work.

- The first goal was to investigate the leaching profile of dried *Spirulina* powder to understand the amount of time required to allow the majority of the C-PC to be released from the algal cells into the buffer solution.
- The next step was to run tests on the existing aspects of the CeBER patented process, such as the performance of the PEG-maltodextrin ATPS, to contextualise the pretreatment and determine if it is able to improve the performance of the C-PC purification.
- After acquiring this context, it was then possible to look at aspects of the pretreatment – specifically the adsorbent concentrations and adsorption time and pH – to determine how they each impacted process performance and to find combinations of variables which optimised the purity of the C-PC produced.
- With this information, it was then possible to test the impact of the pretreatment step in the context of the entire process by measuring the performance of the ATPS and precipitation stages once the adsorption had been performed on the crude extract and determine an optimal process configuration.
- The last set of experimental work looked at aspects of this optimal process such as its effectiveness after changing the physical setup of the adsorption step, and its robustness to differing *Spirulina* feeds.

4.3 Experimental methodology

4.3.1 Materials

Dried Spirulina powder

The dried *Spirulina* used for the majority of the experimental work was purchased from Carbocraft (referred to as CC *Spirulina*), a local South African supplier who imports the powder from China. The powder had a reported C-PC content of between 8% and 13%.

Other samples of *Spirulina* powder were used for both the investigation into leaching behaviour as well as when testing process robustness. For the leaching experiments, the three other *Spirulina* powders were:

- a sample acquired from Brenntag (BT), a South African supplier who sourced the powder from China
- a sample acquired from Green Create Nutra (GCN), a *Spirulina* producer in Mauritius
- an organic *Spirulina* purchased from a supplier in India (referred to as Indian *Spirulina*)

When testing the robustness of the process, an additional three *Spirulina* products were purchased from Dis-Chem South Africa. Two of these, Health Connection Wholefoods (HCW) and Nature's Choice (NC), were products of China and the third, Raw Spirulina Powder (RSP), was a product of India.

Adsorbents

The majority of experimental work in this research project was conducted with DARCO powdered activated charcoal with a mesh size of 100 (Sigma-Aldrich: product code 242276). However, two other powdered activated charcoal samples were acquired to understand what impact a specific powder had on the adsorption process. The one sample was also purchased from Sigma-Aldrich and had the same mesh size of 100 but was not the DARCO brand of activated charcoal (product code 161551). Additionally, this other sample purchased from Sigma-Aldrich was less than half of the cost of the DARCO activated charcoal. The final sample tested was ProCarb powdered activated charcoal with a mesh size of 100-250 µm, purchased from a local South African supplier Rotocarb. Despite having a larger particle size than the two Sigma-Aldrich samples, it was still worthwhile to test this sample, as it would likely be a better representation of what would be used in a commercial C-PC purification process. Table 1 summarises the different powdered activated charcoal samples used throughout the experimental work.

Table 1: Summary of all powdered activated charcoal samples used for C-phycocyanin adsorption within the research study.

Supplier	Brand	Size distribution	Relative cost	Uses
Sigma-Aldrich	DARCO	100 mesh	100	All experimental work
Sigma-Aldrich	-	100 mesh	45	Powdered activated charcoal comparison
Rotocarb	ProCarb	100-250 µm	1.4	Powdered activated charcoal comparison

For the tests making use of the packed adsorption columns, two different sizes of granular activated charcoal were tested. Both samples were DARCO granular activated charcoal

purchased from Sigma-Aldrich where one had a particle size distribution of 4 to 12 mesh (product code 242233) and the other of 12 to 20 mesh (product code 242241).

Low molecular weight chitosan was purchased from Sigma-Aldrich (product code 448869) and used for all experimental work.

It was discussed in Chapter 2.3.2 that properties of both activated charcoal and chitosan products have an impact on their performance. For activated charcoal particles, BET surface area, functional groups and the pore size distribution all have an impact on how effective they are as adsorbents. On the other hand, chitosan's effectiveness is often determined by its degree of deacetylation. It is therefore important to note that for all the activated charcoal and chitosan samples used in this research, none of these properties were specified by the suppliers and no analysis was done to characterise them in this manner. This is naturally something that must be kept in mind and any results generated could, in theory, be unrepresentative of these adsorbents in general and apply only to the specific samples used.

General chemicals

The sources of all other chemicals used will be named when the chemicals are mentioned in the relevant sections of the methodology. All water used in this project as part of C-PC purification was obtained from a Millipore Elix 3 electro-deionisation and reverse osmosis unit. The only exception to this was the water used as part of the diafiltration step of the ultrafiltration stage where this ultrapure (type 1) water was taken from a Millipore Milli-Q Direct-Q 8 UV Water Purification System.

4.3.2 Experimental methods

Each stage of the C-PC purification process is described in the following sections. Figure 53 in Appendix A4 represents the general flow of the purification process with each individual unit operation, however it must be noted that each individual experimental run did not necessarily include all aspects of the process. The methods followed for specific sets of experiments – such as the investigation into leaching duration, the adsorption optimisation, the adsorption runs using a packed column of activated charcoal, and the test of process robustness using different *Spirulina* samples – are also defined in their own individual sections.

Unit operations

Cell disruption and leaching

Cell disruption was performed by suspending the dried *Spirulina* powder into a 5 $g.L^{-1}$ citrate buffer at a concentration of 10% by volume, i.e. 100 g of *Spirulina* was added to a total buffer volume of 1 L in a 3 L plastic beaker. The citrate buffer was composed on a mass basis of 92% of sodium citrate dihydrate and 8% of citric acid monohydrate, both purchased from Merck, to try and achieve a pH of 6 (Hockey, 2022). The weighing out of buffer components and *Spirulina* powder, as well as all other weighing required for this research project, was done using a Radwag PS 4500.R2 balance.

Once the *Spirulina* powder was mixed in the buffer, disruption of the cells took place. This was achieved via bead milling, where 1 kg of 1 mm borosilicate glass beads (acquired from Sigma-Aldrich) were added to the beaker. The milling took place by using a Dillon RDM100A 14" drill press overhead stirrer spinning at 180 rpm for 15 minutes. Once this step was completed, the beads were removed by pouring the sample through a 180 µm aperture sieve into a clean 3 L beaker. The sample of disrupted *Spirulina* was then left at 4°C for approximately 24 hours to allow the C-PC to leach into the buffer solution.

For certain sets of experiments, a slightly different method was used where this approach excluded the step of milling the suspended *Spirulina* powder with the glass beads. Therefore, once the *Spirulina* powder had been mixed into the citrate buffer at a concentration of 10%, the sample was left at room temperature overnight (between 16 and 18 hours) to provide enough time for C-PC to leach out of the cells.

Cell debris removal

Cell debris removal was performed after the leaching period in the same manner, regardless of whether or not bead milling took place. This was completed by pouring the leached solution into Beckman Coulter 500 mL centrifuge bottles and centrifuging for 30 min with a set temperature of 24°C at a speed of 7000 g or 10000 g, using either a Beckman Coulter Avanti J-25 centrifuge or an Avanti J-E centrifuge. The result of this centrifugation can be seen in Figure 7. The blue supernatant from each of the centrifuge bottles was poured off into a 3 L beaker. This supernatant was the crude extract to be used in the next steps of the purification process. The green cell debris pellet remaining in the bottles was discarded.

Figure 7: Example of blue supernatant (the crude extract) separated from green biomass pellet after centrifugation.

Adsorption

Adsorption to purify the crude extract was conducted using two methods. The first method was to directly add powdered activated charcoal and chitosan into suspension. This was used for the initial screening experiments as its setup allowed for a greater degree of control and uniformity between runs. The second approach consisted of passing the crude extract through a column packed with granular activated charcoal particles.

Adsorption performed in suspension

Adsorption using both activated charcoal and chitosan in suspension was conducted directly on the crude extract. The adsorbents were mixed into suspension at different compositions, where the exact adsorbent concentration used was dependent on which set of experiments was being performed. The range of chitosan concentrations added on a mass basis was between 0.1% and 17%, while for activated charcoal this was between 3% and 15%, again by weight. In certain experiments, chitosan was first dissolved to a concentration of 1% in a solution of 1% acetic acid (glacial acetic acid purchased from Sigma-Aldrich) and added in this form to the crude extract. The adsorption step was either conducted in 50 mL falcon tubes

or in 500 mL centrifuge bottles with working volumes of approximately 40 mL and 100 mL, respectively.

Certain adsorption experiments took place where the solution to be purified had its C-PC concentration reduced to half of its original value by diluting the crude extract with an equal volume of 5 $g.L^{-1}$ citrate buffer. In this case, the amount of chitosan was still added based on the total volume, but the quantity of activated charcoal used was scaled down to account for the reduction in C-PC concentration.

The adsorbents were left to mix in the crude extract on a shaking platform at 100-125 rpm for a specific amount of 'contacting' time, with the standard time being 10 minutes. After the contacting time, the activated charcoal and chitosan were removed along with adsorbed impurities by centrifuging at either 4000 rpm for 20 minutes in 50 mL falcon tubes using a Hettich Universal 320 benchtop centrifuge or by using the Avanti J-E or Avanti J-25 centrifuges for 30 minutes at 10000 g. The results of the centrifugation can be seen in Figure 8 where, as with the cell debris removal step, the purified blue supernatant was poured off for further processing while the residual pellet was discarded.

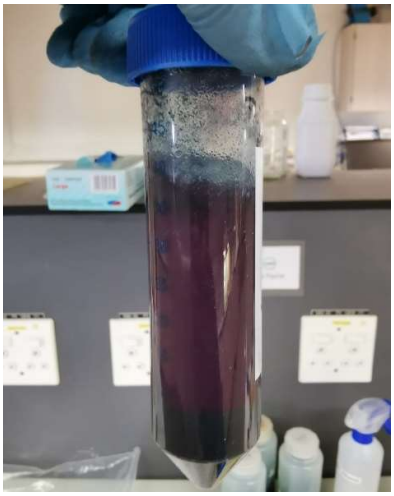

Figure 8: Adsorption step after centrifugation with the blue supernatant above the dark pellet.

Packed adsorption column

As an alternative to mixing the powdered activated charcoal into a suspension, columns were packed with granular activated charcoal over which the C-PC containing solution would be passed. Glass columns with a volume of 100 mL (height of approximately 200 mm and diameter of approximately 25 mm) were packed with 14.87 g of either 8 to 12 mesh or 12 to 20 mesh granular activated charcoal. Duplicate columns were set up for each activated charcoal particle size so that the experimental repeats could be conducted within the same run.

Figure 9: Representation of packed adsorption columns connected to pump with columns seen in more detail.

The columns were orientated vertically in a wooden box with the charcoal particles held in place above and below by 1 mm borosilicate glass beads and Saarchem Unitek glass wool. The setup can be seen in Figure 9 with a Cole Parmer Masterflex peristaltic pump used to feed samples through Masterflex Type 14 tubing so they could flow upwards through the columns at a flowrate of either 3.373 $ml.min^{-1}$ or 1.000 $ml.min^{-1}$. Once these samples had passed through the relevant columns with approximately 20 mL of solution being retained, chitosan was added to the solution at a composition of 0.2% w/v by mixing in 20% w/v of 1% chitosan dissolved in 1% acetic acid before being mixed for a certain amount of time and centrifuged off.

Aqueous two-phase separation

Two types of ATPS were performed, where type used was dependent on the set of experiments being performed. These were a PEG-maltodextrin and a PEG-citrate ATPS. The ATPS purifications were conducted on either a crude extract, directly after leaching, or on the output of the adsorption pretreatment.

The PEG-maltodextrin ATPS was conducted using PEG 10000 (Sigma-Aldrich) at a concentration of 11% of the solution by mass and maltodextrin (Supplement World, South Africa) at a concentration of 22% as suggested by Hockey (2022), where these were added to the C-PC containing supernatant from the previous processing step. This solution was then mixed using the overhead stirrer at 180 rpm for 15 minutes to ensure that it was uniform. The mixture was then poured into 500 mL bottles and centrifuged at 7000 g for 30 minutes in the Avanti J-25 centrifuge. After centrifugation, the system separated into two layers with the PEG 10000 on top and the C-PC rich maltodextrin fraction at the bottom. The top phase was siphoned off so that the phase containing C-PC and maltodextrin could be recovered.

For the PEG-citrate ATPS, the stream to be purified was diluted so that the concentration of C-PC was reduced by a factor of 10, i.e. one part of the C-PC solution was added to nine parts of 5 $g.L^{-1}$ citrate buffer. The PEG 4000 (Merck) was added to make up 11% of the system's mass while citrate was included at 20%, where 92% of this citrate consisted of sodium citrate dihydrate and 8% was citric acid monohydrate. Once the components had been added to the C-PC containing solution, the system was mixed on a shaking platform for 20 minutes at 100-125 rpm before being centrifuged in 50 mL falcon tubes at 4000 rpm for 20 minutes in the Universal 320 centrifuge. The C-PC containing PEG phase settled at the top of the tubes after centrifugation, as seen in Figure 10, and so this top layer was siphoned off and recovered.

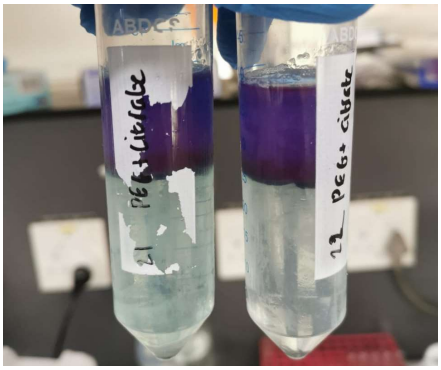

Figure 10: PEG-citrate ATPS with the blue C-PC rich PEG phase above separated from the citrate phase below.

Precipitation

Precipitation of the C-PC was predominantly done after adsorption but was also performed on a crude extract, depending on the specific aspect of the process being tested. The precipitation took place by adding a set amount of solid ammonium sulfate (Merck) to the solution feed, containing C-PC, so that it made up a desired fraction of the saturation concentration. This predominantly meant adding 357 $g.L^{-1}$ of ammonium sulfate to the initial sample volume – equating to approximately 55% of the saturation concentration at 25°C (Wingfield, in press).

After adding the salt, the entire sample was mixed on a shaking platform at 100-125 rpm for 1 hour before being centrifuged at 10000 g for 30 min in the Avanti J-E or Avanti J-25 centrifuge. The clear supernatant was poured off and discarded while the remaining blue pellet was resuspended to a known total volume using 5 $g.L^{-1}$ citrate buffer. The contrast between the pellet and supernatant can be clearly seen in Figure 11. The resuspension volume was chosen depending on the scale of the initial amount of crude extract which underwent purification.

Figure 11: Blue precipitate formed after centrifugation, separating it from the clear supernatant.

Fractional precipitation was tested too, in which lower concentrations of ammonium sulfate were used. At these lower concentrations, the C-PC would not precipitate, but other proteins would still come out of solution and could in theory be removed. For this lower precipitation, ammonium sulfate was added at 110 $g.L^{-1}$ of initial C-PC solution, equating to a concentration of about 14% of saturation. This precipitation stage would then follow the same procedure of mixing the ammonium sulfate on a shaking platform for 1 hour at 100-125 rpm before centrifuging for 30 minutes at 10000 g in the Beckman Avanti J-25 or J-E centrifuge. After the precipitation at this lower concentration, the blue supernatant was poured off and retained while the pellet was discarded. When taking this supernatant on to the second precipitation to precipitate the C-PC, more salt was added to increase the ammonium sulfate concentration from its initial concentration of 110 $g.L^{-1}$ in the initial solution to the target of 357 $g.L^{-1}$ (i.e. only 247 grams need to be added for every litre of solution).

Microfiltration

The resuspended pellet from the 55% ammonium sulfate precipitation was taken through a microfiltration step to remove any unwanted contaminating microorganisms still present with the C-PC containing solution, and thereby prepare the sample for ultrafiltration. This was done using vacuum, dead-end filtration on a 47 mm diameter filter. Microfiltration was done in three stages at reducing filter pore sizes. The first filtration took place through Whatman Type 1 filter papers with a pore size of 11 µm. The second step of the filtration train was passed through Whatman GF/A glass microfibre filter papers containing pore sizes of 1.6 µm. The last stage of this aspect of the process, and the only one of these three steps which is actually an example of microfiltration, was passing the permeate of the glass microfibre filters through sterile FILTER-LAB MCE 0.20 µm or 0.45 µm membrane filter papers.

Ultrafiltration

After passing through microfiltration, the purified sample could then be sent into the ultrafiltration step to desalt the solution. Ultrafiltration was conducted using a Pall Minimate Tangential Flow Filtration System using a Minimate Omega 50 kDa molecular weight cut-off Membrane capsule. A Cole Parmer Masterflex peristaltic pump was used to feed the solution through the filtration unit at a constant flowrate of 40 $mL.min^{-1}$ and a cross-membrane pressure of 2 bar was used to retain the C-PC on the membrane and allow smaller proteins and other contaminants to pass through. Figure 12 shows this system in operation, with the pump feeding the C-PC solution through the membrane capsule.

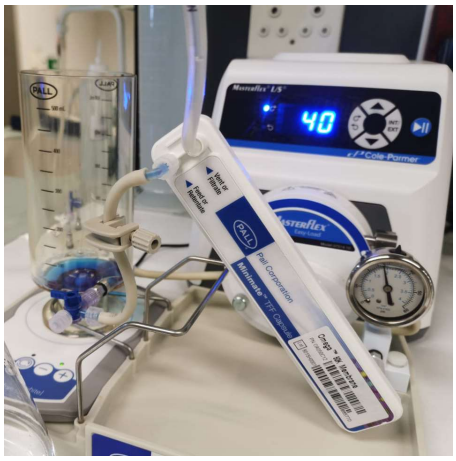

Figure 12: Set up of the ultrafiltration step using a 50 kDa Omega membrane capsule.

Initially, the volume of the feed solution was reduced to approximately 20 mL to concentrate the C-PC. Continuous diafiltration was then used to reduce the concentration of ammonium sulfate by feeding through five volumes of ultrapure water – relative to the solution of C-PC – to replace the high-salt solution. The diafiltered and concentrated C-PC was recycled through the system during these stages before it could then be recovered by flushing the membrane with water at the same flowrate of 40 $mL.min^{-1}$.

Freeze drying

Freeze drying was performed after ultrafiltration to generate C-PC product in a powdered form, as would be done in a commercial process for ease of packaging, storage and transport. An Instruvac freeze dryer was used to prepare the samples, where the drying took place under vacuum conditions at a temperature of -35°C for a period of 72 hours.

Blocks of experiments

A summary of all experimental blocks performed is provided in Table 2.

Table 2: Summary of all experimental blocks performed within the project as well as the rationale behind their inclusion.

Experiment topic	Experiment blocks and associated purpose
Leaching tests	Testing the optimal time, concentration and method for leaching C-PC from different forms of *Spirulina*.
Individual adsorbents	Individually purifying C-PC using chitosan and activated charcoal.
Adsorbent combination	Using chitosan and activated charcoal together to purify C-PC, initially at the same concentrations which had already been tested and then using a central composite design. Different samples of activated charcoal were also tested to compare their effectiveness.
Adsorption followed by ATPS	Including the adsorption pretreatment before an ATPS step to see what impact the adsorption had on its performance.
Proposed adsorption process	Testing a new proposed adsorption process to determine if it produced cosmetic-grade C-PC. The process was adjusted by varying the order of unit operations, including activated charcoal in the form of a packed column and testing the process on different sources of *Spirulina*.

Leaching investigation

Using a new sample of CC *Spirulina*, it was necessary to investigate its leaching profile to understand how much time was required for the C-PC to be released from the cells into the buffer solution. The cell disruption protocol making use of bead milling as described previously was followed. The milled sample was stored at 4°C with regular samples taken every 2 hours for the first 30 hours (apart from hours 10 and 12) and then again at hours 42, 44, 48 and 50. Each sample was placed in a 15 mL falcon tube and spun at 4000 rpm for 15 minutes in the Universal 320 centrifuge. The blue supernatant was poured off and recovered to be tested for C-PC purity and concentration to understand how these changed over time, while the green pellet was disposed.

A separate leaching test was conducted on the CC *Spirulina* as well as the three other sources of *Spirulina* (BT, GCN and Indian), each being leached at a few different concentrations. This test was done without a cell disruption step so the performance of the process without bead milling could be better understood, and it could be determined whether the algal drying process by the manufacturer had disrupted the cells sufficiently to allow C-PC to be released into the solution. Additionally, testing the different samples provided an indication of how variable the leaching period could be for different feed sources. This experiment considered different initial starting concentrations of the *Spirulina* powders, namely 10 $g.L^{-1}$, 20 $g.L^{-1}$, 40 $g.L^{-1}$, 100 $g.L^{-1}$ and 200 $g.L^{-1}$. The appropriate amount of powder to make up these concentrations was weighed out and added to 40 mL of 5 $g.L^{-1}$ citrate buffer in a falcon tube of 50 mL total volume. The samples were placed at room temperature on a shaking platform rotating at 100-125 rpm. A sample was taken in a 1 mL Eppendorf tube every hour for the first six or seven hours with a further sample taken at 24 hours. The samples in the Eppendorf tubes were centrifuged in an Eppendorf MiniSpin Plus centrifuge at 12000 g for 10 min before the blue supernatant was recovered and measured for C-PC purity and concentration, using the method described in Chapter 4.3.3.

Adsorption optimisation

Different aspects of the adsorption pretreatment step were of interest in this study, and resulted in a few different experimental procedures and experimental designs being followed.

Chitosan and activated charcoal performance comparison

Experiments were conducted to compare the performance of the chitosan and activated charcoal when added as adsorbents individually. This was done by conducting the leaching stage at a pH of 6.7, where this pH was reached by adjusting the composition of the citrate buffer. The buffer concentration was still maintained at 5 $g.L^{-1}$ but sodium citrate dihydrate was added at a mass composition of 97% while the citric acid monohydrate was added at 3% by mass. Once, the cell debris was removed, the adsorbents were added individually at a composition of between 0.1% and 17% for chitosan and 3% and 15% for activated charcoal, both on a mass basis. The full summary of the exact concentrations of each adsorbent used can be found in Chapter 6.2 of the results. The mixing of the adsorbent took place for 10 minutes before centrifugation at 4000 rpm for 20 minutes in 50 mL falcon tubes, using a Hettich Universal 320 benchtop centrifuge. Additional tests were performed by adding both adsorbents together, where activated charcoal was added at either 0.5% or 2% by mass and activated charcoal was added at 6% or 10% by mass. Once the adsorbents were in the suspension, the mixing and centrifugation took place as described previously.

Different sources of activated charcoal samples were also investigated at certain adsorbent concentrations. The other sample purchased from Sigma-Aldrich was tested along with the

one obtained from Rotocarb, and these were compared to the DARCO activated charcoal used in all other experiments. The same protocol was followed for these different samples as has already been described.

Adsorption optimisation using central composite design

A central composite design was used to test the impact of four different factors – chitosan concentration, activated charcoal concentration, adsorption time and pH – on the performance of the pretreatment step. Each of the variables was tested at a number of levels to understand if there would be any maxima or minima, rather than simply considering high and low values of each factor. The central composite design was chosen as it was able to test four factors at several levels without requiring the impractical number of runs which would have been needed for a full factorial design. Therefore, each variable had a low, centre and high level along with star points, where these star points were calculated based on the difference between the low and high points as well as a rotatability factor of 2. A full breakdown of the set of runs for the central composite design, as well as the logic behind the choice of values for each variable is presented in Chapter 6.4 and Table 5 with six runs performed on the centre point. Each run followed the same general method, as follows. An initial cell disruption and leaching step including bead milling was performed as described previously, but with a slight alteration. This alteration was to accommodate the testing of adsorption pH by slightly adjusting the relative proportions of citric acid monohydrate and sodium citrate dihydrate used in the 5 $g.L^{-1}$ citrate buffer. The calibration curve (which can be found in Appendix A2) shows how the pH of the system was changed based on the amounts of the two components in the buffer, while still maintaining an overall citrate concentration of 5 $g.L^{-1}$. However, the leaching still took place for 24 hours at 4°C and cell disruption was performed in the same manner for 30 minutes at 7000 g with the supernatant poured off from the rest of the cell debris.

The required amount of activated charcoal and chitosan, as needed based on the specific run being performed, were added to the crude extract in a 50 mL falcon tube before being mixed on an orbital shaking platform at 100-125 rpm for the set amount of time. Centrifugation was then performed using the Universal 320 centrifuge at 4000 rpm for 20 min before the supernatant was again recovered by separating it from the pellet remaining in the tube.

Test of different samples of Spirulina powder

Each *Spirulina* sample (the standard CC as well as the HCW, NC and RSP) was leached at a concentration of 100 $g.L^{-1}$ by adding 3 g of the dried powder in a 50 mL Beckman centrifuge tube to 30 mL of 5 $g.L^{-1}$ citrate buffer. Once the powder had been suspended, each was left overnight to leach before being used in further purification experiments. For each of the powders, this was done in triplicate for both low and high concentration samples of C-PC.

4.3.3 Analytical methods

C-phycocyanin purity, concentration and recovery

The approach to determine C-PC purity and concentration – and therefore also recovery – relied on taking optical density measurements on a spectrophotometer and using these to calculate the desired properties. All absorbance readings were taken on either a Genesys 10S UV-Vis spectrophotometer or a BMG LABTECH FLUOstar Omega microplate reader. The readings taken on the UV-Vis Genysis were at wavelengths of 280 nm, 620 nm and 650 nm on a BRAND GMBH + CO KG UV transmissive Perspex cuvette. For the Omega microplate reader, measurements were taken using a Corning UV 96 microwell plate on a spectrum of wavelengths between 260 nm and 750 nm. For each optical density reading, the samples

were diluted using citrate buffer to fall within the linear range of absorbances and compared to a citrate buffer blank. The calibration curves for the dilutions at the crucial wavelengths of 280 nm, 620 nm and 650 nm can be seen in Appendix A1.

C-phycocyanin purity

The C-PC purity measurement takes into account the ratio between the maximum absorbance of C-PC to the absorbance of all proteins. This is given by Equation 4.1, as was also presented in Chapter 2.2.4.

$$Purity_{C-PC} = \frac{OD_{620}}{OD_{280}} \quad 4.1$$

C-phycocyanin concentration

Equation 4.2 was used for the calculation of C-PC concentration. This quantification method by Yoshikawa and Belay (2008) was both calibrated relative to a known C-PC sample and developed using extinction coefficients from a sample extracted from *S. platensis*. Other methods, such as the one by Bennett and Bogorad (1973) (Equation 2.3), though commonly used in literature, determined the extinction coefficients from other microorganisms and were thus deemed to not be as appropriate for use in this project.

$$C_{C-PC}[\text{mg.m}L^{-1}] = 0.162 \cdot OD_{620} - 0.098 \cdot OD_{650} \quad 4.2$$

C-phycocyanin recovery

The recovery of C-PC for each stage of the downstream process was determined using Equation 4.3:

$$Recovery_{C-PC}[\%] = \frac{V_f \cdot C_{C-PC,f}}{V_i \cdot C_{C-PC,i}} \cdot 100 \quad 4.3$$

Where V_i and $C_{C\text{-}PC,i}$ refer to the total volume and concentration respectively of C-PC solution prior to the purification stage, and V_f and $C_{C\text{-}PC,f}$ refer to the purified solution total volume and C-PC concentration. Volumes were either measured with measuring cylinders or by determining the mass and assuming the volume based on a standard density.

C-phycocyanin E-value

As discussed in Chapter 2.2.4 of the Literature Review, the E-value is an important characteristic for marketing C-PC, particularly for products which will be used in the food and cosmetic industries. It was measured by making a 1% solution of dried C-PC powder in deionised water. This 1% solution of C-PC was then measured on a spectrophotometer, with the reading at 620 nm taken as the E-value.

Microbial contamination

The level of bacterial contamination is an important quality of a C-PC product being sold commercially and therefore this was something that needed to be quantified as part of the purification process. The contamination was measured using a serial dilution and spread plating technique to develop a reasonable understanding on the number of colony forming units (CFU) per gram or millilitre of C-PC. This quantification approach could be used on the initial sample of *Spirulina* biomass as well as after adsorption to understand what levels of contamination were present prior to the downstream process, and how effective the stage was at reducing the numbers of CFU to within the desired levels.

The serial dilutions were done with potassium buffered saline (PBS) using nutrient agar plates on which the colonies could grow. Once the serial dilutions (done in duplicate) and spread plating were completed, the plates were stored at 37°C for approximately 72 hours. All this plating work was done in a sterile environment – underneath a horizontal laminar flow hood – and all buffers and media required were autoclaved at 121°C for 20 minutes before use.

Analysis of data and statistical error

The majority of figures included throughout this report were generated using Microsoft Excel Version 2211 Build 15831.20208. The only exceptions to this are the response surface curves generated as part of adsorption optimisation which were produced using *Statistica* Version 14.0.0.15.

Statistical uncertainty of results was represented by standard error of either analytical repeats – where multiple absorbance readings were taken on the same sample – or of repeats of experimental runs. When error bars are presented on figures or the uncertainty sign ± is used in tables, it will be stated whether these are based on analytical or experimental repeats.

5 Results: Leaching Experiments

5.1 Introduction

As has already been discussed, the overall aim of this research project is to understand what benefit can be gained from including an adsorption pretreatment into a C-PC purification process. However, before the adsorption could be tested, the cell disruption and leaching steps of the process needed to be better understood for the specific *Spirulina* sample used in this research.

The goal of the leaching is to allow the intracellular C-PC protein to move from within the algal cells into the buffer solution, from where it can be recovered. The amount of time required for this leaching to take place is dependent on the nature of the *Spirulina* feedstock. Aspects such as the *Spirulina*'s strain, original source and cultivation method, whether it is present as a wet biomass or dried powder, the drying method used or the cell disruption technique can all impact how easily the C-PC is able to leach into solution. Naturally, the goal of leaching is to try and recover as much of the C-PC as possible and therefore the leaching time needs to be sufficiently long in order for this to occur. However, if the period of leaching is too lengthy, not only does this potentially reduce the viability of the process commercially but there is the possibility of increasing the number of other proteins moving into the solution – decreasing the purity of the C-PC in the crude extract and making it more difficult to successfully purify it in the downstream steps. Additionally, a long leaching time also creates an opportunity for undesired microorganisms – either present from the native environment of the *Spirulina* or introduced into the process – to survive in the solution and increase the level of contamination. Therefore, the leaching profile of the *Spirulina* used for this research project needed to be understood so that an optimal amount of time could be chosen.

5.2 Leaching of bead milled *Spirulina* sample

5.2.1 C-phycocyanin concentration

The results of the first investigation into the leaching performance of C-PC can be seen in Figures 13 and 14. These figures display the change in C-PC concentration and purity as a function of time. To perform the test, two samples needed to undergo leaching in order to fill any gaps in the data which would have been present due to the overnight nature of the study. Sample 1 was started in the morning and Sample 2 was set up in the afternoon. The leaching was conducted at 4°C using a specific concentration (100 $g.L^{-1}$) of CC *Spirulina* which had undergone cell disruption by bead milling.

The results clearly show an increase in concentration from the start of the experiment until the end point at 50 hours. The initial concentration of C-PC, after cell disruption had taken place but before any time for leaching, was only between 2.30 and 2.50 $mg.mL^{-1}$. This increased to a maximum value of 5.39 ± 0.10 $mg.mL^{-1}$ after 48 hours. This demonstrates that this particular *Spirulina* powder required a fairly lengthy period of leaching and that the 2 hours used in the investigation by Hockey (2022) would not be sufficient for this sample. However, despite 48 hours resulting in the highest concentration of C-PC present in the buffer, this was not necessarily the most optimal time period in terms of maximising the efficiency of the process.

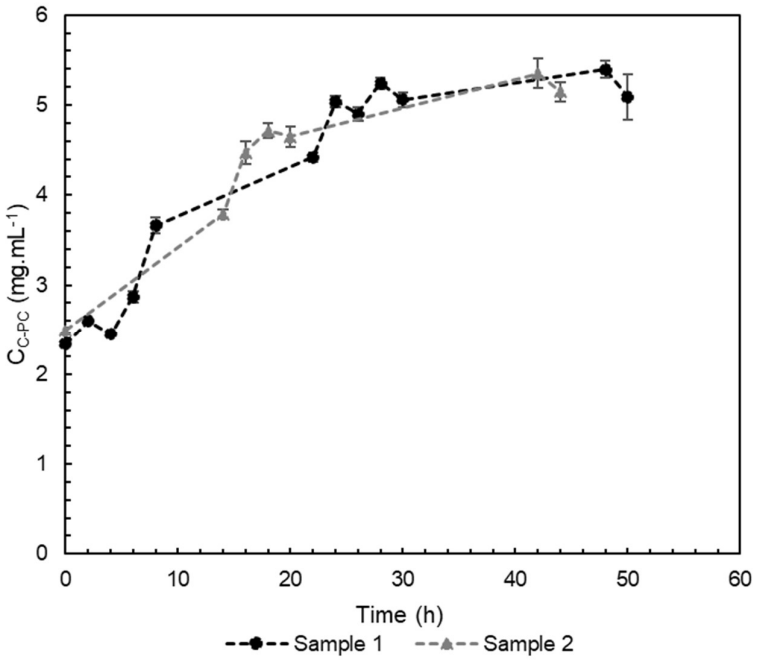

Figure 13: Change in C-PC concentration over time during leaching investigation. Error bars represent the standard error on repeat analysis. Sample 1 refers to *Spirulina* sample leached in the morning while Sample 2 was leached in the afternoon to fill in any gaps during the overnight study.

5.2.2 C-phycocyanin purity

What also needed to be considered was the change in purity of C-PC over time, with this seen in Figure 14. As with the concentration profile, the C-PC purity showed a definite increase over the time period considered. The initial value of 0.348 ± 0.008 increased to a maximum of 0.464 ± 0.003 at 24 hours. However, what Figure 14 also shows is that from about 14 hours, the purity reached a value of 0.44 and remained fairly constant from then on. Therefore, there was no significant increase in purity which could be achieved from leaching for a longer period, but there also was no decrease in purity after a certain point.

However, even though leaching for 48 hours would maximise the concentration of C-PC and hence recovery, as mentioned previously this was not ideal in terms of process efficiency due to the greater potential for microbial contamination as well as reducing the amount of C-PC crude extract which could be generated in a certain time period. Therefore, a leaching period of 24 hours was used for the majority of the research work as this still resulted in a reasonable recovery of C-PC – over 95% of the maximum at 24 hours – while only requiring half the amount of time.

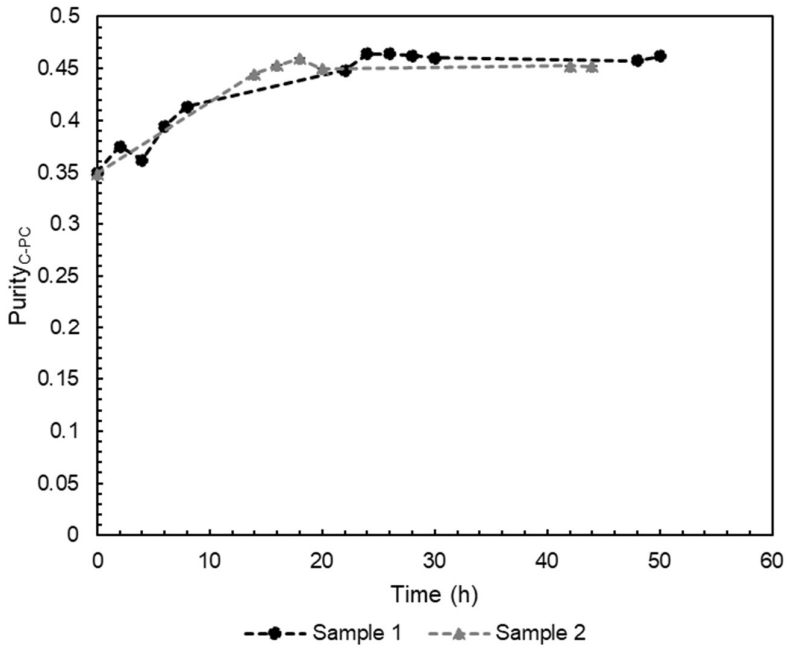

Figure 14: Change in C-PC purity over time during leaching investigation. Error bars represent the standard error on repeat analysis. Sample 1 refers to *Spirulina* sample leached in the morning while Sample 2 was leached in the afternoon to fill in any gaps during the overnight study.

5.3 Leaching investigation into different Spirulina samples

5.3.1 C-phycocyanin concentration of different samples

Further tests were done to consider other aspects of the leaching process by adjusting these variables to understand what impact they have. This encompassed the leaching of *Spirulina* from four different sources – including the CC which had already been presented – at five different concentrations, with leaching at room temperature where no cell disruption step took place beforehand. The results of these experiments can be seen in Figures 15 and 16, where the legend of each refers to the different initial starting concentration (in units of $g.L^{-1}$) of the *Spirulina* powder within the citrate buffer. The recovery of C-PC seen in the figures was calculated, taking into account the differing initial concentrations of *Spirulina* used, by representing it as a percentage of the dry weight of the powder (%DW).

There are a few conclusions which can be drawn from the recovery of C-PC determined from this experiment, the most obvious of which is the poor performance of the Indian *Spirulina*. The recovery of C-PC for this sample only reached a maximum of 1.25 ± 0.00% on a dry weight basis. This is significantly lower than what was seen for the *Spirulina* purchased from BT and CC, which had a maximum C-PC recovery of 4.90 ± 0.06% and 5.24 ± 0.09%, respectively. The performance of GCN powder was even better – apart from the sample tested at an initial *Spirulina* concentration of 40 $g.L^{-1}$ which appears to have been an outlier – with a maximum C-PC recovery of 6.73 ± 0.00%. An additional conclusion which can be drawn based on the results of this experiment is that there seems to be little difference in C-PC recovery based on initial dry weight when using different concentrations of *Spirulina* dissolved in buffer. This was true in particular for the BT, CC and Indian samples. There was little significant difference for these *Spirulina* sources, where the final recovery of C-PC ranged from 4.52 ±

0.00% to 4.90 ± 0.10% for BT, from 4.22 ± 0.01% to 4.78 ± 0.00% for CC and from 0.35 ± 0.01% to 0.94 ± 0.03% for the Indian *Spirulina*. There was a slightly larger degree of variation for GCN – even after excluding the outlier concentration – with a range of C-PC recovery from 5.56 ± 0.08% to 6.73 ± 0.00%.

Another interesting aspect of this investigation was to compare the results to those seen in Figure 13. It is particularly useful to focus on the CC sample at 100 $g.L^{-1}$ as this was the same starting concentration as was used in the initial leaching test done on the bead milled *Spirulina*. When looking at this sample, after 24 hours – which, as discussed, was determined to be the optimal leaching period for this study – the recovery of C-PC was 5.20 ± 0.06% which is equal to a C-PC concentration of 5.20 ± 0.01 $mg.mL^{-1}$ based on the initial *Spirulina* dry weight of 100 $g.L^{-1}$. This is similar to what was seen in Figure 13 with a C-PC concentration of 5.04 ± 0.06 $g.L^{-1}$ after 24 hours. This indicates that there was not a substantial improvement gained from milling the algal powder and this step could potentially be excluded. However, what is also important to note is that the concentration of C-PC reduced between 24 and 48 hours when leaching at room temperature – as shown by Figure 15. This same trend was not observed when leaching at 4°C and the C-PC recovery increased between these points (Figure 13). This could be the result of degradation of C-PC at room temperature as opposed to when leaching took place at 4°C. This shows that for a longer leaching period, there is potentially an advantage to be had from leaching at lower temperatures. For the 24 hour leaching period, however, this was not evident and there was no benefit gained in terms of recovery from increasing costs by including refrigeration within this aspect of the process.

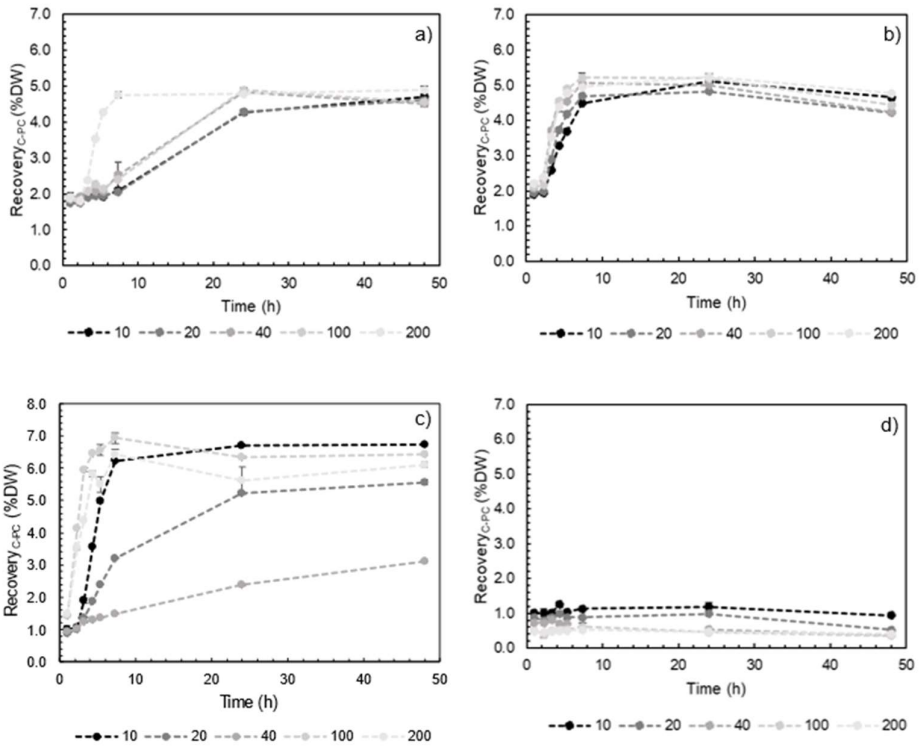

Figure 15: Change in C-PC concentration over time during leaching investigation for a) BT b) CC c) GCN and d) Indian *Spirulina* powders. Error bars represent the standard error on repeat analysis. Recovery determined as a percentage of the dry weight of the powder (%DW). The legend refers to different starting concentrations of *Spirulina* in buffer in units of $g.L^{-1}$.

5.3.2 C-phycocyanin purity of different samples

Similar trends are seen for C-PC purity as were observed for recovery. The Indian *Spirulina* again performed significantly worse than the other three samples. The maximum purity of 0.150 ± 0.002 seen after 4 hours with an initial concentration of 10 $g.L^{-1}$ was still significantly lower than the purities seen from the *Spirulina* obtained from BT, CC and GCN. Again, as with the recovery profiles, the results seen in terms of C-PC purity for BT and CC were similar, where after 24 hours they respectively ranged from 0.432 ± 0.004 to 0.501 ± 0.001 and from 0.435 ± 0.000 to 0.486 ± 0.001. There was also a similar performance seen for the different initial concentrations of *Spirulina*, although there was a trend with the BT and CC that the 100 $g.L^{-1}$ and 200 $g.L^{-1}$ samples resulted in slightly higher C-PC purities. This trend was not seen in the GCN and Indian *Spirulina*, but again there was not a significant difference between the varying concentrations, excluding the GCN outlier of 40 $g.L^{-1}$. This clearly showed that there was no limit to the efficiency of the leaching even up to a concentration of 200 $g.L^{-1}$ of *Spirulina* and that there was no benefit at lower concentrations.

This conclusion, coupled with the recovery results, implied that it was preferable to conduct the leaching at the highest possible concentration of *Spirulina* to maximise the amount of C-PC which could be recovered with the minimal amount of raw materials and smallest equipment size. This would imply that using 200 $g.L^{-1}$ as the starting leaching concentration would be optimal for the CC *Spirulina*. However, at this concentration, the solution became extremely viscous and difficult to work with. This could lead to significant issues when scaling up the process for commercial production. Therefore, the 100 $g.L^{-1}$ concentration as was applied in the first leaching test and in developing the CeBER patented process was chosen to be used in further experimental work throughout the research project.

The C-PC purity results of CC *Spirulina* leached at room temperature at 100 $g.L^{-1}$ without bead milling shown in Figure 16 can also be compared to the 4°C milled results seen in Figure 14. After 24 hours, the C-PC purity in the unmilled room temperature leachate reached a value of 0.486 ± 0.001, while the equivalent purity was 0.464 ± 0.003 with bead milling and leaching at 4°C. There is a high degree of similarity between these values – and in fact, the sample that did not undergo bead milling actually resulted in a higher purity. Therefore, the additional costs associated with creating a bead milling step and refrigerating the leaching sample at 4°C are not necessarily required for this C-PC purification process.

The purity of leached GCN samples was higher than the other three samples, where after 24 hours the purity ranged from 0.486 ± 0.000 to 0.652 ± 0.002. Although this implies there was an improvement in terms of both C-PC purity and recovery relative to the performance of CC, GCN is no longer producing *Spirulina* and therefore this sample could never be used in a commercial cosmetic C-PC production. It is because of this that CC *Spirulina* was used in the majority of remaining work. There was a fair degree of variation of C-PC purity within these samples however they were within the range seen in previous studies, where the purities reported in literature for C-PC crude extracts vary between 0.44 and 1.0. However, the difference in performance of the Indian sample in particular showed that there is a wide variation in the C-PC content of commercially available *Spirulina* products and therefore this is something that needs to be taken into account when attempting to implement larger scale production.

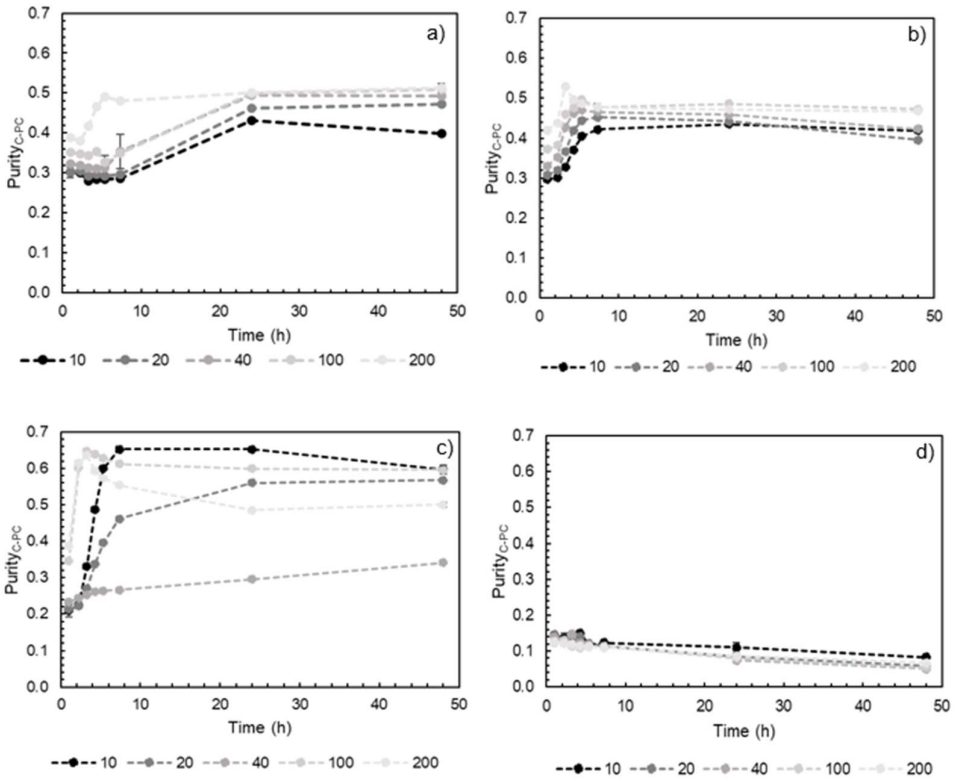

Figure 16: Change in C-PC purity over time during leaching investigation for a) BT b) CC c) GCN and d) Indian *Spirulina* powders. Error bars represent the standard error on repeat analysis. The legend refers to different starting concentrations of *Spirulina* in buffer in units of $g.L^{-1}$.

5.4 Conclusions

The aim of this section of the research project was to better understand the leaching aspect of the existing process. This initially consisted of running tests on the cell disruption and leaching stage of the process to determine an optimal leaching time for the sample of CC *Spirulina* used in the experimental work. It was determined that when leaching at 4°C after cell disruption, a time period of 24 hours would be optimal. This was decided because 24 hours was found to provide a good balance between C-PC recovery – where the concentration of 5.04 ± 0.06 $mg.mL^{-1}$ was 95% of the maximum recovery – and reducing the process time to limit the potential for bacterial contamination. Additionally, 24 hours also led to the maximum observed C-PC purity of 0.464 ± 0.003.

The impact of using different *Spirulina* samples on the leaching step was tested – each at five different initial biomass concentrations. The impact of not bead milling the algal powder was also considered. The results, in terms of both C-PC purity and recovery, showed that the source of the *Spirulina* can have a significant impact on the effectiveness of the leaching. The Indian *Spirulina* consistently had the lowest purity and recovery throughout the period of leaching, while using the GCN sample from Mauritius generally resulted in slightly higher purities and recoveries than the CC *Spirulina*. It was also shown that adjusting the initial concentration of *Spirulina* in the citrate buffer before leaching (from 10 $g.L^{-1}$ to 200 $g.L^{-1}$) did not impact the purities and recoveries achieved to any noticeable degree. Therefore, it was decided to continue to leach at 100 $g.L^{-1}$ for the remainder of the experimental work, as was

done in the development of the patent. This concentration maximised the amount of C-PC generated in each leaching step, while avoiding the issues, such as high viscosity, of leaching at 200 $g.L^{-1}$. Finally, by comparing the results of this experiment to the test where bead milling had taken place, it can be concluded that the cell disruption did not significantly improve the output of the leaching step. The concentration and purity achieved without bead milling after 24 hours of 5.20 ± 0.006 $mg.mL^{-1}$ and 0.486 ± 0.001 respectively, were very similar to what was achieved when cell disruption took place, implying the algal powder is likely sufficiently disrupted through the drying process for the bead milling step to be omitted when using the CC *Spirulina* in any commercial process.

6 Results: Adsorption Pretreatment

6.1 Introduction

Now that the leaching step was better understood and an optimal time period for leaching had been identified for further experiments, the focus moved to the adsorption pretreatment itself. This initially consisted of simply adding each of the adsorbents, chitosan and activated charcoal, to a C-PC crude extract individually, and determining the impact each had on C-PC purity, concentration and recovery where the purity is an expression of the amount of C-PC present in the sample relative to other proteins as defined in Equation 2.1. Following on from this, the next step was to add the two adsorbents in combination with one another to evaluate their combined performance and to determine if this resulted in an improved process. By adding chitosan and activated charcoal together at the same concentrations as was previously done in the individual tests, a direct comparison could be made between their effectiveness when used in combination and when used separately.

In order to add another level of complexity to the adsorption step, the impact of adjusting the pH and contacting time – in combination with varying adsorbent concentrations – was also tested by using a central composite design. These factors were considered as they had previously been shown in literature to have an impact on C-PC purification through adsorption, and therefore the goal of this investigation was to attempt to optimise the output of the pretreatment in terms of C-PC purity and recovery. The advantage of using this central composite design was that it considered the impact of all these factors in combination with one another and any interactions between the variables could be identified.

Finally, a simple test was done to assess the contamination levels in the purified solution after adsorption, thereby to determine how effective pretreatment with the two adsorbents was in reducing the quantity of microorganisms present in the crude extract.

6.2 Individual adsorbents

6.2.1 Chitosan

To begin the investigation into the adsorption, it was decided to try and test the performance of chitosan and activated charcoal individually to fully understand the effects of each. The results of this investigation into activated charcoal and chitosan working as the sole adsorbents for C-PC purification can be seen in Figures 17 to 20. The results seen in Figure 17 clearly indicate that increasing the amount of chitosan added to the crude extract results in an improvement in the purity of C-PC generated after the adsorption. Adding the lowest amount of chitosan on a mass basis of 0.1% resulted in the lowest final purity of 0.475 ± 0.001, while when adding chitosan at 17% per mass, the purity reached a maximum of 0.750 ± 0.001.This was likely due to a greater total area being available for adsorption as more chitosan was added, and a higher number of contaminating proteins could therefore be removed, improving the purity. Attempting to increase the chitosan concentration beyond this point resulted in the centrifuged pellet trapping the entire liquid volume and no supernatant was obtained, hence 17% was the maximum amount of chitosan added. It is also worth noting that the increase in purity was greater at the lower concentrations of chitosan, i.e. at 5% chitosan the purity was improved to 0.615 ± 0.001 while increasing it another 5% to 10% by mass only slightly increased the C-PC purity to 0.652 ± 0.002. This implies that by this point, most of the impurities which could be adsorbed were already removed by the chitosan and so

adding higher quantities of chitosan only had a marginal impact on the improvement in C-PC purity.

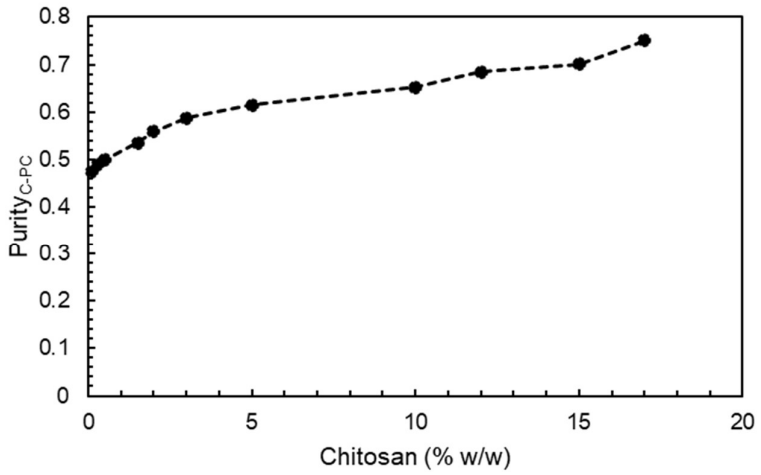

Figure 17: Impact of varying chitosan content on C-PC purity. Error bars represent the standard error on repeat analysis.

When considering the C-PC concentration and recovery based on chitosan content, as represented by Figure 18, a different set of conclusions can be drawn than those relating to the purity. Adjusting the chitosan content did not seem to have a significant impact on the concentration of C-PC after adsorption. Despite the wide range of chitosan percentages used, the C-PC concentration only varied between the values of 4.97 ± 0.04 $mg.mL^{-1}$ and 5.93 ± 0.07 $mg.mL^{-1}$. This implies that the chitosan was able to selectively remove unwanted contaminants from the solution, while leaving the C-PC free to pass through this processing step. Despite the concentration of C-PC not being significantly affected by the changing chitosan amounts, the recovery of the pigment showed a sharp decrease as more chitosan was added to the crude extract. This was seen in the lowest recovery of C-PC of 12.1 ± 0.2% being observed at the maximum chitosan content of 17% by mass, and almost 100% of the C-PC being recovered at the lowest mass fractions of chitosan The reason for this was the use of dead-end centrifugation as the method for removing the purified supernatant from the adsorbent pellet. When centrifuging in this manner, the pellet will always have a certain moisture content associated with it, and hence a significant amount of the desired liquid was retained within the pellet. Naturally, as more of the chitosan was added, the pellet became larger and it was able to retain a greater volume of total liquid, and the recovery of C-PC decreased accordingly. It must be noted that this is a phenomenon consistent with this method of separation and is not specific to the use of chitosan or due to the presence of C-PC in the solution. Therefore, these low recoveries were more a function of how the adsorption step was performed than a function of the adsorbent itself. Hence, when using this approach, the increase in purity at high chitosan composition must be considered by keeping in mind the simultaneous decrease in C-PC recovery. However, by conducting a pellet rinsing step or by using an alternative method of conducting the adsorption, this issue with C-PC recovery at high concentrations of adsorbent can be overcome.

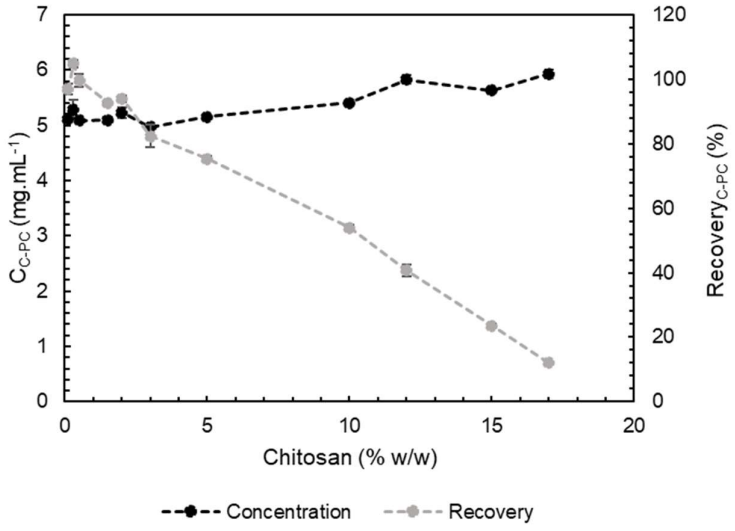

Figure 18: Impact of varying chitosan content on C-PC concentration and recovery. Error bars represent standard error on repeat analysis.

6.2.2 Activated charcoal

A slightly different trend is observed for the impact of activated charcoal on C-PC purity, seen in Figure 19, when compared to what was seen using chitosan. There is not a continual increase in purity when the concentration of activated charcoal increases and a maximum is reached of 0.682 ± 0.002 at an activated charcoal content of 9% by mass. At the low and high compositions of activated charcoal – 3% and 15% by mass – there is a reduction in C-PC purity, when compared to the maximum, to values of 0.636 ± 0.001 and 0.588 ± 0.003 respectively. The explanation behind this is that the low amounts of activated charcoal are not sufficient to take the contaminating proteins out of the solution and therefore there is only a slight increase in C-phycocyanin purity. At the higher fractions of activated charcoal, the adsorbent begins to remove substantial quantities of the desired pigment and hence the C-PC purity begins to decrease. This conclusion is further supported by the C-PC concentration results presented in Figure 20.

Both C-PC concentration and recovery decreased as more activated charcoal was added to the crude extract, as shown in Figure 20. The highest concentration and recovery values of 4.28 ± 0.09 mg.mL^{-1} and 78.5 ± 1.6% were when the activated charcoal content was at its lowest value of 3%. Additionally, the maximum activated charcoal content of 15% resulted in both the lowest C-PC concentration of 2.61 ± 0.03 mg.mL^{-1} and recovery of 25.2 ± 0.3%. The reason for the decreasing concentration of C-PC, as was briefly discussed, was because of the propensity of activated charcoal to adsorb the C-PC and remove it from the solution. Therefore, this lack of selectivity implies that activated charcoal tended to adsorb greater quantities of C-PC when it was added in increasing amounts. This reduced the C-PC concentration and had a negative impact on the recovery of the adsorption step. Further to this, adding greater amounts of solid activated charcoal to the system increased the size of the pellet after centrifugation and simultaneously enhanced its capacity to hold the desired liquid. This resulted in smaller volumes of the purified sample being retained and further reduced the overall recovery of C-PC. Again, this was a consequence of the approach taken

for the solid-liquid separation and could be avoided by adjusting the adsorption configuration, and was not necessarily a result of the specific choice to use activated charcoal.

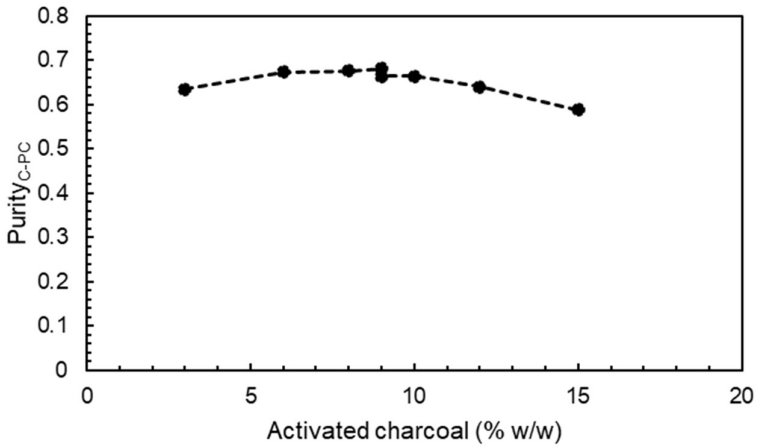

Figure 19: Impact of varying activated charcoal content on C-PC purity. Bars represent standard error on repeat analysis.

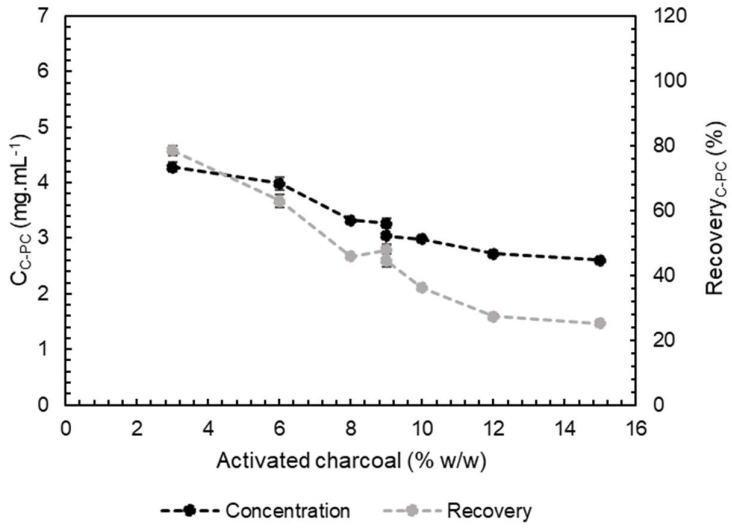

Figure 20: Impact of varying activated charcoal content on C-PC concentration and recovery. Error bars represent standard error on repeat analysis.

6.2.3 Impact of adsorbents on specific wavelengths

It is possible to further support the conclusions that have been discussed in this results section by looking at the impacts of chitosan and activated charcoal on the absorbance of the individual wavelengths – 280 nm, 620 nm and 650 nm – rather than simply focusing on the purity and concentration as a whole. As discussed in the literature review, the absorbance at 280 nm provides a good indication of the level of protein in the solution, while the absorbances

at 620 nm and 650 nm respectively should give an idea of the relative amounts of C-PC and allophycocyanin present. Therefore, looking at how the absorbances at these wavelengths change – as seen in Figure 21 and 22 – for the different amounts of the two adsorbents, should provide a further indication of the effectiveness of each in terms of C-PC purification.

The trends seen in Figures 21 and 22 reinforce the conclusions which had been previously identified from the purity, concentration and recovery data. When chitosan was used for the C-PC purification, there was a clear decrease in the absorbance readings at 280 nm as more of the adsorbent was added, indicating that proteins were being removed from the solution. This same trend was not observed at 620 nm and 650 nm, with the absorbance readings at these wavelengths remaining fairly constant. This implies that the chitosan was not removing the phycobiliproteins from the solution. Thus, the chitosan was able to selectively remove the unwanted proteins while leaving the phycobiliproteins in the solution. This is not what was seen for activated charcoal, which appeared to indiscriminately adsorb all proteins from the solution, with the absorbances at all three wavelengths reducing as more of the activated charcoal was added. What can also be concluded from analysing Figures 21 and 22 is the reduced effectiveness of the two adsorbents when they were added at high concentrations. When using chitosan, there was initially a clear decrease in the absorbance at 280 nm as more was added. However, once its mass composition reached 3% and the absorbance at 280 nm was equal to 0.746 ± 0.007, there was less of an improvement as more was added – seen in the absorbance only being reduced to 0.693 ± 0.010 at the maximum concentration of 17% by mass. A similar result was seen when activated charcoal was applied to the system. The absorbance at 280 nm was reduced efficiently from 0.589 ± 0.012 at 3% by mass to 0.441 ± 0.002 at 8% by mass. From this point however, the decrease in 280 nm was not as substantial when more of the adsorbent was added, and at the maximum mass composition of 15%, the 280 nm optical density was only 0.438 ± 0.007.

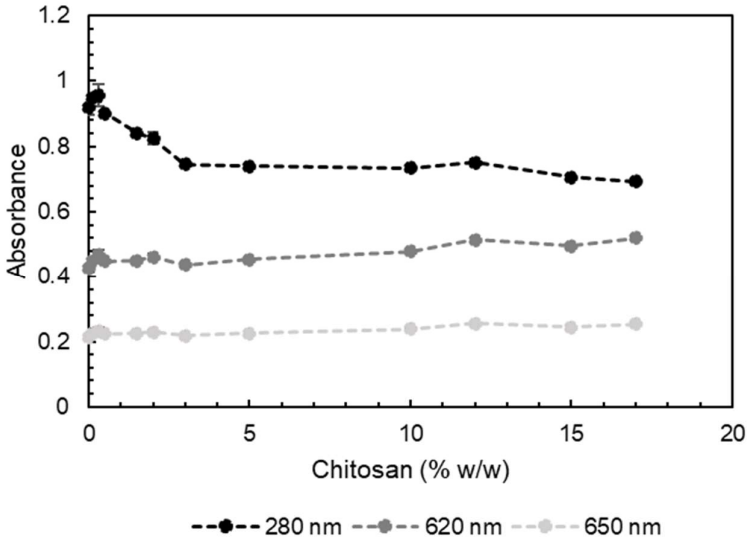

Figure 21: Impact of varying chitosan content on absorbance of the resulting solution at 280 nm, 620 nm and 650 nm. Error bars represent the standard error on repeat analysis.

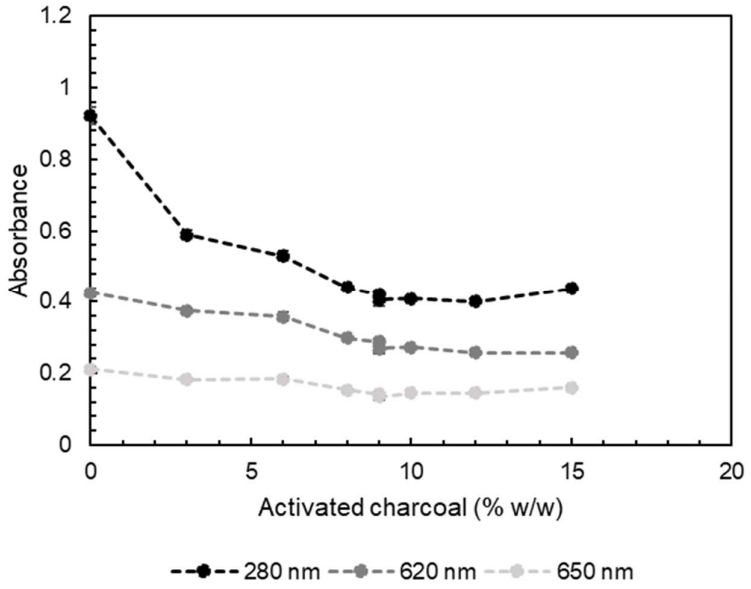

Figure 22: Impact of varying activated charcoal content on absorbance of the resulting solution at 280 nm, 620 nm and 650 nm. Error bars represent the standard error on repeat analysis.

Ultimately, this shows that at a certain point, the slight improvement in protein removal achieved by adding more chitosan and activated charcoal must be weighed against both a further reduction in C-PC recovery as well as the increased cost of the adsorbents, and hence the process overall.

6.2.4 Different samples of activated charcoal

Before considering the adsorbents in combination, it was worth considering the use of alternative samples of activated charcoal. There is a wide range of activated charcoal samples available, which can have different sizes and methods of preparation. It was therefore deemed important to investigate the relative performance of select different samples. In particular, this focused on looking at other examples of powdered activated carbon (PAC) to determine if any significant differences existed in their performance as adsorbents for this application. As presented in the methodology Chapter 4.3.1, the three powdered activated carbon products were tested. This included the DARCO 100 mesh sample which has been used previously for all the preceding experiments. Another 100 mesh sample purchased from Sigma-Aldrich (which is not part of the DARCO brand) was investigated. The third sample was a South African Rotocarb PAC with particle sizes between 100 and 250 µm. The different samples were tested at different weight fractions to also understand if this had any impact on the adsorption performance.

There was a similar performance between the two PAC products obtained from Sigma-Aldrich – namely the DARCO brand and the one named Sigma in Table 3. Although they were sourced from the same company and have the same particle size of 100 mesh, this is still a relatively surprising result, because there was a significant difference in the purchase price of the two adsorbents. The DARCO activated charcoal was more than double the cost of the other option from Sigma-Aldrich, where this is likely due to having more of its properties specified, such as the level of different impurities. This increased price and degree of specification meant that the DARCO sample was expected to have improved adsorptive properties and perform better,

although this clearly was not the case. When using the Rotocarb PAC, the C-PC purity after adsorption was lower than the purities at the equivalent mass compositions of the other samples. It must also be noted that the mesh size of 100 for the other two samples was equivalent to 149 µm, which falls in the lower range of the Rotocarb activated charcoal size distribution. Therefore, the larger particles of the Rotocarb PAC resulted in a lower available surface area for adsorption and this is likely what explains the slightly reduced purity improvement when compared to the other two samples.

What can also be noticed from the data in Table 3 is that the concentration and recovery of the Rotocarb charcoal was higher than when using the other two samples – particularly at the higher mass compositions of activated charcoal. This is likely also explained by the fact that the Rotocarb particles were slightly larger on average and therefore had a lower available surface area. This implies that there would have been less available area on which adsorption could take place and hence undesired proteins were not as effectively removed from the solution, resulting in slightly lower C-PC purities. Additionally, there was less of an opportunity for the C-PC to be adsorbed onto the surface of the activated charcoal particles, and therefore there was an increase in the C-PC concentration in solution after adsorption with the Rotocarb PAC when compared to the other samples.

Table 3: Summary of the purity, C-PC concentration and recovery achieved after adsorption with different powdered activated charcoal samples at various mass compositions. Uncertainty represented by the standard error was based on repeat analysis.

Composition (% w/w)	Brand	$Purity_{C\text{-}PC}$	$C_{C\text{-}PC}$ (mg.mL^{-1})	$Recovery_{C\text{-}PC}$ (%)
	N/A	0.446 ± 0.003	4.63 ± 0.05	N/A
6	DARCO (D)	0.697 ± 0.005	3.79 ± 0.08	60.6 ± 1.2
	Sigma (S)	0.726 ± 0.005	3.92 ± 0.04	63.0 ± 0.6
	Rotocarb (R)	0.528 ± 0.004	4.20 ± 0.22	73.8 ± 3.9
9	DARCO (D)	0.686 ± 0.008	3.39 ± 0.06	45.7 ± 0.8
	Sigma (S)	0.684 ± 0.006	3.56 ± 0.10	48.9 ± 1.4
	Rotocarb (R)	0.547 ± 0.003	4.65 ± 0.19	73.0 ± 3.0
12	DARCO (D)	0.684 ± 0.004	3.03 ± 0.07	33.3 ± 0.8
	Sigma (S)	0.653 ± 0.009	3.17 ± 0.11	35.7 ± 1.2
	Rotocarb (R)	0.557 ± 0.005	4.23 ± 0.15	58.6 ± 2.1

These conclusions are further reinforced by the full wavelength spectrum of the solution after adsorption, using the different samples. Figure 23 shows the impact each of the different activated charcoal samples had on the wavelength spectrum of the final solution when they were added at 9% by mass to the crude extract. The DARCO and other sample from Sigma-Aldrich performed similarly and were both able to effectively remove unwanted proteins from the solution, as seen in the decrease in absorbance readings at 280 nm. However, the reduction in absorbance at 620 nm when compared to the crude extract indicates they also removed C-PC from solution, resulting in the reduced concentrations reported in Table 3. When considering at the Rotocarb sample, the same trends observed in Table 3 can be seen in Figure 23. There was less of a decrease in absorbance at all wavelengths, including at 280 nm, implying that the reduced surface area was less effective at adsorbing impurities. However, this lower available surface area also explains the increased absorbance value at

620 nm – when compared to the other samples of activated charcoal – as less C-PC was removed and its concentration in the purified solution was therefore higher.

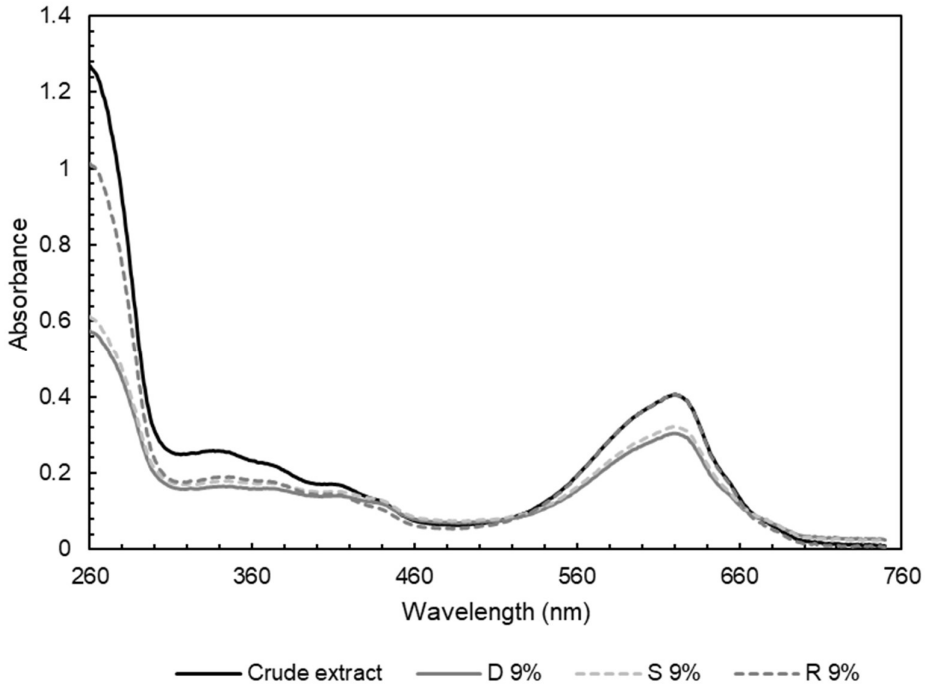

Figure 23: Full wavelength spectrum for different samples of C-PC solution purified using activated charcoal added at a mass composition of 9%. The legend refers to the different activated charcoal types tested with DARCO (D), another Sigma-Aldrich sample (S) and Rotocarb PAC (R) being used.

These conclusions follow the expected trends as presented Chapter 2.3.2. They are important to discuss, nonetheless, particularly when considering the results of the adsorption step in the context of the overall process aiming to generate cosmetic-grade C-PC. When implementing this process commercially, it is unlikely that chemicals will be purchased from suppliers like Sigma-Aldrich at a large scale due to cost considerations. It would make better economic sense to acquire the activated charcoal from a local supplier like Rotocarb, which cost less than 10% of the cheaper of the two Sigma-Aldrich products. This cost consideration is something which needs to be kept in mind when drawing any conclusions from this work about the potential viability of including the pretreatment step in a C-PC purification process.

6.3 Adsorbents used in combination

Investigating how the two adsorbents work when used simultaneously in a C-PC purification process is important because of the possibility of them having a synergistic relationship, where each one helps the other to be more efficient. A simple experiment was done to improve this understanding by adding both adsorbents to a crude extract at various concentrations that had already been tested on each of chitosan and activated charcoal individually. A summary of these results can be seen in Table 4. When trying to analyse the results of the adsorbent combinations, it is important to consider the performance of chitosan and activated charcoal

when they were added individually at the same compositions, i.e. 0.5% and 2% for chitosan and 6% and 10% for activated charcoal.

The comparison within Table 4 between the adsorbents added individually and when they were added in combination shows that there was clearly some benefit in terms of maximising C-PC purity by using the two adsorbents together. The purities reached when chitosan and activated charcoal were both used for removing unwanted proteins were much higher than when they were used individually. Additionally, the improvement from the crude extract – which had a purity of 0.470 ± 0.000 – when the adsorbents were added together was greater than the sum of the purity improvements achieved for the adsorbents individually. As an example, the maximum purity of 0.853 at 2% chitosan and 6% activated charcoal increased the purity by a value of 0.383, which was greater than the sum of the individual chitosan and activated charcoal improvements of 0.089 and 0.204. This same trend was seen at all other combinations of the adsorbents. What is also important to take away from these results is that the C-PC recovery significantly reduced as more of the activated charcoal was added. When the composition was 10% by mass of activated charcoal, the recoveries achieved were below 40%. Because recovery is an important aspect of any commercial application, this is something which needs to be carefully considered when using dead-end centrifugation to remove the adsorption pellet. Therefore, unless alternative configurations for conducting the adsorption are used, it is unlikely that such high concentrations of activated charcoal would be effective in a full scale process when used in this manner.

Table 4: Results of adsorbents used individually and in combination. Uncertainty represented by standard error based on repeat analysis.

Chitosan (% w/w)	Activated charcoal (% w/w)	$Purity_{C\text{-}PC}$	$C_{C\text{-}PC}$ (mg.mL^{-1})	$Recovery_{C\text{-}PC}$ (%)
		0.470 ± 0.000	5.40 ± 0.24	N/A
0.5		0.498 ± 0.001	5.09 ± 0.04	99.6 ± 0.8
2		0.559 ± 0.000	5.23 ± 0.10	94.0 ± 1.9
	6	0.674 ± 0.007	3.99 ± 0.12	63.0 ± 1.9
	10	0.665 ± 0.000	2.99 ± 0.04	36.1 ± 0.4
0.5	6	0.751 ± 0.004	3.51 ± 0.07	59.1 ± 1.1
0.5	10	0.770 ± 0.001	2.90 ± 0.11	36.4 ± 1.4
2	6	0.853 ± 0.004	3.62 ± 0.06	55.3 ± 0.9
2	10	0.826 ± 0.001	2.85 ± 0.08	33.6 ± 0.9

The influence of each adsorbent can be further assessed by looking at the full spectrum of wavelengths. The full wavelength spectrum is represented in Figure 24, with the chitosan and activated charcoal used separately at compositions of 2% and 6% respectively, while also being added at these same concentrations in combination with one another. The different curves in Figure 24 imply that there is some form of beneficial relationship between the two adsorbents at removing contaminants around the 280 nm wavelength. This is seen by the reduction in absorbance at this wavelength for all curves, but with the greatest decrease being achieved for the combination of chitosan and activated charcoal. This suggests that each of the adsorbents may have removed different contaminating proteins from the solution, such that more proteins were removed in total when the chitosan and activated charcoal were both used.

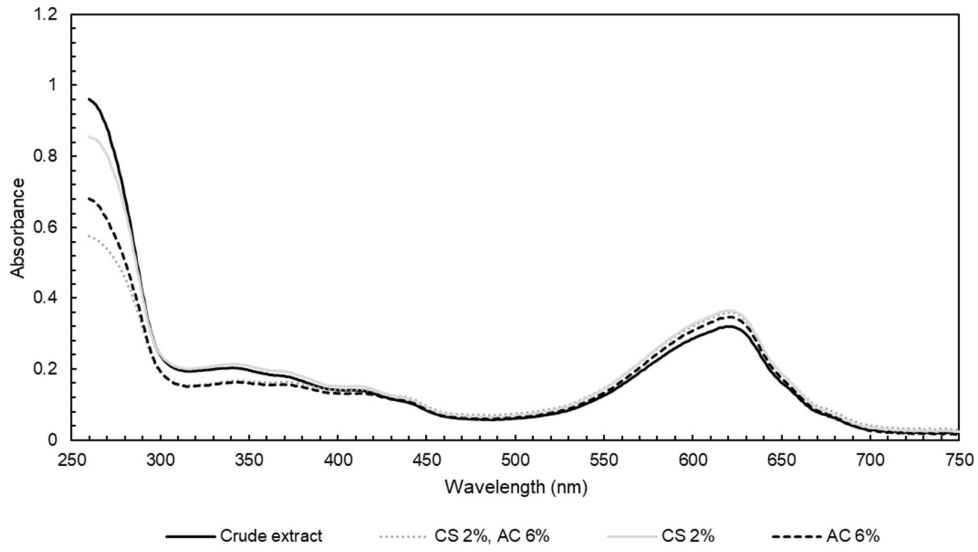

Figure 24: Impact of adding different weight percentages of chitosan (CS) and activated charcoal (AC) on full wavelength spectrum.

6.4 Central composite design

After simply investigating the impacts of varying chitosan and activated charcoal concentrations, it was useful to follow this by attempting to fully optimise all aspects of this adsorption so that the process as a whole can operate in the most optimal manner. The nature of the pretreatment step – namely the adsorption of impurities from the crude extract using chitosan and activated carbon – means that there are a few different variables that could be adjusted with the goal of improving this aspect of the process. The concentrations of the two adsorbents, chitosan and activated carbon, have already been shown to have a significant impact on the removal of impurities. However, it was useful to consider these adsorbent concentrations along with other aspects of the process. The pH of an adsorption step has been shown to have a significant impact on the ultimate purity and concentration of C-PC which can be achieved and therefore it was also necessary to consider this as part of the pretreatment optimisation (Liao et al., 2011). The pretreatment follows certain kinetics and therefore increasing or reducing the adsorption time will likely impact the mechanism of the adsorption and influence the purity of the sample being recovered. This is because the number and type of impurities being removed, as well as the C-PC itself, will be affected by the varying adsorption time (Fekrat et al., 2019). For this reason, the period required for adsorption was another important variable to investigate so that an optimal length of time could be determined. One variable which was not investigated, but could potentially be important to the adsorption rates, was the temperature at which the adsorption was conducted.

It was desired to test these variables at different levels to try and maximise the performance and identify any optimal points rather than simply investigating high and low values. However, testing numerous factors at a number of levels can easily result in an impractical number of experiments required for a full factorial design. For example, testing the concentrations, pH and adsorption time at four levels each – which would be necessary to understand where any maxima or minima lie – would result in 256 individual runs being required. Therefore, it was necessary to use an alternative approach for conducting this investigation into pretreatment optimisation. A central composite design was used by Fekrat et al. (2019) during an

investigation into C-PC purification and therefore this was considered to be a viable method of testing this adsorption step. The advantage of central composite design is that it reduces the number of experimental runs but is still able to fit a second-order model, i.e., it can represent any maxima or minima (Montgomery, 2017). The logic behind a central composite design is that it starts with a traditional 2^k factorial design – two levels for each factor – and augments this 2^k design with axial points and central points to better signify curvature in the output. Repeats of the central point allow for an understanding of experimental variation and thus it is not always necessary to perform repeats on all combinations of variables. By using a central composite design with four factors and six repeats of the central point, the optimisation experiment could be reduced to 30 runs. The choice of variable ranges was guided by similar investigations presented in literature (Fekrat et al., 2019; Liao et al., 2011). The summary of experimental runs with the values of the variables can be seen in Table 5.

Table 5: Breakdown of central composite design experiments for testing the impact of adsorbent concentrations as well as contacting time and pH on an adsorption step to purify C-PC. The repeats around the central point are represented by (C).

Run number	Chitosan (% w/w)	Activated charcoal (% w/w)	Time (min)	pH
1	0.2	6	6	6.5
2	0.2	6	14	6.5
3	0.2	12	6	6.5
4	0.2	12	14	6.5
5	0.4	6	6	6.5
6	0.4	6	14	6.5
7	0.4	12	6	6.5
8	0.4	12	14	6.5
9	0.2	6	6	6.9
10	0.2	6	14	6.9
11	0.2	12	6	6.9
12	0.2	12	14	6.9
13	0.4	6	6	6.9
14	0.4	6	14	6.9
15	0.4	12	6	6.9
16	0.4	12	14	6.9
17 (C)	0.3	9	10	6.7
18 (C)	0.3	9	10	6.7
19 (C)	0.3	9	10	6.7
20 (C)	0.3	9	10	6.7
21 (C)	0.3	9	10	6.7
22 (C)	0.3	9	10	6.7
23	0.3	3	10	6.7
24	0.3	15	10	6.7
25	0.1	9	10	6.7
26	0.5	9	10	6.7
27	0.3	9	2	6.7
28	0.3	9	18	6.7
29	0.3	9	10	6.3
30	0.3	9	10	7.1

The summary of the full set of results of the optimisation experiments can be seen in Table 6. These results need to be considered while keeping in mind the breakdown of each of the runs presented to try and understand the impacts of the different variables. What is immediately obvious is that the adsorption step – at all different combinations of variables – was able to increase the purity of the C-PC when compared to the crude extract. However, despite this improvement, it must be noted that the purity achieved did not vary to a great degree for any of the combinations. The range of purities measured was between 0.635 ± 0.008 to 0.724 ± 0.008, which is significantly lower than the desired value of 1.5 for cosmetic-grade C-PC. Therefore, it appears as though only marginal benefits are realised by attempting to optimise the adsorption. It can be seen that the results presented in Table 6 are similar to what was achieved when conducting the adsorbent combination experiments previously. Although, as can be seen from Table 4, improved C-PC purities were achieved when adding the chitosan at higher concentrations.

The purity results presented in Table 6 are significantly lower than what was achieved by Fekrat et al. (2019) and Liao et al. (2011) at similar conditions. Fekrat et al. (2019) achieved C-PC purities of between 2.19 and 3.47 when adding chitosan and activated charcoal at similar concentrations, while the equivalent range seen in the study conducted by Liao et al. (2011) was approximately between 0.8 and 2.7. However, when considering the results presented by Fekrat et al. (2019), it is important to note that the concentration in the crude extract was only equal to 0.34 $mg.mL^{-1}$, significantly lower than the concentration of 4.78 ± 0.07 reported in Table 6. This indicates that the higher purities achieved by Fekrat et al. (2019) are likely as a result of using a solution with a lower quantity of C-PC, increasing the effectiveness of the adsorbents. Liao et al. (2011) did not report the concentrations of C-PC in either the crude extract or the purified solution, and so it is not possible to compare this aspect of the two sets of results. However, what can be seen from the study conducted by Liao et al. (2011) is that the purity of C-PC in the crude extract was equal to 0.93. Therefore, the higher purities achieved at the end of adsorption, when compared to those in Table 6, can potentially be attributed to the fact that a higher purity solution was initially used. This implies that there was already a significantly lower quantity of impurities in the crude extract and that the use of chitosan and activated charcoal was made more effective. This makes it challenging to directly compare the results of this proposed optimisation to those seen in literature, as there are enough discrepancies between the various process configurations to potentially explain any differences in results.

The struggle when trying to definitively conclude on any optimal combinations is further emphasised when considering the results of runs 17 to 22 – which are the six repeats around the centre points of each variable. The range of purities seen in these runs – from 0.680 ± 0.006 to 0.717 ± 0.008 – was significant when compared to the difference in results for all other runs, which had altered the combinations of variables. This makes it difficult to conclude if any differences observed were due to the adjustment of process parameters or simply experimental variation. This variation was seen even more strongly in the C-PC concentration and recovery data for runs 17 to 22 in Table 6. Once again, this makes it a challenge to understand if any true optimal combinations of variables existed.

However, there did seem to be a general trend for the concentration of C-PC being reduced through the adsorption step, with the final concentrations represented in Table 6 and the initial concentrations in the crude extract being equal to 4.78 ± 0.07 $mg.mL^{-1}$. The final initial observation is that the recovery of C-PC for each run was lower than would be hoped for a commercial process – particularly for runs which had increased amounts of activated charcoal added. However, as discussed previously, this is more a consequence of the method of adding

powdered adsorbents into suspension and coupling it with dead-end centrifugation rather than an issue inherent with the adsorbents themselves.

Table 6: Summary of results for central composite design experiments. Uncertainty represented by standard error based on repeat analysis. The repeats around the central point are represented by (C).

Run number	$Purity_{C\text{-}PC}$	$C_{C\text{-}PC}$ (mg.mL^{-1})	$Recovery_{C\text{-}PC}$ (%)
Crude extract	0.467 ± 0.002	4.78 ± 0.07	N/A
1	0.721 ± 0.003	4.39 ± 0.12	72.4 ± 2.0
2	0.716 ± 0.005	4.01 ± 0.06	62.4 ± 0.9
3	0.707 ± 0.005	3.71 ± 0.11	58.0 ± 1.8
4	0.678 ± 0.005	3.04 ± 0.03	41.7 ± 0.5
5	0.724 ± 0.008	4.09 ± 0.04	65.8 ± 0.7
6	0.709 ± 0.005	3.84 ± 0.07	61.2 ± 1.1
7	0.690 ± 0.004	3.24 ± 0.07	42.7 ± 0.9
8	0.709 ± 0.006	3.24 ± 0.04	44.1 ± 0.5
9	0.689 ± 0.003	4.27 ± 0.10	70.3 ± 1.6
10	0.689 ± 0.006	3.85 ± 0.09	66.4 ± 1.6
11	0.714 ± 0.006	3.29 ± 0.10	45.7 ± 1.4
12	0.686 ± 0.008	2.92 ± 0.02	42.0 ± 0.3
13	0.684 ± 0.004	4.03 ± 0.06	73.1 ± 1.1
14	0.694 ± 0.005	3.96 ± 0.08	62.9 ± 1.2
15	0.677 ± 0.006	3.18 ± 0.04	40.7 ± 0.5
16	0.676 ± 0.004	3.12 ± 0.05	36.6 ± 0.6
17 (C)	0.714 ± 0.006	3.75 ± 0.070	46.0 ± 1.1
18 (C)	0.699 ± 0.005	3.61 ± 0.05	44.4 ± 1.1
19 (C)	0.680 ± 0.006	3.53 ± 0.06	43.4 ± 1.0
20 (C)	0.701 ± 0.005	5.28 ± 0.17	63.1 ± 2.1
21 (C)	0.698 ± 0.009	5.27 ± 0.15	63.0 ± 1.8
22 (C)	0.717 ± 0.008	5.10 ± 0.17	61.0 ± 2.1
23	0.649 ± 0.004	4.24 ± 0.06	72.2 ± 1.0
24	0.635 ± 0.008	2.80 ± 0.080	34.4 ± 0.9
25	0.674 ± 0.007	3.52 ± 0.05	47.1 ± 0.7
26	0.714 ± 0.005	3.41 ± 0.03	44.4 ± 0.4
27	0.706 ± 0.008	3.58 ± 0.10	48.8 ± 1.4
28	0.699 ± 0.006	3.56 ± 0.05	50.6 ± 0.6
29	0.712 ± 0.005	3.76 ± 0.04	56.4 ± 0.6
30	0.692 ± 0.005	3.83 ± 0.04	49.8 ± 0.5

6.4.1 Response surfaces for C-phycocyanin purity

Due to the difficulty in drawing any definitive conclusions from the tabulated central composite design data, response surfaces were drawn to model the impact of the four variables – chitosan and activated charcoal concentrations (measured as a mass percentage), pH and time (in minutes) – on the purity of C-PC. These can be seen in Figures 25 and 26. The

response surfaces exhibited an excellent fit of the experimental data, as seen in the low residual sum of mean squared errors (MS) value of 0.000233. This implies that the curves provided a fair indication of the performance of the adsorption pretreatment in terms of C-PC purity.

The curve seen in Figure 25 focuses particularly on the impact of the adsorbent concentrations on the C-PC purity. As can be seen from the accompanying legend, the darker red colour indicated a higher purity of C-PC while the greener areas of the surface indicated that those combinations of the adsorbents resulted in a lower purity. Figure 25 clearly indicates, therefore, that using the midpoint ranges of the activated charcoal resulted in higher purities of C-PC, while the lower and higher fractions – of around 3% and 15% by mass – did not purify the C-PC to the same extent. The most likely explanation for this is that the low concentrations of activated charcoal did not provide enough of an opportunity for impurities to be removed from solution. By contrast, at a high fraction of activated charcoal, it was possible for the adsorbent to begin to remove the desired C-PC out of solution, reducing its purity.

For chitosan, on the other hand, a similar C-PC purity was seen at all levels and there was less of a steep decline for certain concentrations of the adsorbent. However, there was a slight trend of C-PC purity increasing with a higher chitosan concentration, as the mass percentage of 0.5% led to the darkest red area on the curve. This less obvious impact of chitosan concentration could be partly as a result of its lower initial concentration – implying that any differences in changing concentration would be not as noticeable – or because it was potentially able to more selectively remove other impurities rather than C-PC.

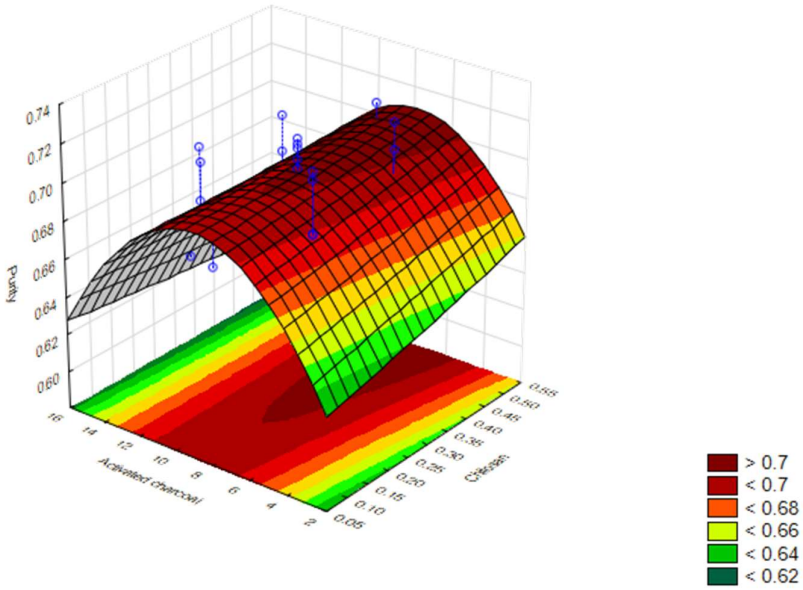

Figure 25: Response surface for C-PC purity based on mass percentages of chitosan and activated charcoal. Curve was drawn using *Statistica* with blue circles representing experimental data.

There was less of an obvious performance trend for the adsorption pH and contact time, as seen in Figure 26. The profile of the response curve was not as steep as that seen in Figure 25, implying that changing the pH and adsorption time did not have as significant an effect on the C-PC purity as compared to the concentration of activated charcoal. The only minor trend

which can be identified from the figure was the slightly higher C-PC purity at the lower pH values and at the high and low values of the contact time. However, as mentioned, this difference was not as significant and the range of purities in the figure was small, from 0.70 to 0.75 . Therefore, it is difficult to develop an effective conclusion behind the physical reason for the slightly better performance at the lower pH and contact time, especially considering the difference in results was similar to what was seen in the experimental variation on the repeat runs of the centre point.

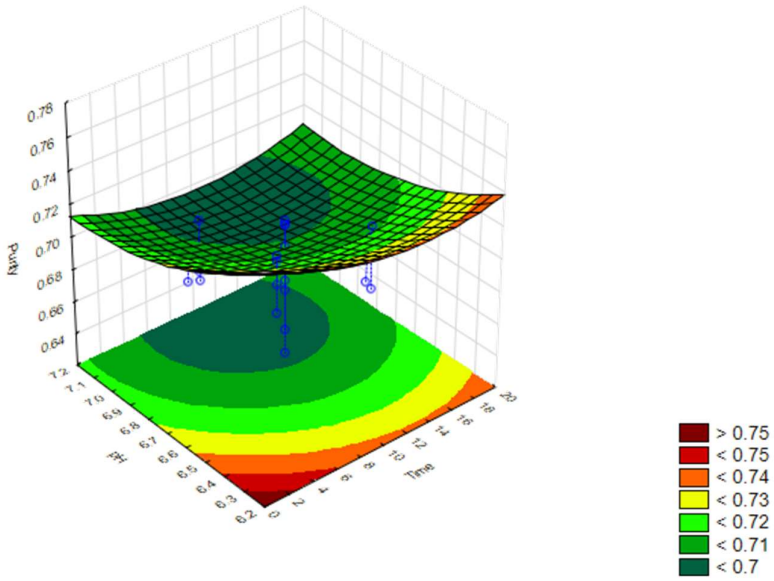

Figure 26: Response surface for C-PC purity based on pH and contact time in minutes. Curve was drawn using *Statistica* with blue circles representing experimental data.

6.4.2 Response surfaces for C-phycocyanin concentration

The impact of the adsorption on the concentration of C-PC can be similarly represented by response surfaces. These are presented in Figures 27 and 28, with the concentration reported in units of $mg.mL^{-1}$. These two response surfaces generated did not fit the measured results as well as those generated for C-PC purity, as indicated by the increased MS value of 0.268. This indicates that there is a greater error between the experimental data itself and the predicted curve, a fact that should be remembered when interpreting the surfaces.

From the response surface for chitosan and activated charcoal concentration in Figure 27, there are a few trends which can be identified. The most obvious of these is that there was a definite decrease in measured C-PC concentration at increased loadings of activated charcoal. At weight percentages of 12% and above, there was a sharp decline in the concentration of C-PC, evident in the colour of the response surface shifting towards yellow and green. This falls in line with the conclusions drawn earlier, that at high fractions of activated charcoal the adsorbent begins to remove the pigment out of solution and therefore the concentration of C-PC is reduced. The optimal concentration appears to have been when adding activated charcoal at approximately 6% with a chitosan percentage of 0.30%. However, there was less of an impact on C-PC concentration from changing the amount of chitosan, as seen in the red colour of the response profile at the majority of chitosan values. Additionally, the profile of the surface was less steep in the direction of the chitosan axis, implying that the

changes were not as significant as for the adsorption caused by activated charcoal, and therefore chitosan was likely more selective at adsorbing other impurities rather than the desired pigment.

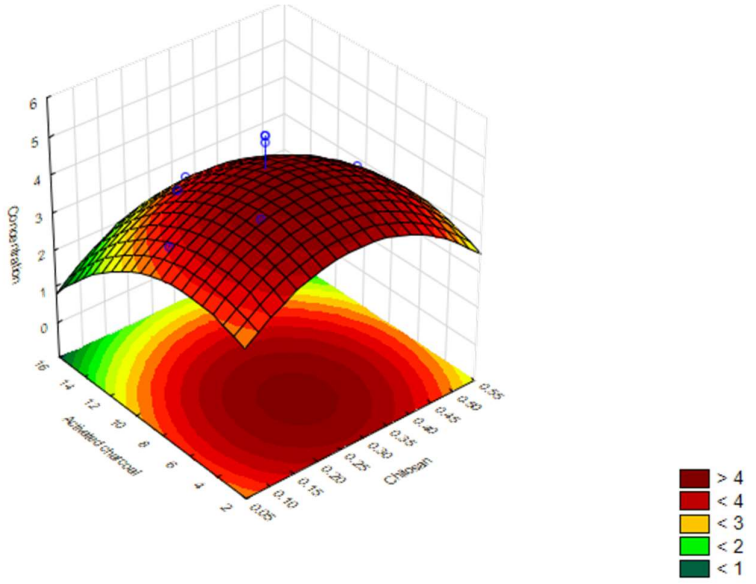

Figure 27: Response surface for C-PC concentration in mg.mL^{-1} based on mass percentages of chitosan and activated charcoal. Curve was drawn using *Statistica* with blue circles representing experimental data.

The response curve based on pH and adsorption time (Figure 28) has a similar appearance to that of the chitosan and activated charcoal. The is because the optimal C-PC concentration was seen towards the centre points of the two variables, with the lowest results seen at the extreme high and low combinations. It is possible that at extreme values of pH, the protein was not able to remain stable in solution and there was degradation of C-PC occurring. In terms of the adsorption time, the most logical explanation for the reduced concentration seen at around 2 minutes is that the contact time was not sufficient to remove other impurities out of the solution and therefore the concentration of C-PC was slightly lower. At the longer process times of around 18 minutes, it is likely that more of the C-PC was adsorbed due to the extended period of contact and hence its concentration was lower. However, despite these tentative conclusions and explanations, it must be noted that the low MS residual reported as well as the high degree of experimental variation seen on the repeats does make it difficult for these supposed optimal combinations to be completely reliable.

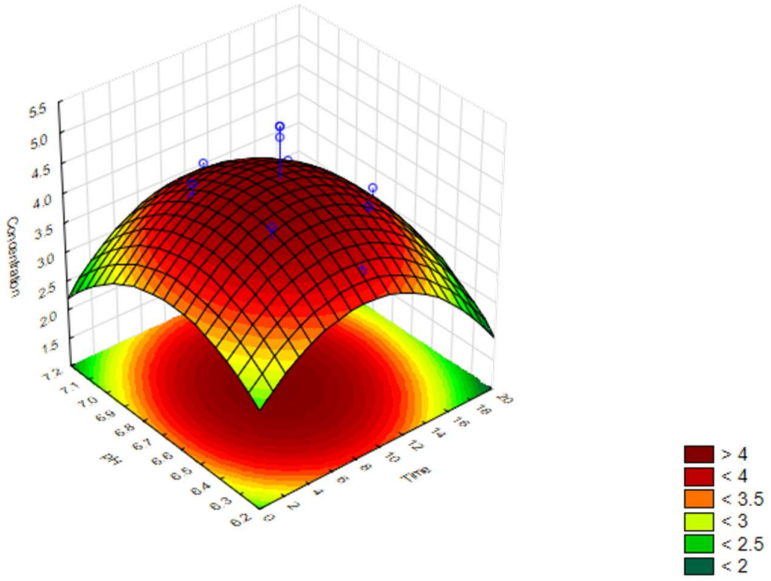

Figure 28: Response surface for C-PC concentration in mg.mL^{-1} based on pH and contact time in minutes. Curve was drawn using *Statistica* with blue circles representing experimental data.

6.4.3 Response surfaces for C-phycocyanin recovery

The recovery of C-PC through the adsorption step is impacted by the C-PC concentration measured on the purified sample – as has been discussed above – but also takes into account the volume of solution retained. Therefore, it is worth presenting response surfaces based on this C-PC recovery – seen in Figures 29 and 30 – so that the impact of the four variables on this particular aspect of the adsorption step can be discussed. However, it is important to note at this point that the MS residual for the recovery response surfaces was equal to 53.3, representing a substantial error between the recovery measured and what was predicted by the model output. Therefore, although it still useful to analyse the response surfaces based on C-PC recovery and discuss any trends which can be identified, it would be misleading to draw any firm conclusions on the specific impacts of any of the variables.

The results represented by Figure 29 seem to suggest a clear trend with regards to the impact of activated charcoal concentration on C-PC recovery. The response surface indicates that the recovery of C-PC sharply decreased as the amount of activated charcoal increased. This was a result of both a reduction in C-PC concentration at these higher values – as discussed in Chapter 6.4.2 – and the reduction in retained volume as a result of the additional liquid contained within the adsorbent pellet after centrifugation. Therefore, the highest recovery of C-PC was seen at the lowest composition of activated charcoal of 2%. As a contrast to this, because the chitosan was only added at a much lower level than the activated charcoal, there was less of a change in the volume of solution contained within the pellet as the amount of chitosan was increased, and therefore there was not as noticeable an impact on the C-PC recovery.

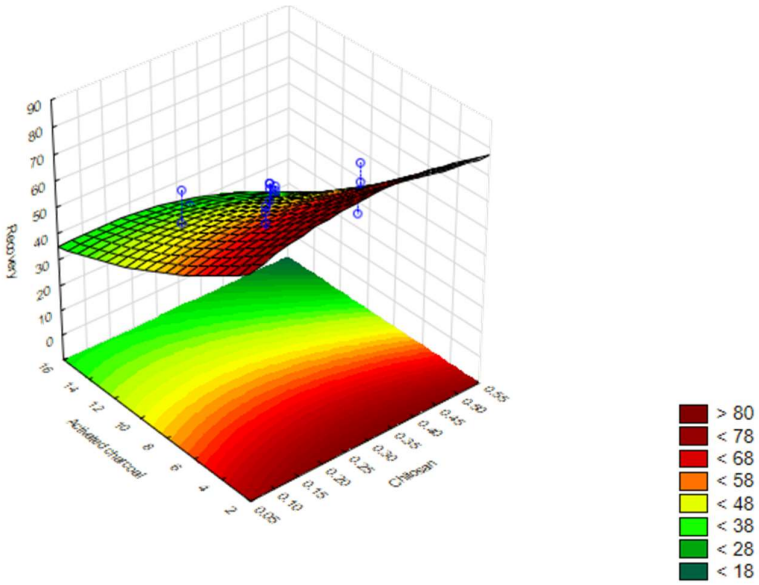

Figure 29: Response surface for C-PC recovery based on mass percentages of chitosan and activated charcoal. Curve was drawn using *Statistica* with blue circles representing experimental data.

When considering the effects of time and pH on C-PC recovery, represented in Figure 30, there was also not as obvious a trend which can be observed. The response surface does not have as steep a profile as was observed for activated charcoal content and therefore the pH and contact time did not have as significant an impact on recovery. The most reasonable explanation for this conclusion is that neither the pH nor adsorption time would have much of an impact on the volume of liquid held within the pellet after adsorption – and this change in volume is what predominantly determined how much of the C-PC was lost in the adsorption step. Having said this, based on the response surface, there does seem to be a trend which suggests that the recovery of C-PC was reduced at longer contacting times, as indicated by the dark green regions of the curve at the time period of 18 minutes. Additionally, it appears that conducting the adsorption at a combination of a shorter time period and a lower pH could lead to an improvement in the maximum recovery.

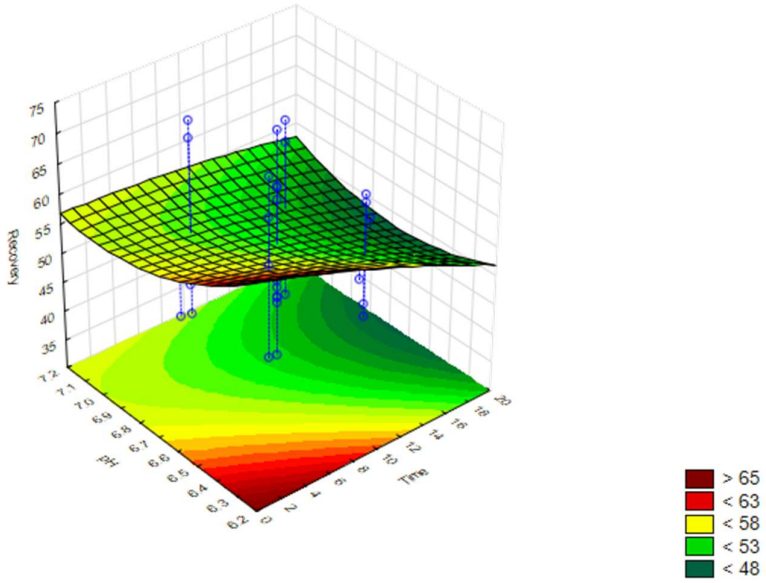

Figure 30: Response surface for C-PC recovery based on pH and contact time in minutes. Curve was drawn using *Statistica* with blue circles representing experimental data.

Ultimately, although the various response surfaces represented by Figures 25 to 30 do suggest certain trends in the performance of the adsorption step, it is difficult to take away anything conclusive from this attempted optimisation. The predominant reason for this was due to the narrow range of C-PC purities which were achieved even when adjusting the variables to extreme high and low values (in the context of the literature on this topic). This implies that even the suggested optimal values do not necessarily improve the process significantly and it is not possible to conclude that any differences in performances are attributable to the changing of variables and not to other factors such as experimental variation.

6.5 Microbial contamination

Commercial samples of C-PC used for cosmetic applications require the microbial contamination in the sample to be below a certain level. As reported in Chapter 2.2.4, one value reported is a maximum count of 1000 CFU.g^{-1} (Sensient, 2021). The results of this contamination check can be seen in Table 7, where the method of plating used to quantify the number of microorganisms can be found in Chapter 4.3.3. The microbial contamination was measured in the crude extract and at the end of adsorption. In this manner, the impact of chitosan and activated charcoal on the level of microbial contamination could be determined.

As can be concluded from Table 7, there was a benefit in including the adsorption step in terms of reducing the level of microbial contamination within the system, when compared to what was present in the crude extract. The measured contamination was reduced by two orders of magnitude, i.e., approximately by a factor of 100. However, what is also clearly evident from the table was that the microbial contamination at the end of this adsorption step was significantly higher than the desired final threshold of 1000 CFU.g^{-1}. This indicates that, although removing a certain number of microorganisms was an advantage of using adsorption, it was not sufficient as an isolated step to ensure the process meets the required specifications. Therefore, it is important that the subsequent purification steps are able to

further remove the unwanted microorganisms so that the final product meets the required specifications in this regard.

Table 7: Summary of levels of microbial contamination for different stages of process. Uncertainty represented by standard error based on repeat analysis.

Process stage	Contamination (CFU.mL^{-1})	Contamination (CFU.g^{-1})
Crude extract	70000 ± 30000	1 x 10^7 ± 5 x 10^6
Adsorption	500 ± 200	1 x 10^5 ± 7 x 10^4

Despite the general trends suggested by these results, it would be beneficial for more work to be done on this aspect of quantifying the level of microbial contamination. The process of generating data by serial dilution and spread plating is prone to experimental error, and therefore more accurate and precise results could be presented after conducting further repeats. Additionally, using other plating media might allow microorganisms present in the solution, but which did not form colonies on the nutrient agar, to be quantified. Finally, it could be beneficial to better understand the antimicrobial impacts of the adsorbents used. It would be helpful to determine if the chitosan and activated charcoal are physically able to remove the microorganisms from the solution or if the reduction in contamination through adsorption is simply a function of the unwanted microbes forming part of the pellet after centrifugation.

6.6 Conclusions

In order to initially test the adsorption pretreatment, it was decided to perform it by only adding one adsorbent at a time. This made it simpler to try and understand the impact each had on the purity, concentration and recovery of C-PC. The purity of C-PC increased as more chitosan was added to the solution, while for activated charcoal the purity reached a maximum when included at mass compositions of between 6% and 10%; at higher concentrations, the purity began to decrease. This was coupled with the C-PC concentration trends, where the concentration remained fairly constant as the amount of chitosan was varied, but decreased as the activated charcoal content increased. These sets of results seemed to suggest that the chitosan was effective at selectively removing unwanted proteins from the solution, hence the continual increase in C-PC purity and the constant concentration as more chitosan was added. Activated charcoal, on the other hand, was less selective and seemed to adsorb all proteins from the solution, including the C-PC. This was seen in the reduced C-PC concentration as more activated charcoal was added and also explains the purity profile – where a maximum was reached and then began to decrease. The results for C-PC recovery when using either chitosan or activated charcoal followed similar trends to one another with a decrease as more of the adsorbents were added. The main reason for this was due to the reduced volume recovered when the concentration of adsorbent increased as a result of the capacity of both chitosan and activated charcoal powders to contain liquid within the solid pellet after centrifugation. Therefore, the lower amount of solution retained after adsorption resulted in a decrease in recovery. As discussed, this is a consequence of operating a dead-end centrifugation step and is something which needs to be considered when attempting to implement a large scale process.

As part of the investigation into using activated charcoal as an isolated adsorbent, the performance of slightly different activated charcoal samples was tested. The two purchased

from Sigma-Aldrich with the same particle size, despite having considerably varying cost prices, performed similarly, while the third sample of slightly larger particles obtained from Rotocarb did not generate in C-PC with as high purities. This was likely due to the reduction in available surface area when using these larger activated charcoal particles, although this reduced surface area also resulted in less C-PC being adsorbed, improving its concentration and recovery when compared to the Sigma-Aldrich samples. It must be noted that the local Rotocarb sample is likely the better representation of what would be used in a full scale process due to its significantly lower cost and easier availability. Therefore, one needs to keep in mind the slightly lower purities achieved using the Rotocarb sample when attempting to use the results of this research to implement a commercial C-PC purification process.

After looking at the adsorbents individually, an investigation was then done to test the adsorbents when they were added in combination with one another. When different combinations of chitosan and activated charcoal were added together as part of the adsorption step, the purity of C-PC was increased when compared to their respective individual performances. This indicates a synergistic effect between the two adsorbents and that they were able to operate more effectively when they were used together as opposed to in isolation. A full wavelength spectrum was generated on a sample purified using both chitosan and activated charcoal, and was compared to spectra generated by chitosan and activated charcoal separately to confirm the results which had been obtained previously.

A central composite design was used to attempt to optimise all crucial operating variables of the pretreatment – such as chitosan and activated charcoal content, pH and adsorption time. The goal was to test different levels of each variable to find a combination which would be able to maximise the purity and recovery of the C-PC. However, when analysing the results of this central composite design, it was found that adjusting the variables did not have a significant impact on the C-PC purity achieved. The purity across the 30 runs performed only ranged between 0.635 ± 0.008 to 0.724 ± 0.008, where this narrow range made it difficult to draw any definite conclusions about the adsorption step. Additionally, the high degree of experimental variation seen, based on the repeat runs on the centre point, made it challenging to determine if any observed differences in process effectiveness were as a result of adjusting variables, or this experimental variation. Despite this, a few minor trends – particularly in terms of the impact of adsorbent concentration – were still discernible after generating response surfaces to model the performance of the central composite design. Ultimately, after completing all of these different investigations into the performance of the adsorption, it was then possible to try and incorporate this pretreatment into the full downstream process.

Finally, serial dilution and spread plating was used to try and quantify the effectiveness of adsorption at removing microorganisms from the system. It was found that the adsorption step was able to reduce the measured level of contamination by a factor of 100 when compared to what was present in the crude extract. This showed the potential benefit of including chitosan and activated charcoal in this aspect of the process. However, it was found that the contamination level measured after adsorption of $1 \times 10^5 \pm 7 \times 10^4$ CFU.g^{-1} was still significantly higher than the reported allowable maximum of 1000 CFU.g^{-1}. This implied that the adsorption was not sufficient to meet this aspect of the process and that the subsequent purification stages would need to remove more of the contaminants.

7 Results: Adsorption in Purification Process

7.1 Introduction

Chapter 6 of this research project focused on the adsorption pretreatment in great detail as an isolated step. However, even after better understanding its operation, it was still important to couple it with the existing steps of the process to fully appreciate the potential benefit to including it in C-PC purification. This was done by sending a stream purified by chitosan and activated charcoal adsorption through a PEG-citrate ATPS. The outputs of this process would be evaluated in terms of C-PC purity, concentration and recovery and they would be compared to running a PEG-citrate as well as PEG-maltodextrin ATPS on a C-PC crude extract.

7.2 Adsorption coupled with ATPS

7.2.1 Negative control runs

Based on the work done by Hockey (2022), it was discussed that the optimal configuration for the CeBER process was to include a PEG and citrate ATPS step before the patented PEG-maltodextrin ATPS in order to make the overall process more efficient and effective. Therefore, the goal of this aspect of the research project was to test the impact of the adsorption pretreatment on the performance of this PEG 4000 and citrate ATPS. This test was done on the same concentrations of chitosan and activated charcoal seen in Table 4, so it would be possible to understand if different compositions of the adsorbents impacted the ATPS in contrasting ways. The results of this investigation can be seen in Figures 31, 32 and 33 which each consider the C-PC purity, concentration and recovery respectively.

However, before presenting the results of the adsorption and ATPS combination, it was worth first running the ATPS on the crude extract to understand how effectively it worked as an isolated step. This was done for both a PEG 4000-citrate ATPS with the C-PC reporting to the PEG phase as well as a PEG10000-maltodextrin ATPS where the C-PC was recovered with the maltodextrin. As discussed previously, this PEG 10000-maltodextrin ATPS was the configuration suggested by the CeBER patent and thus was useful to test (Harrison et al., 2020). The results of these negative control runs can be seen in Table 8.

When considering the PEG-maltodextrin ATPS, it can be seen that there is only a small increase in C-PC purity that could be achieved through the use of this one ATPS step. There was, however, a substantial increase in C-PC concentration from 4.69 ± 0.04 $mg.mL^{-1}$ to 6.44 ± 0.5 $mg.mL^{-1}$ due to the portioning of the pigment into a smaller volume. This increase in concentration does imply that a smaller working volume would then be sent to the subsequent downstream steps – potentially making them more efficient – but this benefit does not outweigh the lack of improvement in the purity of the C-PC. Naturally, following this ATPS with a subsequent ammonium sulfate precipitation could still increase the purity of the C-PC to above the 1.5 required for cosmetic-grade. However, there is clearly great potential benefit in including the adsorption step if it is able to increase the purity of the C-PC to a value higher than what can be achieved using the PEG-maltodextrin ATPS.

Similarly, the control run on the PEG-citrate ATPS clearly indicates that there are inherent limitations of the ATPS in its current configuration. The C-PC purity of 0.522 ± 0.005 achieved

after the ATPS was only slightly higher than was observed in the crude extract, and the concentration or recovery of C-PC post ATPS were both lower than would be desired for a commercial process. The concentration of 0.356 ± 0.007 was significantly lower than was present in the crude extract because of the requirement to dilute the crude extract by a factor of 10 times before it could be sent to the ATPS (Hockey, 2022). Without this dilution, the ATPS does not operate as effectively and the purity of C-PC obtained in the PEG phase is reduced. However, having to dilute the C-PC to this extent using citrate buffer makes the process significantly more challenging to scale up and implement in a commercial setting. This is because the raw material input needed to successfully operate the ATPS – predominantly the PEG 4000 and citrate salts – will be substantially higher for every gram of C-PC recovered due to the fact that only 10% of the original C-PC was present in the purified solution. Additionally, the process equipment for this ATPS and any downstream steps, such as mixing vessels and centrifuges, will also need to be scaled up accordingly or the amount of purified C-PC recovered in a set amount of time will be significantly reduced.

The low recovery seen in the PEG-citrate ATPS is also a concern for the commercial viability of this step in its current form. The main reason for this low recovery of C-PC from the ATPS was due to the formation of a sizeable layer of apparent remaining cell debris as well other impurities in which much of the C-PC appears to be held. This layer formed between the blue PEG phase on top and the clear citrate phase below and occupied a significant volume of the system. Because the C-PC in this layer was trapped within other proteins and remaining cell debris, it was not possible to obtain the pigment from within it. This was thus responsible for the low overall recovery of the ATPS step. Unlike the low recoveries for the adsorption step presented in Chapter 6.2, this low recovery of the ATPS cannot be improved by changing the manner of conducting the separation step. However, now that the ATPS had been considered in isolation, it was possible to add the adsorption as a pretreatment to determine what impact it had on the performance of the ATPS.

Table 8: Results of two different ATPS performed on crude extract. Uncertainty represented by standard error based on *repeat analysis and †triplicate repeat experiments.

Stage	$Purity_{C\text{-}PC}$	$C_{C\text{-}PC}$ (mg.mL^{-1})	$Recovery_{C\text{-}PC}$ (%)
Crude extract	0.466 ± 0.005	4.69 ± 0.04	N/A
PEG 10000-maltodextrin ATPS†	0.496 ± 0.019	6.44 ± 0.54	-
PEG 4000-citrate ATPS*	0.522 ± 0.002	0.356 ± 0.01	27.8 ± 0.6

7.2.2 C-phycocyanin purity

The C-PC purity seen in Figure 31 indicates that the combination of the adsorption step coupled with the ATPS was effective at generating cosmetic C-PC. The purities achieved after the ATPS ranged between 1.42 ± 0.15 and 1.84 ± 0.14, which was either already above the minimum purity of cosmetic-grade C-PC or just below the required value of 1.5. This implies that even before the second PEG-maltodextrin ATPS or a potential precipitation stage, the purity requirement could already be met. Additionally, these purities are also significantly higher than was achieved when conducting the PEG-citrate ATPS on the C-PC crude extract. Thus, the incorporation of the adsorption pretreatment would appear to have achieved the desired result. It also is clear from Figure 31 that the purity results after adsorption were not necessarily a good indication of the purity that would be achieved after the ATPS. The two

combinations of adsorbents which used 2% chitosan produced similar purities after adsorption of 0.800 ± 0.054 and 0.779 ± 0.047 for activated charcoal concentrations of 6% and 10%, respectively. Despite these results being not being significantly different, after going through ATPS the purities were calculated to be 1.53 ± 0.16 and 1.84 ± 0.14, respectively. This was a more noticeable difference between the two combinations and indicates that C-PC purity after adsorption was not necessarily related to purity after ATPS.

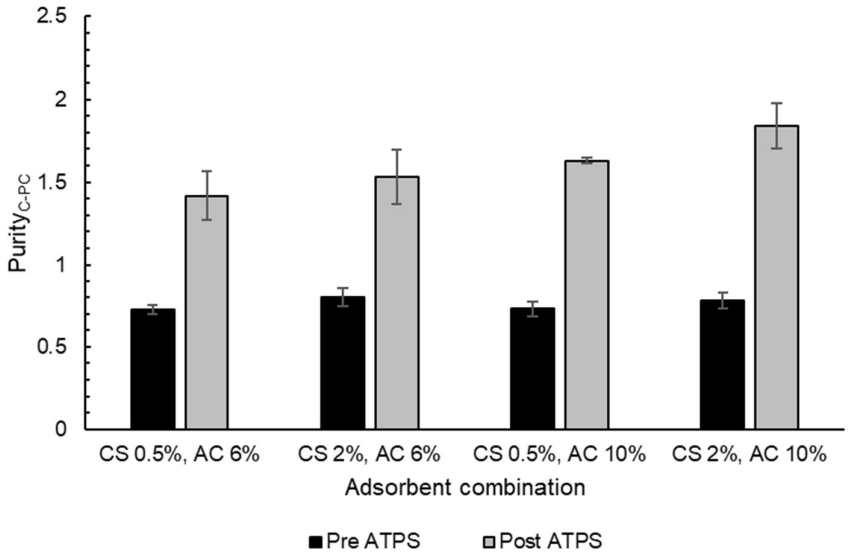

Figure 31: C-PC purity results following adsorption (Pre ATPS) and a PEG-citrate aqueous two-phase separation (ATPS) (Post ATPS) for different mass percentages of chitosan (CS) and activated charcoal (AC). Error bars represent the uncertainty based on duplicate repeat experiments.

7.2.3 C-phycocyanin concentration

Figure 32 considers the concentration of C-PC after the adsorption and ATPS. This shows quite clearly one of the major disadvantages of the PEG-citrate ATPS – the low concentration of C-PC that reported in the PEG phase. The concentration of C-PC recovered from the ATPS ranged from 0.345 ± 0.014 $mg.mL^{-1}$ to 0.410 ± 0.041 $mg.mL^{-1}$, which was significantly lower than the minimum value of 3.00 ± 0.14 $mg.mL^{-1}$ after adsorption. As discussed when considering the PEG-citrate ATPS as a negative control, the reason for this low concentration of C-PC was due to diluting the purified adsorption stream by a factor of 10 before adding the PEG and citrate as part of the ATPS. This dilution clearly helped the ATPS to perform effectively, as seen in the purity results in Figure 31 but this made the ATPS unfeasible to scale up commercially.

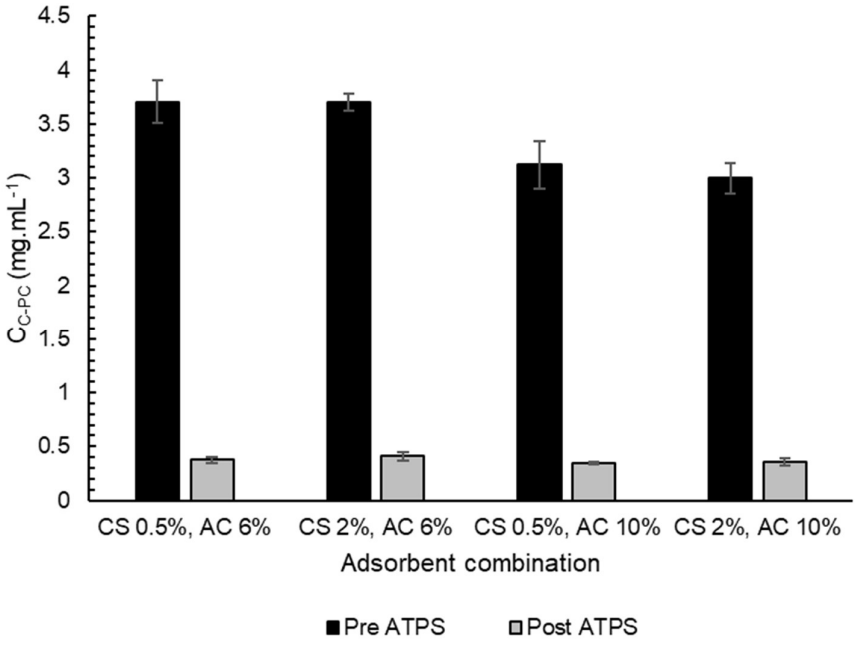

Figure 32: C-PC concentration results following adsorption (Pre ATPS) and a PEG-citrate aqueous two-phase separation (ATPS) (Post ATPS) for different mass percentages of chitosan (CS) and activated charcoal (AC). Error bars represent the uncertainty based on duplicate repeat experiments.

7.2.4 C-phycocyanin recovery

Further to the issues around the low C-PC concentration, there were also concerns with the recovery achieved in the ATPS step, shown in Figure 33. The recovery of C-PC over the ATPS step was consistently lower than 50% – with a minimum value of 37.4 ± 0.8% and a maximum of only 44.5 ± 6.3%. As was discussed, the main reason for this low recovery of C-PC from the ATPS was due to what appears to be remaining cell debris forming a noticeable layer between the PEG and citrate layers. This layer of debris contained significant portions of C-PC and thus impacted the recovery that could be achieved, as it was not possible to separate this C-PC from the remaining proteins and cell debris trapped in this interface.

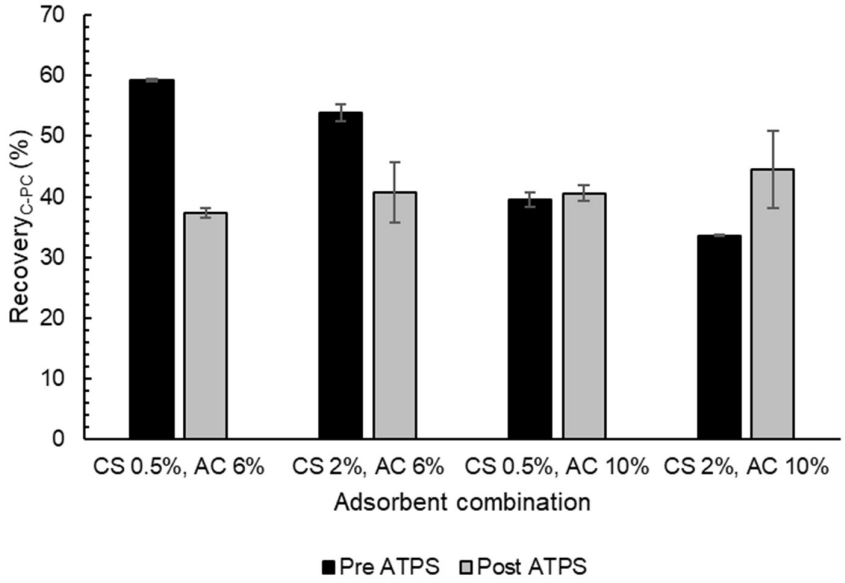

Figure 33: C-PC recovery results following adsorption (Pre ATPS) and a PEG-citrate aqueous two-phase separation (ATPS) (Post ATPS) for different mass percentages of chitosan (CS) and activated charcoal (AC). Error bars represent the uncertainty based on duplicate repeat experiments.

7.3 Conclusions

After considering the adsorption step at different combinations of chitosan and activated charcoal concentrations, the pretreatment was performed in combination with a PEG 4000-citrate ATPS to understand what impact the adsorption had on its performance. Negative control runs were conducted by performing PEG-citrate and PEG-maltodextrin ATPS stages on a C-PC crude extract. Both of these steps were unable to significantly improve the purity of the C-PC where they only reached purities of 0.496 ± 0.019 and 0.522 ± 0.002, respectively. Additionally, the PEG-citrate ATPS resulted in low C-PC concentration and recovery. When running the adsorption pretreatment before the PEG-citrate ATPS, the purity after the ATPS was consistently high for all combinations of adsorbents and either reached the cosmetic-grade purity of 1.5 or was slightly below. However, despite this increased purity, the issues with the PEG-citrate ATPS seen previously of low C-PC concentration and recovery were still evident. These poor results, which have been discussed, do not bode well for the combination of the adsorption step and PEG-citrate ATPS. But, as has been shown, this has more to do with limitations of the ATPS than the inclusion of the adsorption pretreatment. For this reason, as well as much of the parallel research work done by Griffiths (personal communication, 2022), it was decided to move away from coupling the adsorption with the ATPS and to rather focus on taking the purified solution after adsorption into a precipitation step.

8 Results: Performance of Proposed Process

8.1 Introduction

As presented in Chapter 6, a significant amount of research was done considering the adsorption as an isolated step and investigating the performance of the chitosan and activated charcoal by trying to understand what impact each has and how they work when used together. Further research was then conducted including the adsorption as a pretreatment to a PEG and citrate ATPS. However, it was found that although the adsorption improved the performance of the ATPS in terms of increasing the purity of C-PC, the ATPS itself had issues with poor recovery, and only being able to operate with highly diluted solutions of C-PC. It was also found that the adsorption worked more effectively as an individual step than the ATPS when each was performed on a C-PC crude extract. For this reason, it was decided to move away from the ATPS entirely and simply include the adsorption as a pretreatment to the remaining steps of the CeBER process, with particular focus on the ammonium sulfate precipitation.

Along with certain results presented in Chapter 7, much of this part of the research project was based on previous work done by Griffiths (personal communication, 2022) and Kadir (personal communication, 2022) who investigated aspects of both the adsorption and precipitation stages, as well as including a filtration step, to try and understand how best they can be used in combination with one another to generate cosmetic-grade C-PC. Therefore, the goal of this chapter was to initially run the C-PC purification process as suggested by Griffiths (personal communication, 2022) to determine if the final purity of C-PC could consistently reach the minimum purity of 1.5 in an efficient manner. This process includes leaching without a prior cell disruption, an adsorption step using chitosan and activated charcoal, and finally an ammonium sulfate precipitation. In a full scale process, these steps would also be followed by microfiltration and ultrafiltration as well as a drying step to generate the final C-PC product in the desired form. However, not all process runs included these final stages and the majority of the tests were performed until the end of the precipitation.

After evaluating the proposed method for C-PC purification, there was then the opportunity to adjust aspects of the process configuration – particularly with regards to the order of unit operations as well as the possibility of including additional steps – to determine whether this could potentially improve the final outputs. This was achieved by testing the performance of running the precipitation prior to the adsorption and by including a second adsorption step once precipitation had taken place. Additionally, an investigation was included which focused on running part of the adsorption step as a packed activated charcoal column rather than mixing the powdered activated charcoal into suspension. This was done in an attempt to improve the recovery of this step of the process while still maintaining the final desired purity.

Certain experimental runs were also conducted which included the steps of filtration and freeze drying to understand the impacts they had on the process outputs. These samples had been purified via adsorption and precipitation and were then taken through the microfiltration and ultrafiltration units before undergoing freeze drying. Finally, a robustness experiment was performed with different samples of *Spirulina* to understand how sensitive the proposed process was to the initial feed and confirming it did not only operate efficiently when using a specific powder.

8.2 Proposed C-phycocyanin purification process

8.2.1 Runs of proposed process

As mentioned, the proposed process was designed by taking into account certain results presented in Chapters 5.3 and 7.2, such as the fact that the cell disruption step was not required, and the poor performance of the ATPS. This was coupled with the work done by Griffiths (personal communication, 2022) and Kadir (personal communication, 2022) which focused predominantly on the ammonium sulfate precipitation but also tested aspects of the adsorption step as well as including microfiltration and ultrafiltration in the process. The breakdown of the proposed process to generate cosmetic-grade C-PC can thus be seen below with it also being represented in Figure 34. Within this description, details of certain features of the process, such as centrifugation and the mixing aspect of adsorption and precipitation steps, can be found in Chapter 4.3.2.

- Leaching of the *Spirulina* powder was done overnight at room temperature and at a concentration of 100 $g.L^{-1}$.This was done without a full cell disruption step, rather simply dissolving the powder in the citrate buffer. This was followed by centrifugation to remove the cell debris before the blue crude extract was poured off and recovered separately from the green pellet.
- The adsorption step was performed at set concentrations of chitosan and activated charcoal throughout the investigation into this proposed process. This was because the impact of varying adsorbent composition was already extensively covered in Chapter 6, and this section of the report was instead focused on configurations of the process as a whole rather than attempting to adjust one step. Two sets of conditions were used for adsorption, where either the crude extract was treated with chitosan and activated charcoal, or an equal volume of citrate buffer was added to the crude extract to reduce the concentration of C-PC to half of its original value. The chitosan was included in the process in a slightly different form as to what had been done previously. Based on the work by Griffiths (personal communication, 2022) and Fekrat et al. (2019), a 1% solution of chitosan was generated by dissolving it in 1% acetic acid. Chitosan was added to either solution at a concentration of 0.2% w/v – per volume of initial solution – by adding 20% w/v of the 1% solution of chitosan dissolved in 1% acetic acid. Powdered activated charcoal was added to the crude extract at a composition of 8% w/v, again where this volume was that of the starting solution. If, however, the C-PC concentration had been reduced through dilution, the amount of activated charcoal was then scaled accordingly and therefore only 4% w/v was added per total initial volume, i.e. the volume of both the crude extract and buffer. This step would then undergo mixing to provide sufficient adsorption contact time before centrifugation took place. The black pellet containing the adsorbents and unwanted proteins was then discarded with the blue, purified supernatant being recovered.
- A single precipitation stage was deemed sufficient, as attempting to fractionally precipitate out undesired proteins at lower mass fractions of ammonium sulfate was not found to improve the process in a noticeable manner (Griffiths, personal communication, 2022). Therefore, this one precipitation step took place at a mass composition of 35.7% of ammonium sulfate, based on the volume of liquid which was fed to the purification stage. This implied that the concentration of ammonium sulfate – based on the total final volume – was 299 $g.L^{-1}$ which was equivalent to 55% of the saturation ammonium sulfate concentration at 25°C. The salt was then mixed into the solution before centrifugation was performed to separate the clear supernatant from

the blue pellet. The supernatant was removed by pouring it off and the blue pellet was resuspended in citrate buffer to a known volume.

- Subsequently, this C-PC solution was sent through microfiltration and ultrafiltration steps as outlined in Chapter 4.3.2.
- The final step of the process was to prepare powdered samples of C-PC through freeze drying; the method used for this is given in Chapter 4.3.2.

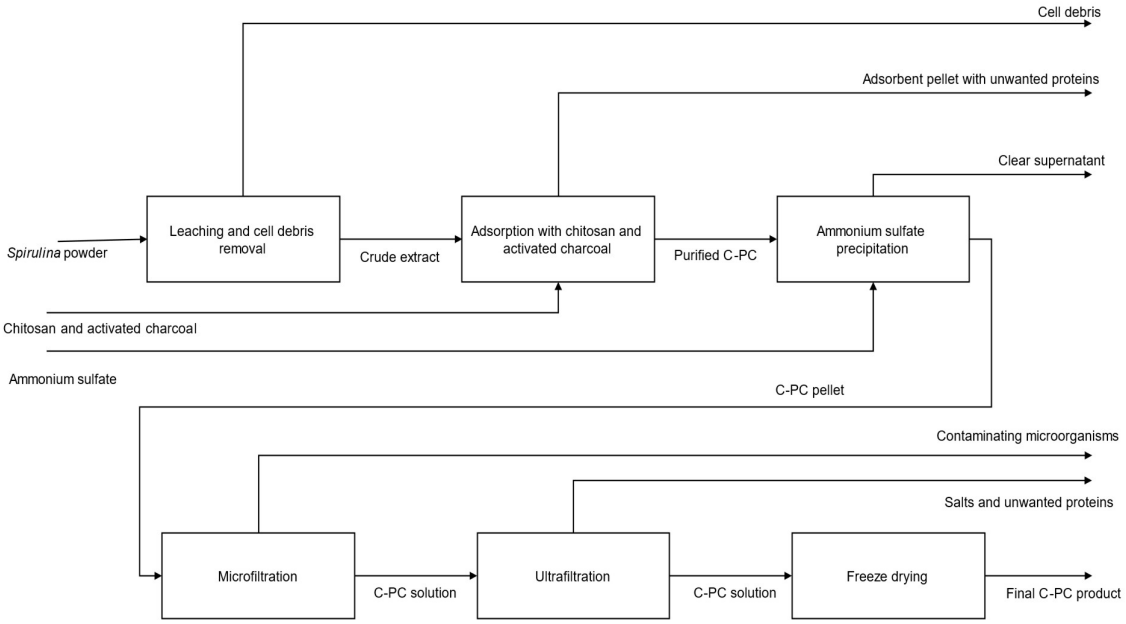

Figure 34: Block flow diagram of proposed C-PC purification process.

The goal was to perform this process (until the end of precipitation) with multiple repeats to understand the change in C-PC purity, concentration and recovery over each stage. This would indicate the effectiveness of each stage of the process as well as the combination of the adsorption and precipitation. As discussed, this proposed process was tested on the crude extract obtained after centrifugation as well as on a crude extract which had its concentration of C-PC reduced by 50% – done by mixing an equal volume of the crude extract with citrate buffer. The rationale behind this dilution was firstly to understand if the adsorption and precipitation would work more effectively with this reduced concentration of C-PC. Additionally, in a commercial process, there is the requirement to try and recover as much C-PC in each step as possible. The centrifugation step to remove cell debris is a prime target for this because of the liquid containing C-PC held within the green pellet. This C-PC can be recovered by resuspending the pellet in more citrate buffer and centrifuging it a second time. In this manner, more of the C-PC will be recovered and this new supernatant can be added to the crude extract already obtained from the first centrifugation. Once these solutions are added together, the overall concentration of C-PC should reduce. If the same volume of buffer as was initially used was used to resuspend the pellet, the C-PC concentration of the combined solutions should be approximately equal to half of its initial value. Therefore, testing the adsorption and precipitation on a diluted sample of crude extract not only has the potential to make them more efficient but was also a reasonable representation of what would take place if this process was implemented commercially. The results of testing the standard crude

extract as well as one with lower C-PC concentration can be seen in Figures 35 to 37, where each reports the achieved purity, concentration and recovery at various stages of the process.

Figure 35 demonstrates the change in purity at each stage of the proposed process for both the standard crude extract as well as the sample which had its C-PC concentration reduced. There were a few obvious conclusions that could be drawn from this set of results about the potential of this process to be used in commercially generating cosmetic-grade C-PC. It is first seen that the purity of crude extract of 0.479 ± 0.006 was very similar to what was obtained in the various experiments performed in Chapters 6 and 7 of this report, again emphasising that the choice to not include a cell disruption step as part of this process did not have a negative impact on the success of the C-PC leaching.

Following on from the crude extract, the next key result seen from Figure 35 was the effectiveness of the adsorption step, particularly on the sample with the reduced C-PC concentration. When conducting the adsorption after reducing the concentration of the crude extract by diluting it with citrate buffer to a value of 2.71 ± 0.03 $mg.mL^{-1}$, it reached an extremely high purity. As can be seen from Figure 35, the purity reached 1.93 ± 0.25 after undergoing adsorption with chitosan and activated charcoal. Despite this high variation, it is still clear that the purity was comfortably higher than the 1.5 required for cosmetic C-PC even before the precipitation step had taken place. Clearly, the reduction of C-PC concentration beforehand helped the adsorption to operate effectively, because this purity was higher than the 1.10 ± 0.03 when chitosan and activated charcoal were added directly to the crude extract. However, even if this purity was lower than the diluted sample, it was still significantly higher than any of the purities achieved in Chapter 6 when using adsorption. This indicates that the configuration including chitosan dissolved in acetic acid was able to operate more efficiently.

Again, by considering the purity results seen in Figure 35, it could be determined that the precipitation with ammonium sulfate was not able to increase the purity to the same degree as the adsorption but that it still had a positive impact on the process. When taking into account the purification train of the standard crude extract, the purity was increased from 1.10 ± 0.03 after adsorption to a value of 1.27 ± 0.03; while for the lower concentration sample, the purity was increased from 1.94 ± 0.25 to 2.00 ± 0.09. These increases are considerably lower than was seen between the crude extract and adsorption stages, but the precipitation was clearly still able to remove certain undesired proteins from the solution.

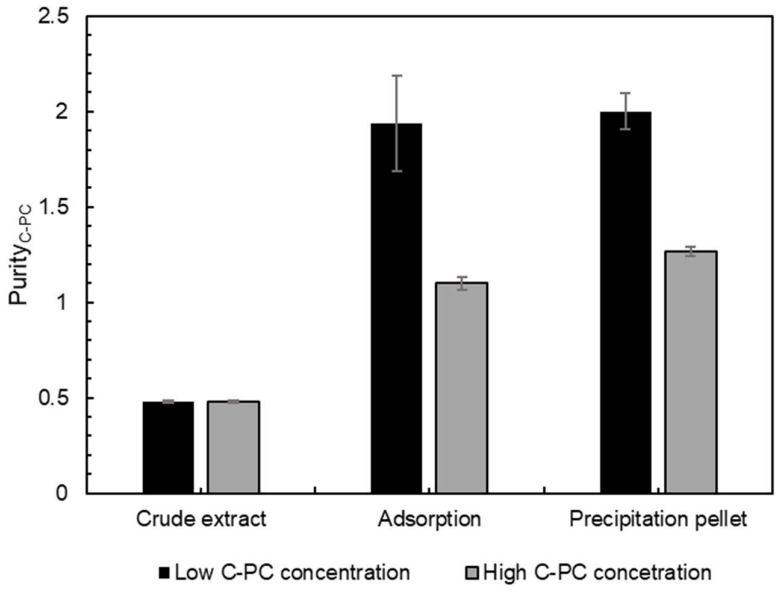

Figure 35: C-PC purity following various stages of proposed process. Error bars represent standard error on six repeat experiments.

The main benefit to including the ammonium sulfate precipitation, apart from the increase in purity it was able to achieve, was its ability to increase the concentration of C-PC in the solution. This is seen in Figure 36, where the concentration of C-PC was higher after precipitation when compared to adsorption for both samples which were tested. The increase on the standard crude extract sample was from 3.58 ± 0.06 $mg.mL^{-1}$ to 6.76 ± 0.13 $mg.mL^{-1}$ while the lower C-PC solution had its concentration increased from 1.58 ± 0.04 $mg.mL^{-1}$ to 3.23 ± 0.11 $mg.mL^{-1}$. The reason the precipitation was able to increase the concentration of C-PC in this manner was because once the clear supernatant had been removed through centrifugation, the blue pellet could be resuspended to any volume using the citrate buffer. Therefore, it was possible to only resuspend the pellet to a small volume – which makes further downstream processing more efficient as it reduces the size requirements of any other pieces of equipment. However, it must also be noted that if the resuspended volume is too low, the viscosity of the solution becomes significant, making it more difficult to work with, especially when working on larger scales.

The advantage of the precipitation increasing the concentration of C-PC was especially useful when considering the fact that the adsorption, although significantly increasing the purity, did tend to reduce the concentration. The C-PC in the crude extract had a concentration of 5.24 ± 0.07 $mg.mL^{-1}$ which became 2.71 ± 0.03 $mg.mL^{-1}$ when the equivalent volume of citrate buffer was used to dilute it. These concentrations though were noticeably higher than the 3.58 ± 0.06 $mg.mL^{-1}$ and 1.58 ± 0.04 $mg.mL^{-1}$ respectively obtained after adsorption. This demonstrated the disadvantage with the adsorption step – and using the activated charcoal in particular – and did negatively impact the overall recovery of C-PC in the process.

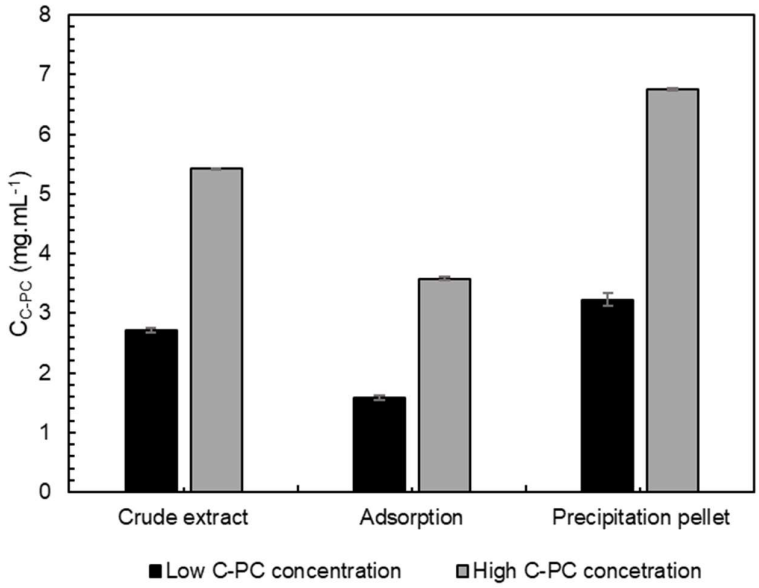

Figure 36: C-PC concentration following various stages of proposed process. Error bars represent standard error on six repeat experiments.

As discussed, the recovery of C-PC is an important factor in trying to design a commercially viable large scale process, and hence it was important to understand what the respective recoveries were at each stage. From Figure 37, it is clear that the main issue with recovery for the proposed process was due to the losses around the adsorption stage. When testing both the crude extract and the lower C-PC concentration sample, the recoveries of the adsorption stage were found to only be 61.0 ± 0.9% and 60.9 ± 1.1% respectively. This low recovery implies that a significant amount of the C-PC was remaining within the disposed pellet after centrifugation, where these losses were two-fold. Part of the losses occur from the C-PC being adsorbed out of solution and onto the surface of the activated charcoal particles – as was discussed in detail in Chapter 6.2. However, as was also mentioned previously, the recovery of the pigment was simultaneously negatively impacted by the ability of both chitosan and activated charcoal powders to hold a set amount of liquid in the pellet when separated out using dead-end centrifugation. As a result of this, only a reduced volume of purified sample could be retained at the completion of adsorption when conducting the purification stage in this manner.

With the precipitation step, on the other hand, essentially all of the C-PC was recovered and almost none was lost to the supernatant. The recovery of the precipitation was calculated to be 97.7 ± 2.7% for the lower C-PC sample and 102 ± 1.9% for the higher concentration solution. It is clearly not physically possible for the recovery to be greater than 100% and so this does imply that some sort of experimental error must have been present. The source of this error was predominantly due to the inaccuracies in trying to resuspend the C-PC pellet after precipitation to a specific volume. If the volume was overestimated, it was possible that the calculated recovery could be greater than 100%, even if that was not necessarily the case. However, by considering the results for the C-PC recovery of the precipitation supernatant, it was still clear that very little of the pigment is lost in this step. The C-PC lost in the higher concentration solution was only equal to 0.113 ± 0.017%, while the equivalent value for the lower concentration sample was 0.347 ± 0.082%. Naturally, these losses were almost

completely negligible, implying that the recovery of the precipitation step would not be a concern when developing a larger scale process.

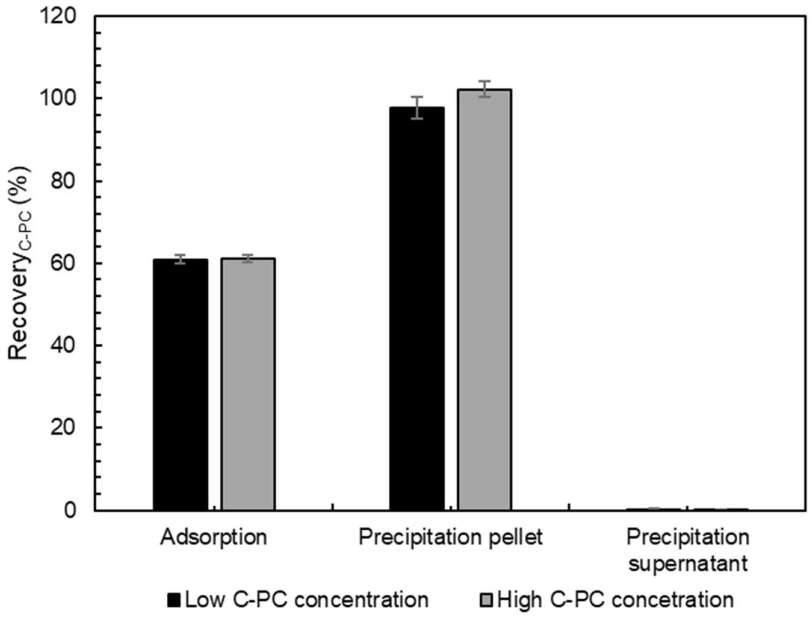

Figure 37: C-PC recovery following various stages of proposed process. Error bars represent standard error on six repeat experiments.

Figures 35 to 37 clearly show there is a great deal of potential in implementing this proposed process. The positive results included the significant improvement in purity achieved by the chitosan and activated charcoal adsorption, as well as the ability of the precipitation step to recover almost all the C-PC and increase its concentration in solution. However, despite these promising aspects, there were still a couple of issues – such as the poor recovery of the adsorption step in its current form and the fact that the final purity of the standard crude extract sample did not reach the desired value of 1.5 – and so it was therefore worth attempting alternative configurations to try and get around these problems and improve the overall process.

8.2.2 Adjustment of order of process units

One of these proposed adjustments was to switch around the order of the adsorption and precipitation steps. The rationale behind this was to try and understand if the adsorption step could be made even more effective by removing some of the impurities beforehand through the precipitation. On top of this, running the process in this manner provided an indication of the performance of the precipitation as an isolated step. As with the proposed process described above, the testing of this variation would also consist of running the purification steps on a standard crude extract as well as a sample which had its C-PC concentration reduced by 50%, for the same reasons as discussed previously. The results in terms of C-PC purity for these two samples can be seen in Figure 38.

As would be expected, the results shown for crude extract purity in Figure 38 were comparable with the purity measured as part of the proposed process (Figure 35). The value for purity of 0.477 ± 0.006 was almost identical to the 0.479 ± 0.006 measured previously, which made

sense considering that this aspect of the process was unchanged. What can be seen, though, is that when ammonium sulfate precipitation was performed on the crude extract, the purities achieved were not as high as what was seen when the adsorption was the first purification step in the process. For the high C-PC concentration sample the purity of 0.768 ± 0.002 reached after precipitation was lower than the equivalent of 1.10 ± 0.03 after adsorption. Similarly, when performing the precipitation on the low C-PC solution, the purity of 0.873 ± 0.004 was not as high as the adsorption purity of 1.94 ± 0.25. Again, it can be seen that the first purification step in the process was made more efficient by initially reducing the concentration of C-PC, although this difference was not as large as was seen after adsorption.

As can also be understood from Figure 38, there was a significant improvement in the purity once the adsorption had taken place on the resuspended pellet after precipitation. When considering the high concentration sample of C-PC, the purity was increased from 0.768 ± 0.002 after precipitation – as was mentioned previously – to a value of 1.42 ± 0.09 post adsorption. On the solution with a lower concentration of C-PC, the equivalent increase was from 0.873 ± 0.004 to 1.61 ± 0.31. When comparing this to what was achieved at the completion of the proposed process using the standard crude extract, the purity achieved is higher than the 1.27 ± 0.03 which was obtained previously. On the other hand, the purity for the initially diluted sample was lower for the adjusted process than the value of 2.00 ± 0.09 measured when adsorption was followed by precipitation. These results – particularly the fact that the desired purity of 1.5 was still unobtainable for the high concentration C-PC sample – implied there was no obvious benefit to placing adsorption after precipitation in the purification train.

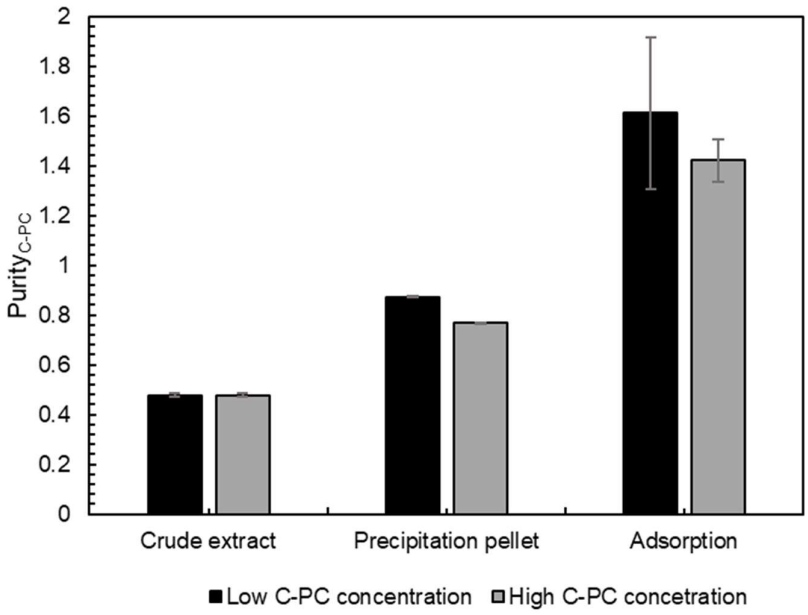

Figure 38: C-PC purity following various stages of adjusted process. Error bars represent standard error on triplicate repeat experiments.

It is also important to consider what impact changing the order of units had on the concentration of C-PC throughout the process, as seen in Figure 39. The concentration of the crude extract of 5.21 ± 0.03 mg.mL^{-1} was similar to what was achieved previously. This was

again an unsurprising result due to the leaching step of the process remaining unchanged. Sending this crude extract to a precipitation step did enable the concentration of the C-PC to be significantly increased – again because the ammonium sulfate precipitation had the advantage of allowing the pellet to be resuspended to any desired volume. It was because of this that the C-PC concentration increased to 10.7 ± 0.2 $mg.mL^{-1}$ after precipitation from the crude extract, and the precipitation was able to increase the concentration of the diluted C-PC solution to 5.45 ± 0.20 $mg.mL^{-1}$. As discussed previously, the adsorption step reduced the concentration of C-PC in solution because of the ability of activated charcoal to adsorb C-PC onto its surface. Because of this, it was unsurprising the that the concentrations of both the high and low C-PC leachates were lower after the completion of the adsorption step – 7.78 ± 0.23 $mg.mL^{-1}$ and 3.81 ± 0.07 $mg.mL^{-1}$, respectively. However, it must be noted that these concentration values were still higher than what was obtained at the end of the proposed process (Figure 36).

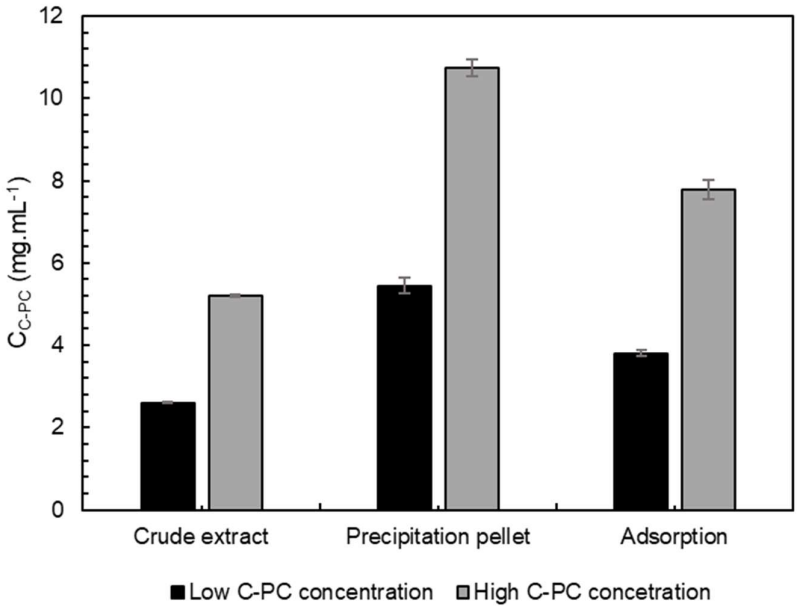

Figure 39: C-PC concentration following various stages of adjusted process. Error bars represent standard error on triplicate repeat experiments.

One of the main advantages to being able to measure the concentration of C-PC in a solution was to allow its recovery to be tracked throughout the process, as can be seen in Figure 40. The trends in recovery for each individual stage were similar to what was determined in the proposed process (Figure 37). The precipitation was able to completely retain almost all of the C-PC which was present in the crude extract, as could be concluded from the recovery values of 103 ± 2.3% and 105 ± 4.2% for the high and low C-PC concentration samples, respectively. As discussed previously, there was the possibility of errors arising when resuspending the precipitation pellet to a specific volume, and this potentially explains the recoveries of greater than 100%, which cannot physically be achieved. Despite these minor errors, the excellent recovery of the precipitation step was further confirmed by considering the C-PC lost to the supernatant where these values were only 0.119 ± 0.007% and 0.178 ± 0.014% for the undiluted and diluted crude extracts, respectively.

The adsorption step again did not achieve as high recoveries, due to some of the C-PC being removed out of solution – hence its lower concentration – and some of the solution being retained with the adsorbent pellet after centrifugation. It was for this reason that the recovery of the adsorption step was only 68.2 ± 2.9% for the higher concentration C-PC solution and 70.7 ± 2.7% for the one which had its C-PC content reduced initially. As has been discussed, improved recoveries were needed if this process is going to be successfully implemented to produce cosmetic-grade C-PC. Therefore, an alternative approach of conducting the adsorption step had to be considered – particularly the method of including and then separating the activated charcoal, as this makes the biggest contribution to the reduced recoveries.

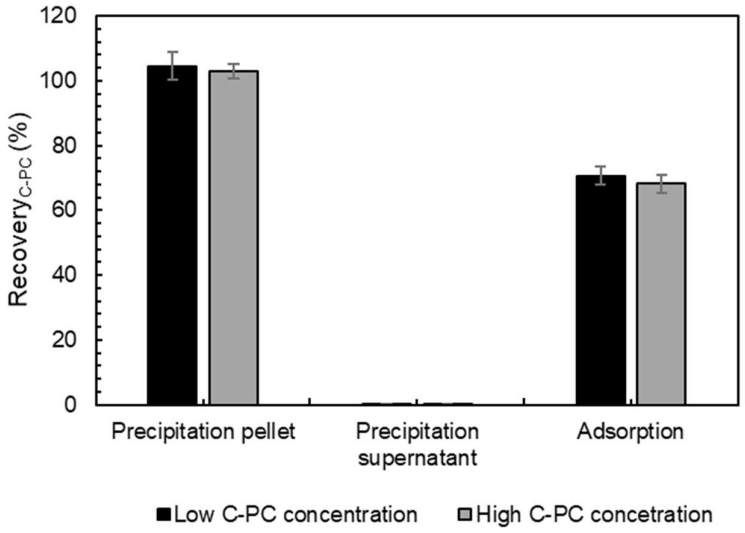

Figure 40: C-PC recovery following various stages of adjusted process. Error bars represent standard error on triplicate repeat experiments.

8.2.3 Attempted additional adsorption step

Before considering the option of altering the adsorption setup, it was first decided to test the impact of incorporating an additional adsorption step – after precipitation had taken place – to see if the purity of the higher C-PC concentration sample could reach 1.5. This was done on the higher C-PC sample at a variety of activated charcoal concentrations to understand what impact this had, while the chitosan in its dissolved form was still added at 0.2% by mass. A summary of these results can be seen in Table 9, where the treatment used is reported along with the C-PC purity, concentration and recovery following each of the steps.

The results of the attempted secondary adsorption clearly demonstrate that including an additional adsorption step did not improve the output of the process sufficiently to generate cosmetic-grade C-PC. Despite the purity before the secondary adsorption step being between 1.24 and 1.27, adding various amounts of activated charcoal and 0.2% chitosan by mass did not increase the purity to above 1.5. In fact, in the runs which included activated charcoal, the purity of C-PC decreased from their previous values. This is likely because, at these increased initial purities, the activated charcoal began to remove the C-PC out of the solution to a greater extent than the other impurities, which were present in lower concentrations. But even in the run in which no activated charcoal was included, the increase in purity from 1.27 ± 0.01 to 1.32

± 0.00 was minor and did not significantly benefit the process. Furthermore, this secondary adsorption step reduced the concentration of C-PC in the solution and reduced the overall recovery of the process – again particularly at higher activated charcoal contents. Ultimately, it can be concluded that increasing the complexity of the process by including this additional adsorption stage did not have the desired effect of enabling a C-PC product of purity of 1.5 to be reached.

Table 9: Results of secondary adsorption step for high concentration C-PC starting solution. Uncertainty represented by standard error based on *repeat analysis and †duplicate repeat experiments.

Activated charcoal (% w/w)	Stage	$Purity_{C\text{-}PC}$	$C_{C\text{-}PC}$ ($mg.mL^{-1}$)	$Recovery_{C\text{-}PC}$ (%)
0*	Before second adsorption	1.27 ± 0.01	7.19 ± 0.14	N/A
	After second adsorption	1.32 ± 0.05	6.09 ± 0.32	96.3 ± 5.0
4†	Before second adsorption	1.27 ± 0.06	6.67 ± 0.02	N/A
	After second adsorption	1.21 ± 0.10	5.27 ± 0.22	81.4 ± 2.6
8*	Before second adsorption	1.24 ± 0.01	6.29 ± 0.23	N/A
	After second adsorption	1.17 ± 0.01	4.62 ± 0.25	68.2 ± 3.6

8.3 Adsorption column runs

The biggest issue with the process in its current form – even when considering the high purities achieved when using the diluted crude extract – was the low recovery of the C-PC over the adsorption step. The adsorption, however, was crucial to maximising the purity which can be achieved, as can be seen from the results when it had not been included in the process. More specifically, the issue with the adsorption was that the use of high quantities of activated charcoal formed a large pellet after dead-end centrifugation which, as discussed, resulted in a significant amount of the purified liquid (including the desired C-PC) being lost with the pellet. This motivated for the testing of alternative configurations of the activated charcoal adsorption step, with the aim of improving the recovery while maintaining the degree of C-PC purification.

The configuration which was proposed and tested was to feed the crude extract through a column packed with granular activated charcoal. This hoped to benefit the process in a number of ways. Firstly, crude extract could be fed through the same column numerous times, allowing the activated charcoal particles to be reused. This was not possible for the powdered activated charcoal, as once the adsorbent pellet had been separated from the purified solution, it needed to be discarded and could not be regenerated. Secondly, the use of the column would eliminate the problem experienced previously where the adsorption pellet, formed after

centrifugation, trapped significant volumes of the C-PC solution, reducing the recovery achieved. The last potential advantage to this new configuration was that the larger particle sizes of activated charcoal used in the column, when compared to what was previously added into suspension, would not adsorb as high quantities of the C-PC itself when the C-PC solution was only passed once through the column, resulting in a further increase in the recovery achieved across this step of the process.

When using the columns for sets of experiments, it was important to flush them with citrate buffer between every C-PC sample to ensure that each run could be analysed accurately without the concern of contamination between the different tests. However, due to imperfect plug flow occurring within the packed columns, flushing them with the buffer resulted in axial mixing between the buffer and the C-PC solution still present in the column. Therefore, when attempting to recover the maximum amount of C-PC, it was inevitable that the C-PC was going to be diluted by the flushing buffer and its concentration would be lower than what would ordinarily be expected. However, the recovery of the C-PC could still be determined by taking into account the starting and final volumes and the respective concentrations of each. As discussed in Chapter 4.3.2, two sizes of granular activated charcoal particles were tested for use in the packed adsorption columns – 12 to 20 mesh and 4 to 12 mesh. Each column was tested for the level of maximum C-PC recovery, where these results can be seen in Table 10.

There was almost complete recovery of C-PC over the packed activated charcoal adsorption columns and there were significantly lower losses of the desired product when compared to the adsorption results presented previously. This indicated that the C-PC was able to pass successfully through the column, with very little of the solution being retained within the activated charcoal particles once it had been flushed with the citrate buffer. Additionally, the pigment itself was not being adsorbed out of the solution onto the surface of the particles and hence the losses of C-PC were also minimised in this manner. Therefore, this initial test of the packed adsorption columns showed potential in improving the C-PC purification process. However, it was still necessary to understand other aspects of the columns' performance.

Table 10: Results of C-PC recovery for packed adsorption columns. Uncertainty represented by standard error based on duplicate repeat experiments.

Activated charcoal mesh size	$Recovery_{C\text{-}PC}$ (%)
12 to 20 mesh	99.0 ± 1.6
4 to 12 mesh	96.4 ± 3.3

One way of doing this was to perform a residence time distribution (RTD) on the packed columns to visualise the flow profile of the liquid as it moved through the activated charcoal particles. A step tracer experiment was conducted for the purposes of this RTD as a constant concentration of C-PC was fed at the beginning of the test. In this case, the RTD was represented by a cumulative distribution function F(t) where this characterised the fraction of the tracer (the C-PC) which had left the reactor. The end point of this step tracer experiment was the point where the outlet concentration of the C-PC was equal to the concentration in the feed stream. The cumulative distribution function was calculated based on the concentration of the tracer in the exit stream, as can be seen in Equation 8.1.

$$F(t) = \frac{C(t)}{C_0} \quad 8.1$$

Within the equation to determine F(t), it must be noted that C(t) refers to the exit concentration of the tracer at a certain time, t, and C_0 is the constant tracer concentration fed in the inlet stream.

The RTD was performed on the column containing 12 to 20 mesh size particles by feeding the C-PC solution at a flowrate of 3.373 mL.min^{-1} and the results of this can be seen in Figure 41. The tracer profile represented by the cumulative distribution function was fairly close to what would be seen for a packed bed reactor, which is similar to the adsorption column used in the study. As discussed previously, there was not perfect plug flow within the column – which would not be expected due to the nonuniformity of the particle sizes and packing – and there was clearly some level of axial mixing taking place. There was an initial plug flow region seen in the short delay as the C-PC moved through the column. But after a period of approximately 25 minutes, the vast majority of the C-PC had left the column. Ultimately, this RTD investigation simply demonstrated that the column performed in a manner which was to be expected and that testing it as part of the C-PC purification process would hopefully provide reliable results which could be applied to other, similar systems.

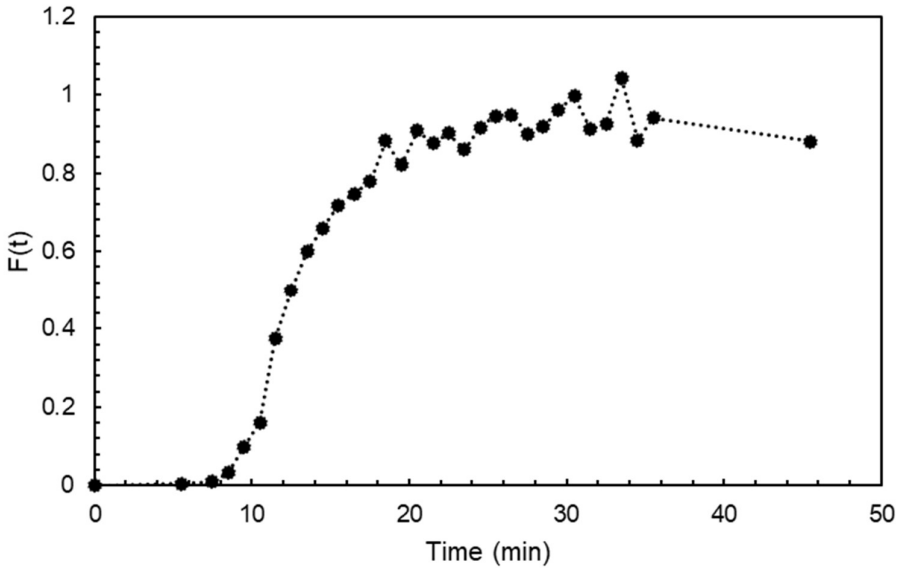

Figure 41: Residence time distribution of packed activated charcoal column using particles with mesh size of 12 to 20.

The next step in considering the performance of the packed columns was to understand how effective they were at improving the purity of C-PC and what impact they had on the other stages of the purification process. In order for this to be done in a manner that would be representative of an actual commercial process, the columns could not be run while trying to maximise the recovery of C-PC. The reason for this, as has been discussed previously, is because of the requirement to flush the column between runs and how this led to mixing between the C-PC solution and the citrate buffer, reducing the concentration of the C-PC in the sample. This is in contrast to an industrial process, where it would not be necessary to flush the column with buffer at such regular intervals and where many batches of C-PC crude

extract could be fed to the adsorption stage in succession. In order for this problem to be overcome – and for the solution exiting the columns to be as close to what would be expected for a commercial process – small sample volumes were recovered for analysis and fed to the further purification steps. Put differently, instead of trying to retain all of the C-PC which passed through the columns, the choice was made to limit the recovered volume to ensure that this smaller sample had not been mixed with the flushing buffer and therefore did not have its concentration unnecessarily lowered. This was important because, as has been shown, the concentration of C-PC in solution entering other purification stages – such as chitosan adsorption and precipitation – impacts the performance of these stages. Therefore, it was important for these concentrations to be as close to what would be expected when performing this process in a commercial setting.

The C-PC purity experiments on the activated charcoal columns also presented an opportunity to investigate different aspects of the columns' operation. One of these was to understand the impact of varying particle size on the effectiveness of the adsorption columns. Therefore two size distributions – 4 to 12 mesh and 12 to 20 mesh – were tested to identify if there were any noticeable differences. Additionally, the impact of varying the residence time within the columns was investigated by feeding the crude extract into the columns at two different flowrates – 3.373 $mL.min^{-1}$ and 1.000 $mL.min^{-1}$. Finally, as was done when adding powdered activated charcoal into suspension, the effect of feeding a low concentration C-PC sample – by diluting the crude extract with an equal volume of citrate buffer – was tested to understand if the columns could operate more effectively with this reduced concentration of C-PC.

A crude C-PC extract, once the cell debris had been removed, was fed to the columns with the output of this undergoing adsorption with chitosan added at 0.2% by mass, followed by ammonium sulfate precipitation taking place in the manner described previously. It was initially hoped to mix the chitosan – which had been dissolved in acetic acid – into the crude extract and feed this combined solution through the columns to allow for the chitosan and activated charcoal to positively interact with one another. However, the chitosan would not remain soluble while the solution was being fed, resulting in it blocking the tubing leading to the column. It was for this reason that it was decided to simply run the crude extract through the column and then include chitosan adsorption as a distinct step. Ultimately, the results of the several different runs can be seen both in terms of the performance of the columns themselves as well as the impact they had on the subsequent purification steps.

Figure 42 displays the results of the packed adsorption column tests by focusing on three different aspects of the purification stage – namely the feed flowrate, the concentration of C-PC in the crude extract as well as the particle size of activated charcoal used in the column. The impacts of each of these is seen in the column outputs as well as after chitosan adsorption (simply listed as chitosan on the axis of the figure) and ammonium sulfate precipitation (referred to as pptation for simplicity). Although Figure 42 presents a large amount of data, it is worth focusing on a few key results which allow for the most definitive conclusions to be drawn about the performance of the adsorption columns and their usefulness in the process as a whole. One of the most obvious trends was the significantly improved purity performance at the completion of the process for the samples which used the low C-PC concentration feed. The final purity for this low concentration sample was between 1.68 ± 0.18 and 2.61 ± 0.44 for the various combinations of particle sizes and flowrates, which was significantly higher than the equivalent range of 1.09 ± 0.02 to 1.16 ± 0.16 for the higher C-PC concentration solution. However, what is also interesting to note is that this difference in purity was smaller when considering the results immediately after the column adsorption – seen in the purity range of 0.61 ± 0.03 to 0.74 ± 0.01 for the low concentration solution and a range of 0.62 ± 0.02 to 0.78 ± 0.04 for the sample containing a higher level of C-PC. This implies that although there was

no significant improvement in the purity of C-PC using the diluted sample, when measured immediately after the column, the other purification steps are made more efficient and cosmetic-grade C-PC can be produced.

There are also trends that can be identified in Figure 42 as a result of adjusting both the liquid flowrate through the column and the particle size used. The various results seen when using 12 to 20 mesh size activated charcoal particles – which, as has been discussed, are smaller and therefore have a greater available surface area – showed an improvement in performance when compared to the 4 to 12 mesh size equivalents. At all stages of the process, for the different C-PC concentrations and volumetric flowrates, the purities of the samples purified, using 12 to 20 mesh activated charcoal, were always slightly higher. This difference was greater when specifically considering the purities of the low C-PC concentration runs after chitosan adsorption and precipitation. However, these results showed increased uncertainty and experimental error and therefore it was not possible to draw any definitive conclusions based on the suggested trends. Ultimately, the increased available surface area provided by the 12 to 20 mesh did lead to a slightly more efficient purification step by enabling higher numbers of unwanted contaminants to be removed. However, the fact that the improvement was only marginal can be explained by the closeness of the two particle size distributions – 12 to 20 mesh size and 4 to 12 mesh size – and therefore there was not a substantial difference in the average particle size within the two different columns. This implies that if even smaller granular particles were used, there could have been a more noticeable increase in the C-PC purity achieved, however these smaller particles might have had an adverse effect on the flow of the solution through the column if the feed pressure to the column remains the same.

When considering the impact of feed flowrate to the columns, there was a similar trend of results. The solution recovered when feeding the column at 1.000 $mL.min^{-1}$ tended to have higher C-PC purities than those attained with the flowrate of 3.373 $mL.min^{-1}$. But these differences were not as significant as those observed as a result of changing the C-PC concentration of the feed. As with the variable particle size, the most significant improvements as a consequence of using the lower flowrate appeared to be for the low C-PC concentration sample after chitosan adsorption and ammonium sulfate precipitation. However, these sets of data had significantly increased uncertainty due to the large experimental error, and therefore these apparent trends could not be deemed statistically significant. The slower feed flowrate naturally allowed for a greater residence time for the solution to remain in contact with the adsorbent present in the column. This, theoretically, should have improved the ability of the activated charcoal to remove the unwanted proteins and can explain the increase in C-PC purity seen when using the lower flowrate of 1.000 $mL.min^{-1}$. However, as was discussed in Chapter 2.3.2, it is reported in a few literature sources that only very short contacting times are required for activated charcoal adsorption within a C-PC purification process (Liao et al., 2011; Fekrat et al., 2019). This was therefore the likely explanation for why there was no significant benefit to increasing the residence time within the column and that the higher flowrate of 3.373 $mL.min^{-1}$ allowed for sufficient contacting between the unwanted proteins and the surface of the activated charcoal particles.

Therefore, it could be concluded that adjusting the flowrate to 1.000 $mL.min^{-1}$ and using the smaller activated charcoal particles did not significantly improve the process.

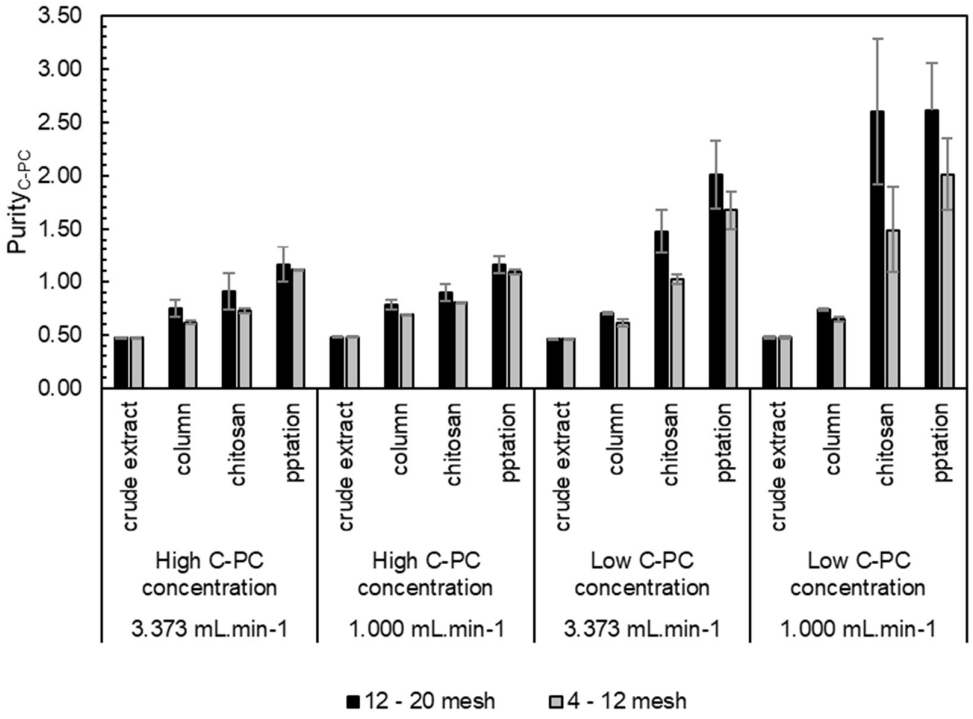

Figure 42: Summary of purity results for various tests on packed adsorption columns. Error bars represent standard error on duplicate repeat experiments. Column refers to solution obtained from packed adsorption column, chitosan refers to solution obtained after chitosan adsorption and pptation refers to solution obtained after ammonium sulfate precipitation.

As with the previous experiments, C-PC concentration was also tracked, presented in Figure 43. The C-PC concentration post-precipitation was not represented in Figure 43 as it was easily altered by adjusting the volume of resuspension and therefore the recovery (Figure 44) was a better indicator of the success of that stage of the process.

The data in Figure 43 demonstrates how the concentration of C-PC present in the solution was impacted by the packed adsorption columns. There was a clear reduction in the C-PC concentration from what was initially fed after the solution had passed through the columns – where this was true when using different activated charcoal particle sizes and different volumetric flowrates. As seen in Table 10, there was almost complete recovery of all C-PC within the columns and therefore this reduction in concentration was likely due to mixing of the C-PC crude extract and the citrate buffer, and not because C-PC was being adsorbed out of solution. As mentioned, this buffer was used to initially prepare the columns and to flush them out once the experimental run had been completed. Smaller volumes were recovered from the adsorption columns to try and minimise this effect, but there was clearly a certain degree of mixing even in these samples. What can be seen from Figure 43, other than the reduction in concentration after column adsorption, is that there was no noticeable impact of either adjusting flowrate or charcoal particle size on the concentration of C-PC. When using flowrates of either 1.000 $mL.min^{-1}$ or 3.373 $mL.min^{-1}$, there were no clear trends in terms of C-PC concentration as a result of this changing flowrate and all equivalent concentration values – i.e., when considering samples which have the same initial C-PC concentration, and which were treated using the same particle sizes – were within the level of uncertainty of one another. A similar conclusion could be easily drawn for the impact of activated charcoal particle size. The concentration levels for the black and grey bars in Figure 43 – which represent the two

different particle size ranges – were close to being identical for almost every combination of variables and stage of the process. For the only occasions where there was a difference in the observed concentrations, this difference was smaller than the level of uncertainty, as calculated from the standard error, and therefore it was possible to conclude that using slightly differently sized particles did not significantly impact the concentration of C-PC throughout the process.

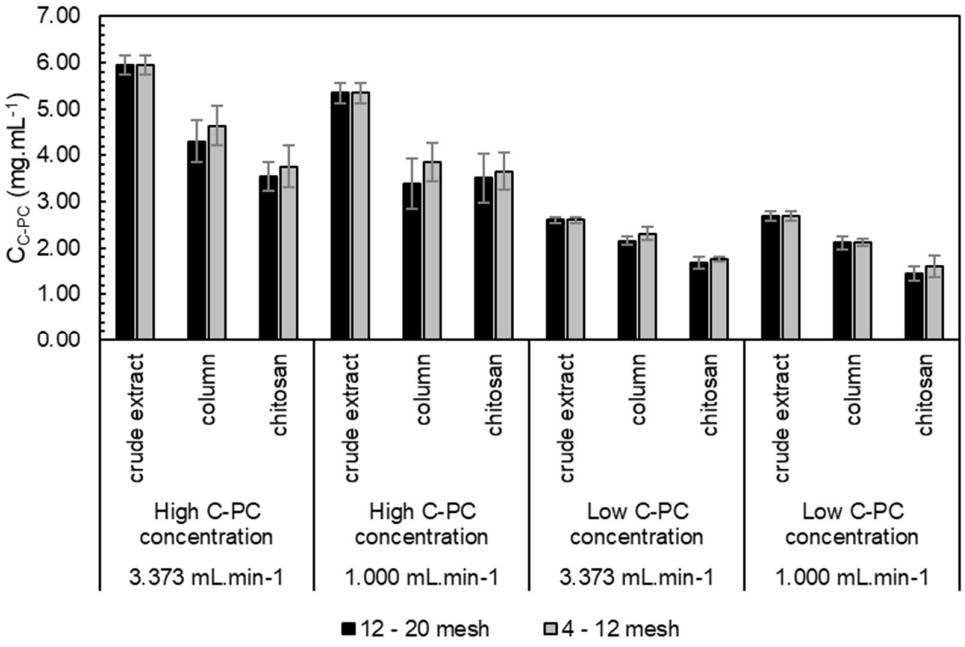

Figure 43: Summary of concentration results for various tests on packed adsorption columns. Error bars represent standard error on duplicate repeat experiments. Column refers to solution obtained from packed adsorption column, chitosan refers to solution obtained after chitosan adsorption and pptation refers to solution obtained after ammonium sulfate precipitation.

As was discussed in Chapter 8.2, the proposed process, including an adsorption step with powdered activated charcoal mixed into suspension, was able to consistently reach cosmetic-grade C-PC levels on a diluted crude extract sample. However, the issue with this configuration was the low recovery of C-PC in the adsorption step due to the nature of using powdered activated charcoal and dead-end centrifugation. Therefore, the idea to use the packed adsorption columns was to alleviate this issue and for this reason, the recovery results presented in Figure 44 are important in understanding if this had been achieved. The recovery of C-PC after the adsorption column step was not included in Figure 44 for the reasons discussed previously, where the small sample volume collected did not enable an accurate calculation of the recovery to be performed. However, what can be seen in Figure 44 is that the adsorption step containing only chitosan was able to achieve significantly higher recoveries than what were achieved previously. The recoveries across all the results presented in Figure 44 were more representative of what would be expected commercially, with a minimum recovery of 76.5 ± 3.2%, where this increased the possibility of the proposed process being able to operate profitably.

Within these results, it was difficult to draw any definitive conclusions on the impact of the varying flowrates or activated charcoal particle sizes, due to the similar results achieved and the high degree of uncertainty within certain aspects of the data. However, what can be taken away from Figure 44 is that the ammonium sulfate precipitation still showed negligible losses to the supernatant. Therefore, the recovery values reported for the ammonium sulfate precipitation were still likely impacted by the inaccuracies in taking volume measurements and in reality, the recovery across the precipitation step for all runs of the process was closer to 100%. The volume inaccuracies were also what likely contributed to the physically unobtainable recoveries of greater than 100% reported for certain results of the chitosan adsorption aspect of the process. Despite these potential minor errors, the general trend (namely that running the process using the adsorption column significantly improved the overall recovery) was still clear and could be used in further decisions about the viability of the process in producing C-PC commercially.

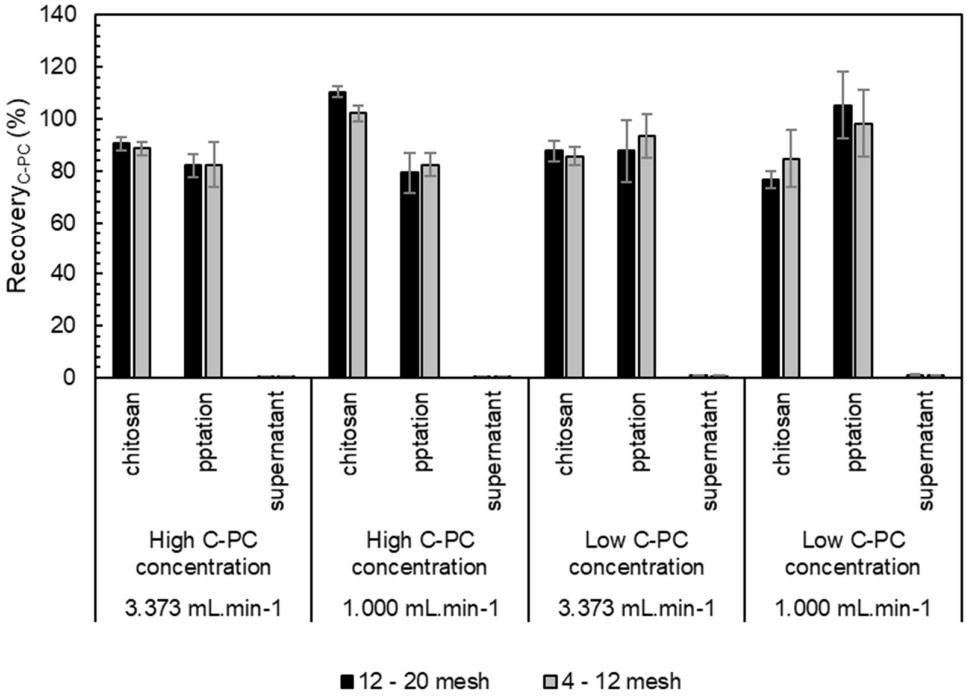

Figure 44: Summary of recovery results for various tests on packed adsorption columns. Error bars represent standard error on duplicate repeat experiments. Column refers to solution obtained from packed adsorption column, chitosan refers to solution obtained after chitosan adsorption and pptation refers to solution obtained after ammonium sulfate precipitation.

To better understand each step of the process, it was necessary to run it while excluding first the packed column and then the chitosan adsorption. In this manner, it would be possible to conclude if all aspects of the process were equally important and if certain steps could potentially be excluded without negatively impacting the final output. The results of this investigation can be seen in Table 11, where the test was only done on the low concentration C-PC sample – as this is the one which was shown to be able to reach the desired level for use in cosmetics (purity > 1.5). These experiments were also only conducted at a column flowrate of 3.373 $mL.min^{-1}$ through particle sizes of 12 to 20 mesh on the runs which excluded the chitosan adsorption.

The results presented in Table 11 make it clear that including both the packed column as well as the chitosan adsorption was essential to the process achieving its desired aim of generating C-PC with a purity of at least 1.5. From the previous results, when using the column packed with activated charcoal of sizes 12 to 20 mesh and feeding at a flowrate of 3.373 $mL.min^{-1}$, the purity achieved was 1.48 ± 0.21 after the chitosan adsorption step. This was significantly higher than the purities of 0.554 ± 0.001 and 0.646 ± 0.030 when only including either the chitosan or the packed columns respectively, as part of the adsorption step. This clearly indicates that both of these adsorption steps were crucial to the success of the overall process and when either one was not included, the final purities after precipitation of either 1.07 ± 0.03 or 0.972 ± 0.005 were lower than the 1.5 required.

Table 11: Results as part of test into packed adsorption columns for C-PC purification. Column excluded refers to control run in which crude extract was fed straight into chitosan adsorption. Chitosan excluded refers to control run in which output of packed column was fed straight to ammonium sulfate precipitation. Uncertainty represented by standard error based on *repeat analysis and †duplicate repeat experiments.

Run Type	$Purity_{C\text{-}PC}$ (%)		
	Crude extract	Adsorption	Precipitation
Column excluded*	0.467 ± 0.004	0.554 ± 0.001	1.07 ± 0.03
Chitosan excluded†	0.472 ± 0.001	0.646 ± 0.030	0.972 ± 0.005

This investigation into the use of a packed adsorption column as part of the C-PC purification process allows for a few conclusions to be drawn. The first is that the column step itself was able to achieve a high maximum recovery of C-PC and this, coupled with the minimal losses over both the chitosan adsorption and ammonium sulfate precipitation steps, made the process more likely to be successful commercially. Secondly, operating the adsorption step as a packed column with the larger particles of activated charcoal did not reduce the ability of this step to remove unwanted proteins, and the final purity when including the columns – no matter the particle size used or feed flowrate – was always significantly greater than the cosmetic-grade of 1.5. Finally, it was shown that the activated charcoal column and chitosan adsorption are both crucial to the success of the process.

However, in future it would be useful to try and incorporate the chitosan and activated charcoal adsorptions into one stage rather than conducting them as two distinct steps. This could be done by attempting to keep the chitosan in solution as it is fed through the column, or by physically incorporating the chitosan into the column itself by using it in a different physical form with larger particles, or by coating the powder onto glass beads, as an example, and adding them to the packed column. Ultimately, this could improve the performance of the purification by allowing the activated charcoal and chitosan to interact within the column and reduce the need for the additional centrifugation step to remove the chitosan pellet.

Additionally, when running the experiments with the packed adsorption columns, the columns were flushed with citrate buffer between each different test to ensure that each set of conditions could be evaluated without the concern that there would be contamination between the different samples. This process of flushing the columns may have removed some of the unwanted contaminants that remained after purifying the C-PC solution and enabled the activated charcoal particles to be regenerated. It was discussed previously that in a commercial process this period of column flushing is unlikely to take place as regularly, and

that the columns would either be run continuously or would only be flushed after several batches of crude extract had been purified. Therefore, over time there is the potential for these activated charcoal particles, and hence the packed adsorption columns, to become less effective. Because of this, it would be necessary to consider the required frequency of column regeneration or replacement of the adsorbent in the scaling-up process.

8.4 Performance of ultrafiltration

As has been previously discussed in Chapter 2.3.2, there are numerous benefits to including a filtration step within a C-PC purification process apart from attempting to improve the purity of the final product. In the case of the proposed process, there was already a sufficiently pure product generated at the completion of precipitation for the samples with the initially lower C-PC concentration. Therefore, the use of filtration in the process was not necessarily to further increase the C-PC purity – although this would naturally still be advantageous. Instead, the benefit to including microfiltration and ultrafiltration steps was to decrease both the amount of ammonium sulfate salt in the final product as well as the level of microbial contamination. Operating a microfiltration step with a 0.2 µm filter should be able to remove all bacteria and larger microorganisms and reduce the amount of contamination to an acceptable level. As seen in Chapter 6.5, adsorption was not able to achieve this successfully and so there is a considerable advantage in including microfiltration. Additionally, performing a buffer exchange as part of ultrafiltration results in the majority of the ammonium sulfate and other salts exiting in the filtrate, with the C-PC being recovered in the retentate. Salts present in the final product reduce the intensity of the blue colour, and removing them should thus increase the E-value of the sample and make it more commercially viable. The results of including filtration steps for several runs for both low and high concentration C-PC starting solutions can be seen in Tables 12 and 13.

Table 12 shows that the purities of the samples being fed to the filtration steps were already greater than the 1.5 required for cosmetic-grade C-PC, so the microfiltration and ultrafiltration were not required in order to meet this aspect of the product specifications. However, it should be noted that there was not a great deal of consistency in terms of the impact of the filtration on the purity of C-PC achieved. There were examples of the purity of the C-PC being increased by both the microfiltration and ultrafiltration while there were also examples of these steps slightly reducing the C-PC purity from what was in the initial solution. The reason for this could have been as a result of changes in the different purification steps used to generate the solution being fed to the filtration – i.e., the exact nature of the adsorption and precipitation stages included as well as the order in which they were performed. However, it must be noted that at these high purity values, there were lower concentrations of unwanted proteins and therefore reduced absorbance readings at a wavelength of 280 nm. This had an impact on the level of experimental error, because at the low values of the 280 nm absorbance, small changes in this specific absorbance reading could significantly impact the purity calculation due to the fact that it is a ratio with the OD_{280} present in the denominator, as can be seen from Equation 2.1. However, the final C-PC purity remained sufficiently high in all the samples.

Table 12: Summary of purity results of filtration steps for low concentration C-PC starting solution. Uncertainty represented by standard error based on repeat analysis.

Run Type	$Purity_{C\text{-}PC}$ (%)		
	Before microfiltration	Before ultrafiltration	After ultrafiltration
Run 1	1.57 ± 0.03	2.01 ± 0.08	2.23 ± 0.29
Run 2	1.88 ± 0.064	1.54 ± 0.03	2.13 ± 0.19
Run 3	2.34 ± 0.17	1.81 ± 0.13	2.13 ± 0.05
Run 4	1.97 ± 0.13	2.27 ± 0.03	2.17 ± 0.14
Run 5	2.00 ± 0.04	1.76 ± 0.14	1.83 ± 0.00
Run 6	2.85 ± 0.15	2.93 ± 0.08	2.85 ± 0.10

The results presented in Table 13 for the samples with high initial concentrations of C-PC – i.e. those crude extracts which were not diluted with citrate buffer after cell debris removal – showed similar impacts of the filtration steps on the purity of the C-PC. The purity was occasionally increased by both filtration steps, but the purities after microfiltration and ultrafiltration could also be seen to be lower than what was initially fed. With these samples the purity before filtration was generally lower than the 1.5 desired and it could be seen that the filtration step of the process was not able to consistently and reliably increase the purity to above what would be classified as cosmetic grade. This implies that the process – even with the inclusion of the filtration – was not able to generate cosmetic-grade C-PC if the crude extract was not diluted prior to the purification steps.

Table 13: Summary of purity results of filtration steps for high concentration C-PC starting solution. Uncertainty represented by standard error based on repeat analysis.

Run Type	$Purity_{C\text{-}PC}$ (%)		
	Before microfiltration	Before ultrafiltration	After ultrafiltration
Run 1	1.39 ± 0.01	1.66 ± 0.01	1.89 ± 0.13
Run 2	1.35 ± 0.01	1.36 ± 0.03	1.30 ± 0.11
Run 3	1.40 ± 0.03	1.25 ± 0.03	1.37 ± 0.02
Run 4	1.34 ± 0.00	1.40 ± 0.06	1.54 ± 0.01
Run 5	1.57 ± 0.02	1.79 ± 0.05	1.62 ± 0.20
Run 6	1.31 ± 0.02	1.58 ± 0.06	1.52 ± 0.02

It was also important to understand if there were any losses of C-PC within the filtration stages, as this could negatively impact the commercial viability of the proposed process. Naturally, being able to recover as much of the C-PC within each step was essential to ensuring that the process could operate profitably. The recoveries of the ultrafiltration step, as well as the losses associated with C-PC passing through the membrane and exiting in the filtrate, can be seen in Table 14. Importantly, the C-PC concentration in the filtrate was reported in $mg.L^{-1}$ as opposed to the $mg.mL^{-1}$ which had been used previously due to the low values of the concentrations.

The results presented in Table 14 show a fairly wide range of recoveries being achieved in the ultrafiltration step. The lowest recovery of 32.8 ± 1.1% was significantly lower than the maximum recovery achieved of 86.8 ± 0.6%. This implies that there was a level of unpredictability associated with running the ultrafiltration step as it was not always known how much C-PC would be retained in the output. However, what is important to note is that the low recoveries were not as a result of C-PC passing through the ultrafiltration membrane and exiting the process in the filtrate waste stream. This is seen in the extremely low concentrations of C-PC present in the filtrates – where the highest concentration measured was only equal to 3.67 ± 0.53 $mg.L^{-1}$ which was considerably lower than the equivalent concentration in the retentate of 3.03 ± 0.18 $mg.mL^{-1}$. This implies that the low recoveries were more likely as a result of the manner of conducting the ultrafiltration on the small scale – particularly the losses due to C-PC remaining in the tubing of the tangential flow filtration unit. These losses, although appearing to be significant based on the results in Table 14, are likely not representative of what would occur when running the process on an industrial scale – either continuously or with multiple batches. Therefore, the recoveries obtained within the ultrafiltration do not detract from the positive aspects of including filtration in the process – such as the removal of ammonium sulfate and unwanted microorganisms.

Table 14: Summary of recovery results of ultrafiltration. Uncertainty represented by standard error based on repeat analysis.

Run Type	Low C-PC concentration		High C-PC concentration	
	Recovery$_{C\text{-}PC}$ Ultrafiltration (%)	**$C_{C\text{-}PC}$ in Filtrate ($mg.L^{-1}$)**	**Recovery$_{C\text{-}PC}$ Ultrafiltration (%)**	**$C_{C\text{-}PC}$ in Filtrate ($mg.L^{-1}$)**
Run 1	53.5 ± 1.3	1.99 ± 0. 11	54.0 ± 2.6	3.24 ± 1.20
Run 2	79.4 ± 1.4	2.03 ± 0.68	32.8 ± 1.1	1.78 ± 0.00
Run 3	86.6 ± 0.6	1.90 ± 0.51	78.4 ± 5.1	1.97 ± 0.76
Run 4	74.8 ± 4.3	3.67 ± 0.53	69.3 ± 2.6	3.45 ± 0.78
Run 5	85.4 ± 1.2	3.54 ± 1.10	82.4 ± 0.5	2.47 ± 6.90
Run 6	70.8 ± 0.9	2.91 ± 0.00	77.1 ± 3.6	0.648 ± 0.46

8.5 Inclusion of freeze drying

Certain samples which had undergone microfiltration and ultrafiltration were sent through a freeze dryer to prepare C-PC in powdered form, as would be done in a commercial process. The powdered samples were then redissolved in distilled water to make a 1% solution and tested for purity, concentration and E-value. The results of the resuspended powder samples were then compared to those of the liquid samples prior to freeze drying to understand what impacts this step had on the C-PC. The results of testing the freeze dried samples can be seen in Table 15, where this focused on the samples which had an initially reduced concentration of C-PC in the crude extract. Table 16 displays similar results, but focuses on samples prepared using the high C-PC concentration crude extract solutions. The breakdown of the exact purification techniques used in Runs A to E can be found in Appendix A3.

Before considering the results presented in Tables 15 and 16, it must be noted that due to inefficiencies in the performance of the freeze drying equipment, the samples were not able to be consistently dried to the same extent. Specifically, the samples from Runs A and B were not as effectively dried and therefore it was challenging to extract a reasonable amount of the dried powder in order to make a 1% solution. For this reason, it is likely that there were

inaccuracies in the measurements taken from these two runs. This, coupled with the reduced C-PC concentration for these samples initially, as seen from Tables 15 and 16, potentially explains why the E-values and final concentrations for these samples were considerably lower than the other samples.

What is clear from the results in Tables 15 and 16, especially when only considering Runs C to E, is that the purity of C-PC remained fairly stable throughout the process of freezing the samples, storing them, and running them through the freeze dryer. The purity did drop slightly in Runs C and D, but this was only a minor decrease and did not significantly impact the quality of the C-PC product being generated. There was the potential of degradation of the C-PC throughout the storage and freeze drying of the samples and so it is a positive result that this did not seem to occur and that this stage can be incorporated without the concern that it would have a significant detrimental impact on the process. It must be noted that with Run E, there was an increase in purity from 2.85 ± 0.10 to 3.24 ± 0.01 for the low concentration sample and from 1.52 ± 0.02 to 2.49 ± 0.02 for the high concentration sample. This significant improvement in purity between the original liquid samples and the 1% solution of the C-PC powder is difficult to explain. There was no logical reason why the purity would increase to this extent, especially when this did not occur for the remaining samples.

As can be expected though, the concentration of C-PC was considerably higher in the dried powder than was present in the liquid solutions. Naturally, the evaporation of a significant amount of the water present through the drying process increased the relative concentration of the C-PC remaining. The increase in concentration ranged from a factor of 3.86 to a factor of 14.8, depending on the starting concentration and the success of the drying for each sample. This was one of the main advantages of including a drying stage in the process as it reduced the volume of the samples which would need to be stored and transported, making it easier and cheaper to sell the C-PC commercially.

The last important aspect of the results presented in Tables 15 and 16 is the calculated E-values for the various samples. Before discussing these results, it is useful to first confirm what a typical E-value would be for cosmetic-grade C-PC and hence how these samples compared with what was available. Three commercial samples of C-PC powder were obtained from Carbocraft, where they were marketed as E10, E18 and E30. Similar tests were done on these samples where the purity, concentration and E-value were determined and these can be seen in Table 17.

It can be concluded from Table 17 that the calculated E-values for each of the commercial samples was almost equivalent to the marketed value. This confirmed the accuracy of the method used to determine these E-values. What is interesting to note, however, is that despite the vastly different E-values for the three samples, they all had similar C-PC purities and the E30 powder – which had the highest E-value and market price – had the lowest purity. This further emphasised, as was mentioned previously, that the E-value is independent of the purity and that both properties need to be considered when attempting to market a C-PC product.

As was discussed in Chapters 8.2 and 8.3, the proposed process showed a great deal of promise when used to prepare C-PC from a low concentration crude extract and would likely be used in any commercial application moving forward. Therefore, it was important to compare these runs, seen in Table 15, to the commercial C-PC samples. Excluding Runs A and B, which as discussed were not truly representative, the remaining samples all had purities considerably higher than cosmetic grade and had E-values higher than the E10 powder and were of similar quality to E18 (this was also true for the E-values calculated on Runs C to E of the high concentration samples). Adding to this, the sample from Run E had an E-value of almost equivalent to the highest of the commercial powders, E30. It was shown in great detail

previously that the proposed process was able to generate C-PC with adequate purity for cosmetic applications when using a diluted crude extract. But further to this, the results indicate that the inclusion of the ultrafiltration step was able to sufficiently reduce the quantity of ammonium sulfate and other salts and ensured that the E-value of the resulting product was competitive with alternatives available commercially.

Table 15: Summary of results on freeze dried low concentration C-PC starting solution. Initial liquid sample refers to sample initially purified and analysed before being stored in freezer. 1% solution of C-PC powder refers to C-PC powder which had been freeze dried and was diluted in water to make a 1% solution. Uncertainty represented by standard error based on repeat analysis. Breakdown of purification techniques used for Runs A to E can be found in Appendix A3.

Run No.	Initial liquid sample		1% solution of C-PC powder		
	$Purity_{C\text{-}PC}$	$C_{C\text{-}PC}$ ($mg.mL^{-1}$)	$Purity_{C\text{-}PC}$	$C_{C\text{-}PC}$ ($mg.mg\ powder^{-1}$)	E-value
Run A	2.23 ± 0.29	0.863 ± 0.021	1.64 ± 0.26	3.33 ± 0.13	2.78 ± 0.19
Run B	2.13 ± 0.19	0.452 ± 0.008	1.53 ± 0.15	2.01 ± 0.05	1.66 ± 0.06
Run C	2.17 ± 0.14	3.03 ± 0.180	2.12 ± 0.02	24.6 ± 0.40	21.2 ± 0.33
Run D	1.83 ± 0.00	4.59 ± 0.066	1.64 ± 0.03	20.3 ± 0.35	17.6 ± 0.31
Run E	2.85 ± 0.10	2.14 ± 0.046	3.24 ± 0.01	31.6 ± 0.15	26.5 ± 0.12

Table 16: Summary of results on freeze dried high concentration C-PC starting solution. Initial liquid sample refers to sample initially purified and analysed before being stored in freezer. 1% solution of C-PC powder refers to C-PC powder which had been freeze dried and was diluted in water to make a 1% solution. Uncertainty represented by standard error based on repeat analysis. Breakdown of purification techniques used for Runs A to E can be found in Appendix A3.

Run No.	Initial liquid sample		1% solution of C-PC powder		
	$Purity_{C\text{-}PC}$	$C_{C\text{-}PC}$ ($mg.mL^{-1}$)	$Purity_{C\text{-}PC}$	$C_{C\text{-}PC}$ ($mg.mg\ powder^{-1}$)	E-value
Run A	1.95 ± 0.08	1.19 ± 0.04	1.44 ± 0.05	7.13 ± 0.06	5.90 ± 0.05
Run B	1.30 ± 0.11	1.16 ± 0.04	1.20 ± 0.04	10.3 ± 0.07	8.73 ± 0.08
Run C	1.54 ± 0.01	3.89 ± 0.15	1.44 ± 0.01	23.1 ± 0.09	20.0 ± 0.08
Run D	1.62 ± 0.20	2.56 ± 0.02	1.57 ± 0.02	17.1 ± 0.04	14.8 ± 0.09
Run E	1.52 ± 0.02	3.61 ± 0.17	2.49 ± 0.02	19.7 ± 0.14	16.8 ± 0.11

Table 17: Summary of results on commercial C-PC samples. 1% solution of C-PC powder refers to C-PC powder which had been freeze dried and was diluted in water to make a 1% solution. Uncertainty represented by standard error based on repeat analysis.

Sample	1% solution of C-PC powder		
	$Purity_{C\text{-}PC}$	$C_{C\text{-}PC}$ (mg.mg powder^{-1})	E-value
E10	2.03 ± 0.04	12.8 ± 0.3	10.8 ± 0.2
E18	2.07 ± 0.03	22.1 ± 0.1	19.1 ± 0.09
E30	1.90 ± 0.01	33.4 ± 0.1	30.2 ± 0.1

8.6 Process robustness

The positive results achieved when using the proposed process for purification of C-PC – as have been discussed in great detail and presented throughout this chapter – have all been achieved on the same sample of initial *Spirulina* feed. Therefore, before definitively concluding that the process was successful at generating cosmetic-grade C-PC, it was important to test other sources of *Spirulina* to understand if any of the positive aspects seen until this point were simply associated with the specific algal powder used or if the process was flexible and robust enough to accommodate variations in the feed. As was discussed in Chapter 4.3.2 within the methodology chapter, three other sources of *Spirulina* were tested in addition to the original CC sample.

Each powder was fed to the process and underwent the same purification steps, beginning with an initial leaching followed by cell debris removal, chitosan and activated charcoal adsorption and, finally, ammonium sulfate precipitation. This was done on a sample with high concentration of C-PC and was also tested on lower concentration samples by diluting the crude extract of each powder with equivalent volumes of citrate buffer, as was done previously.

Running the process on the different *Spirulina* samples by using the high concentration C-PC solution, as seen in Figure 45, gave rise to interesting results and allowed certain conclusions to be drawn. The first noticeable result was the extremely similar crude extract purities between the CC, HCW and NC samples. The range of purities between these three samples was only from 0.462 ± 0.013 to 0.466 ± 0.007. This very narrow distribution was noteworthy because the three powders were all originally sourced from China through South African suppliers. Therefore, there is the possibility that they were purchased from the same algae producer in China and that the samples were not actually distinct. When looking at the sample from India however, the RSP, it can be seen that the crude extract purity of 0.556 ± 0.012 was slightly higher than the other three which were tested. This improvement was not substantial however and so it can be concluded that the crude extracts generated after leaching and cell debris removal were all fairly similar.

There were slightly more obvious differences in performance once these different samples underwent purification. This implies slightly different levels of unwanted proteins and other contaminants in the various crude extracts and could have had an impact on the effectiveness of the purification steps. The lowest purity achieved after adsorption was 1.22 ± 0.02 for the CC sample – which was similar to the equivalent purity reported in Figure 35. The three other samples all performed better with the highest average purity obtained using the NC *Spirulina* – with a value of 1.77 ± 0.33. This indicates that despite the similar purities of the crude extract,

this was not necessarily a reflection of the situation after undergoing purification. This is seen further when considering the results after the ammonium sulfate precipitation where the purity difference between the CC *Spirulina* and the three newly tested samples was even greater. The CC purity of 1.33 ± 0.02 – again in line with what was obtained previously – was substantially lower than the next performing purity of 1.67 ± 0.14 from the HCW. The RSP and NC achieved even higher purities of 2.05 ± 0.22 and 2.12 ± 0.43, respectively. All the results seen in Figure 45 and discussed here are positive for the potential robustness of the process. The fact that the lowest purities achieved were for the CC sample which has been thoroughly tested makes it clear that the proposed process was able to operate at its same level of efficiency even if the *Spirulina* powder used was changed. However, as has been discussed previously, it was not sufficient to only study the purity results to understand the effectiveness of a C-PC purification process; the recoveries of the different steps also needed to be considered. For this reason, Figure 46 shows the recoveries of the different *Spirulina* powders throughout the purification stages to understand if this aspect of the process was also able to handle varying feeds.

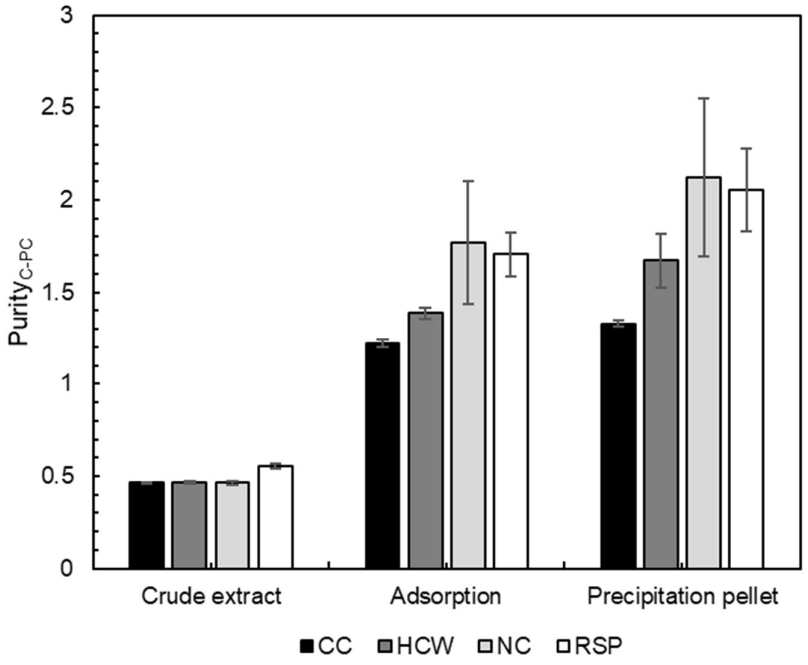

Figure 45: C-PC purity following various stages of the extraction and purification process for different *Spirulina* samples (CC, HCW, NC and RSP) for high concentration C-PC starting solution. Error bars represent standard error on triplicate repeat experiments.

Fortunately, as can be seen from Figure 46, the recovery of the process stages was not significantly impacted by the changing *Spirulina* powder. The range of recovery after adsorption was between 59.8 ± 1.9% and 67.1 ± 2.0%, which shows that it was not very dependent on the choice of feed. As discussed previously, the recoveries when mixing the adsorbents into suspensions and using dead-end centrifugation were lower than would be desired for a commercial process, and hence the idea of conducting the activated charcoal adsorption in a packed column is so attractive. Similar recoveries were achieved through the precipitation step for each sample. The recovery was the lowest when using the CC *Spirulina* with a value of 88.3 ± 0.3% and a maximum of 95.6 ± 0.4% for the HCW. Again, this showed

a fairly narrow range of recoveries and implied that changing *Spirulina* did not impact this part of the process. As has been previously discussed, these recoveries were fairly susceptible to experimental error, due to inaccuracies in taking volume measurements of the resuspended precipitation pellet. It was therefore important to consider the losses to the supernatant from the precipitation, which could be more accurately determined. These values again did not vary significantly for the different samples of *Spirulina*, ranging between 0.304 ± 0.059% and 0.350 ± 0.021%. These extremely low losses to the supernatant indicated that there was almost complete recovery of the C-PC for all sources of *Spirulina*. Based on this, and the other results presented in Figures 45 and 46, it can be concluded that the purification stages operated at similar performance levels for the different feed sources when the higher C-PC concentration starting solution was used.

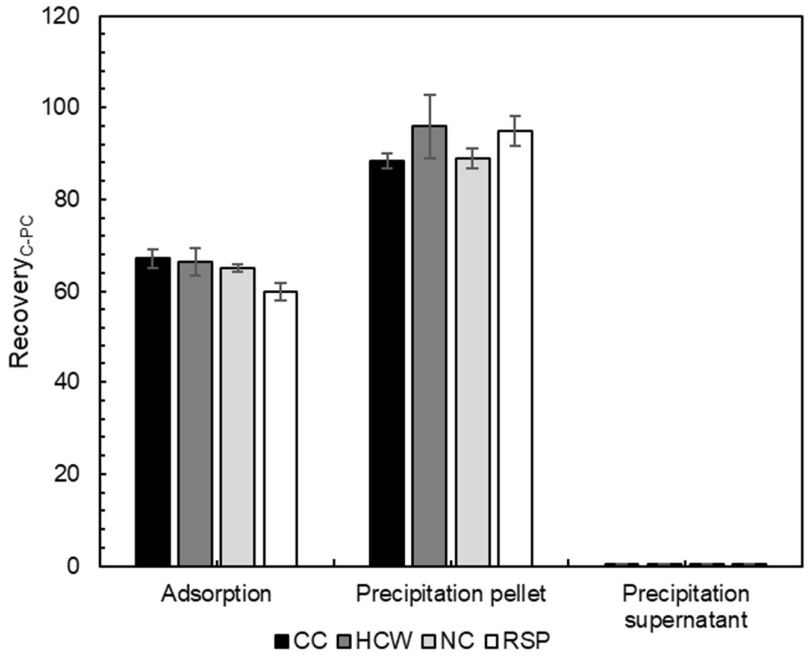

Figure 46: C-PC recovery following various stages of the extraction and purification process for different *Spirulina* samples (CC, HCW, NC and RSP) for high concentration C-PC starting solution. Error bars represent standard error on triplicate repeat experiments.

Purities and recoveries achieved using a low C-PC concentration starting solution are presented in Figures 47 and 48. When considering Figure 47, it can be seen that a similar set of results was observed as that seen for the high concentration starting solution. The range of crude extract purities was still very narrow for the CC, HCW and NC samples, where the purities seen were between 0.440 ± 0.004 and 0.475 ± 0.004. The RSP again had a slightly higher crude extract purity but its value of 0.539 ± 0.008 was not substantially greater than what was obtained for the other three samples. However, there was a greater difference in purity once the adsorption stage had taken place, as was seen previously. The CC sample produced a C-PC purity of 1.70 ± 0.17 – which it must be noted was already higher than what was needed for cosmetic-grade C-PC – but was still lower than the other three samples. These ranged from 2.02 ± 0.05 to 2.07 ± 0.11 and clearly showed that the process was still able to operate effectively when the crude extracts prepared from the different *Spirulina* sources were diluted and treated with activated charcoal and chitosan. This effectiveness continued when

considering the ammonium sulfate precipitation, where the lowest purity achieved was for CC with the other samples performing noticeably better. The CC purity obtained of 1.97 ± 0.06 was similar to what was seen in the initial tests of the proposed process, presented in Figure 35, and was substantially higher than what would be needed for C-PC used in cosmetic applications. However, the other samples had an even better performance, with the purities achieved being equal to 2.22 ± 0.01, 2.25 ± 0.10 and 2.34 ± 0.09 for RSP, NC and HCW, respectively. This further emphasised the idea that the process was able to sufficiently deal with different feeds and its effectiveness was not simply limited to the use of a specific *Spirulina* source.

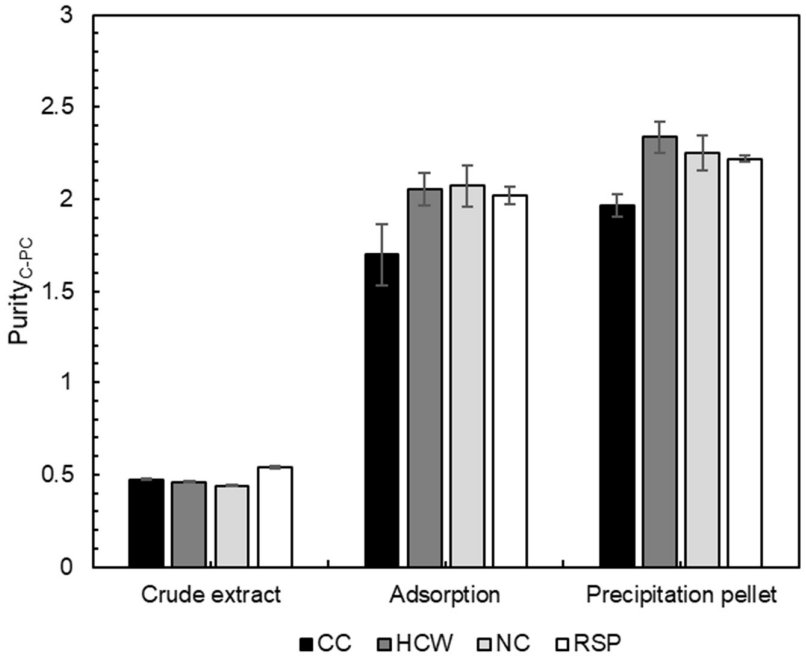

Figure 47: C-PC purity following various stages of the extraction and purification process for different *Spirulina* samples (CC, HCW, NC and RSP) for low concentration C-PC starting solution. Error bars represent standard error on triplicate repeat experiments.

This conclusion was further confirmed by considering the variations in C-PC recovery for the low concentration starting solutions, shown in Figure 48. The adsorption recoveries were again within a very narrow range, where the lowest recovery obtained was equal to 56.2 ± 2.7% and the highest was 60.2 ± 1.5%. These recoveries were lower than what would be desired for commercial applications, but that is an issue which could be mitigated by changing the configuration of the adsorption step, as has been previously discussed. What is important to take away from the adsorption aspect of Figure 48 was that the use of the different *Spirulina* sources did not have an adverse effect on the recovery which could be achieved, and that all the powders performed similarly. This was also true for the recovery within the precipitation pellet, where the range of values was between 86.9 ± 2.9% and 91.4 ± 3.9%. As was discussed for the higher C-PC concentration samples, the fact that the losses due to the supernatant were only between 0.848 ± 0.150% and 1.19 ± 0.23% implied that the precipitation recoveries were likely underestimated due to issues with measuring the volume of the resuspended pellet. But again, the important conclusion to draw from Figure 48 is that the precipitation recovery was not negatively impacted by the use of the different *Spirulina*

powders and that all aspects of the proposed process seemed to show a high degree of robustness.

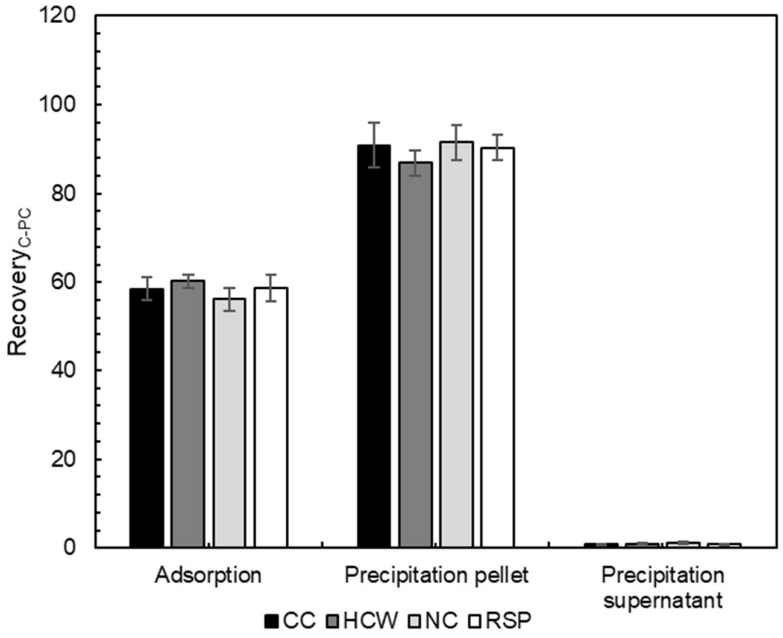

Figure 48: C-PC recovery following various stages of the extraction and purification process for different *Spirulina* samples (CC, HCW, NC and RSP) for low concentration C-PC starting solution. Error bars represent standard error on triplicate repeat experiments.

8.7 Conclusions

This chapter focused on the process designed for the production and purification of C-PC from *Spirulina* developed and suggested by Griffiths (personal communication, 2022). The process in its proposed form begins with an initial overnight leaching period after suspending the algal powder in citrate buffer without the inclusion of cell disruption. The crude C-PC extract is then treated with chitosan and activated charcoal as part of an adsorption step and further purified using ammonium sulfate precipitation. The resuspended pellet then undergoes microfiltration and ultrafiltration before the C-PC powder is prepared by freeze drying. The initial goal of this part of the research project was to test the overall process in its current form to understand if it was able to successfully and reliably produce cosmetic-grade C-PC.

Multiple repeats of the process were conducted and the results were analysed in terms of C-PC purity, concentration and recovery. It was found that when the crude extract was mixed with an equal volume of citrate buffer prior to adsorption, the process was able to generate a C-PC purity of 2.00 ± 0.10 at the completion of the precipitation step. When the concentration of the C-PC in the crude extract was not reduced, the final purity only reached a value of 1.27 ± 0.03. This implied that the process showed potential for generating C-PC for cosmetic applications but dilution of the crude extract was crucial to its overall success. The biggest concern with respect to C-PC recovery was the low recovery achieved over the adsorption stage with activated charcoal and chitosan, which was only 60.9 ± 1.1% and 61.0 ± 0.9% for the low and high concentration crude extracts. This was significantly lower than would be

hoped for a viable commercial process and therefore this was an aspect of the process to attempt to improve.

Other process configurations were tested, with the aim of increasing the obtainable purity for the high concentration starting solution and attempting to reach the desired minimum value of 1.5. The first process adjustment made was to rearrange the order of the adsorption and precipitation steps. This was done with the anticipation that the adsorption would potentially be made more efficient after some of the contaminating proteins had been removed through precipitation. Ultimately, this did not have the desired effect. Although improved from what was seen previously, the same issues were still evident, including a low recovery over the adsorption step (70.7 ± 2.7%). The final purities obtained after adsorption were 1.61 ± 0.31 and 1.42 ± 0.09, for the diluted and undiluted crude extracts respectively. This indicated that adjusting the order of the process units was not sufficient to enable the high concentration sample to reach the goal of a purity of 1.5, while it also reduced the effectiveness of the process for the solution with low C-PC concentration.

Another configuration tested was to include a second adsorption step after the initial adsorption and precipitation had taken place. Different quantities of activated charcoal – 0%, 4% and 8% on a mass basis – were tested for this step to determine what would be the most effective. However, it was found that none of the purities obtained – 1.32 ± 0.00, 1.21 ± 0.10 and 1.17 ± 0.01 – were at the desired level. The two samples which had higher activated charcoal contents actually resulted in reduced C-PC purities when compared to the solutions which were fed to this additional step. Ultimately, this implied that it was not possible to reach the goal of a purity of 1.5 for the higher concentration sample and instead it was decided to rather focus on improving the recovery of the adsorption step.

This was done by changing the way in which the activated charcoal was included in the adsorption. Rather than adding activated charcoal in powdered form into suspension, the C-PC solution was fed through columns packed with granular activated charcoal particles. Two different particles size distributions were used – 4 to 12 mesh and 12 to 20 mesh. The solution was also pumped through the columns at two different flowrates – 1.000 $mL.min^{-1}$ and 3.373 $mL.min^{-1}$ – to understand what impact the flowrate (and so residence time in the column) had on the performance. As with the previous tests, two different concentrations of C-PC were fed to the column – one which was the standard crude extract and another which had first been diluted with citrate buffer. As part of this investigation, it was shown that the maximum recovery of C-PC through the columns was equal to 99.0 ± 1.6% and 96.4 ± 3.3% for the 12 to 20 mesh and 4 to 12 mesh particles, respectively. This was a significant improvement on the recovery achieved with the adsorption suspension and subsequent dead-end centrifugation, and thus demonstrated the potential benefit of using the packed columns. Using these adsorption columns in the C-PC purification process also enabled high purity C-PC to be produced for the low concentration crude extract, with the range of purities at the end of the process being between 1.68 ± 0.18 and 2.61 ± 0.44. Although slightly higher purities were achieved at the lower flowrate and smaller particle sizes (the 12 to 20 mesh distribution), these differences were not significant, and all configurations were able to produce cosmetic-grade C-PC. When high concentration crude extract was fed to the adsorption columns, the purification was not as successful. The purity in this case ranged between 1.09 ± 0.02 and 1.16 ± 0.16.

The major benefit of using the columns was the improved recovery. All the steps in this configuration of the process – the packed activated charcoal column, chitosan adsorption and ammonium sulfate precipitation – were able to achieve high recoveries, with the lowest value seen across all of these steps being only 76.5 ± 3.2%. There was also no noticeable effect

caused by changing the particle size of the activated charcoal or the flowrate on the recovery achieved over the columns. The higher recovery over the adsorption step meant that the overall recovery of C-PC across the entire process was also significantly improved, relative to when the adsorption was conducted with powdered activated charcoal. This means that there is greater potential for it to operate in a commercially viable manner. The performance of the process was also tested without the packed activated charcoal column or the chitosan adsorption step. This was done using a low concentration crude extract. The final purities achieved in these runs were only 1.07 ± 0.03 and 0.972 ± 0.005, respectively. These significantly reduced purities confirm that both of these steps are required to meet the desired purity of 1.5 and imply that the process is not able to operate as efficiently when even one of them is not included.

The next set of results investigated the impact of microfiltration and ultrafiltration on the output of the process. The purpose of including both microfiltration and ultrafiltration was to remove unwanted microorganisms and reduce the amount of ammonium sulfate in the final product. The success of the ultrafiltration step can be seen in the E-values obtained for the final freeze dried products, which were comparable to samples available commercially. The filtration steps did not consistently improve the purity of C-PC and, on occasion, the purity was lower after the filtration when compared to what was fed to that stage of the process. However, for the low concentration samples, the purity before filtration was already comfortably above the 1.5 required.

Despite these positive results, the recovery of C-PC across the ultrafiltration step was found to show a high degree of variation – with a range from 32.8 ± 1.1% to 86.6 ± 0.6% – with some of these being lower than would be desired for a commercial process. Yet, the negligible C-PC concentrations measured in the filtrate implied that the losses were minimal. Therefore, the low recoveries obtained in some runs of the ultrafiltration were more likely due to conducting this step on the small scale and the impact of C-PC remaining within the tubing of the tangential flow filtration unit. Thus, this was not considered to be a concern for the larger scale applications of the process.

Finally, the proposed process configuration was tested using different samples of *Spirulina* to understand how robust it was with respect to with variations in the feed. The tests with the different *Spirulina* powders found that the process seemed able to handle the feed variation. This was because the purities obtained by the end of the precipitation stage were higher for the other samples than for the original CC one. For the low concentration crude extract runs, the purity achieved for CC was 1.97 ± 0.06 while the range for the other three samples was between 2.20 ± 0.01 and 2.34 ± 0.09. Similarly, for the samples with higher initial concentrations of C-PC, the CC *Spirulina* generated a final purity of 1.33 ± 0.02, noticeably lower than the purities achieved for the other three powders of 1.67 ± 0.14 to 2.12 ± 0.43. On top of this, the results suggest that adjusting the feed to the process did not significantly impact the recovery of either the adsorption or precipitation stages. When testing both the high and low concentration crude extracts, the recoveries achieved for the different sources of *Spirulina* at each stage differed by less than 10%. This confirmed that the process, in its current form, was not dependent on the particular source of *Spirulina* used.

9 Conclusions and Recommendations

9.1 Conclusions

A C-PC purification process was developed and patented by Harrison et al. (2020), with further work done by Hockey (2022). This process utilised a sequence of ATPS and precipitation stages in an attempt to generate cosmetic-grade C-PC with a purity of greater than 1.5. It was recommended by Hockey (2022) that including an adsorption pretreatment step to the start of the purification train could potentially improve the ability of the process to reliably produce C-PC of the required quality. The ultimate goal of this research project was therefore to investigate this pretreatment option – with chitosan and activated charcoal chosen to be used as the adsorbents.

Prior to commencement of the adsorption testing, preparative tests were done on the *Spirulina* powder leaching which produces the C-PC containing crude extract for purification. It was determined that a longer leaching period would be required for the CC *Spirulina* sample used in this study when compared to the 2 hours reported by Hockey (2022). The leaching of the CC *Spirulina* at an initial biomass concentration of 100 $g.L^{-1}$ required a period of between 17 and 24 hours to ensure that the majority of the C-PC recovered from the biomass, while still attempting to limit the leaching time to avoid microbial contamination. Additionally, it was found that no improvement in the process was achieved through the incorporation of bead milling and that the *Spirulina* powders were sufficiently disrupted to allow the C-PC to move into the buffer. Finally, it was seen that the leaching profiles of different sources of *Spirulina* varied significantly, and that the optimal leaching method and time for one *Spirulina* powder would not necessarily apply to others, which is something to consider when scaling up the process.

The adsorption pretreatment itself was then investigated to understand how it performed when treating a crude extract, and to what extent the different adsorbents were able to improve the purity of the C-PC in solution. When added individually to the crude extract, chitosan and activated charcoal were found to have different effects. Chitosan selectively adsorbed other proteins while leaving the C-PC in solution, while activated charcoal was not as selective and removed C-PC along with the other proteins. When using either adsorbent, it was seen that the recovery of C-PC decreased as more of the chitosan or activated charcoal were added. However, this was predominantly as a result of adding the powdered adsorbents into suspension and removing them, along with the adsorbed impurities, by dead-end centrifugation. As more of the adsorbents were added, the size of the centrifugation pellet increased and therefore more of the purified C-PC solution was trapped in this pellet. Achieving poor recoveries is a concern when trying to operate a commercial process but, in this case, this was more due to the configuration of the adsorption experiments rather than the adsorbents themselves. When adding chitosan and activated charcoal together into a crude extract, it was shown that there was a beneficial effect on the process and the purities obtained were higher than what was achieved previously. When attempting to optimise this adsorption using a central composite design, it was difficult to draw any definitive conclusions, especially around the impact of varying the contact time and pH of the system, due to the high degree of experimental variation and the narrow range of purities achieved. The adsorption was also tested in terms of its ability to remove unwanted microorganisms, where it was shown to reduce the contamination in the crude extract by a factor of 100. However, this was not sufficient to meet the desired target of 1000 $CFU.g^{-1}$ and further contaminant removal would have to be achieved in further processing steps.

After investigating these aspects of the adsorption, it was necessary to couple it with the existing stages of the CeBER process. This meant using the adsorption as a pretreatment before a PEG-citrate ATPS. It was found that combining these two stages resulted in approximately cosmetic-grade C-PC purities being obtained. However, the ATPS required a significant dilution of the C-PC containing solution in order for it to operate effectively, resulting in a low concentration of C-PC in the purified stream. This would make the process more expensive to scale up, as both equipment sizes and quantities of consumables would increase. Problematically, the recovery of C-PC over the ATPS was consistently lower than 40%, due to C-PC being retained amongst remaining cell debris in the interface between the two phases. This cell debris layer appeared despite the C-PC containing solution having undergone two centrifugation steps – to remove the biomass and to remove the adsorbents. Unlike with the poor adsorption recovery, this was not a consequence of the particular configuration chosen and thus this recovery could not be improved. Because of these issues with the PEG-citrate ATPS, another process configuration was required.

The subsequent process configuration was chosen based on the work done by Griffiths (personal communication, 2022) and removed all stages of the ATPS, and instead took the output of the adsorption straight into an ammonium sulfate precipitation. Microfiltration and ultrafiltration steps were also included to prepare a product which would meet all requirements of cosmetic-grade C-PC. The microfiltration was required to remove microbial contaminants and the ultrafiltration was required to desalt the solution following the ammonium sulfate precipitation step. This process was evaluated, and it was shown that C-PC with a purity of significantly greater than 1.5 could be consistently produced if an initial dilution of the crude extract took place. When this reduction of the C-PC concentration in the crude extract was not performed, the purity could not reach the same desired level of 1.5. The buffer for the dilution could be incorporated first as a secondary rinse of the centrifugation pellet after cell debris removal – to recover more of the C-PC. This would therefore benefit the overall C-PC recovery as well as support the attainment of the higher final C-PC purities. Following microfiltration and ultrafiltration, to remove unwanted microorganisms and ammonium sulfate from the final product, and freeze drying, C-PC was produced with an E-value comparable to commercially available samples. It was also confirmed that the process, in its proposed form, was able to operate effectively even when adjusting the feed source of the *Spirulina,* and that its positive performance was not simply limited to a specific powder.

An issue with this proposed process configuration was conducting the adsorption by mixing the activated charcoal into suspension, as it reduced the recovery of C-PC that could be achieved. Therefore, packed activated charcoal columns were tested in place of the adsorbent suspension in an attempt to mitigate this problem. It was shown that the purity of the final product was not negatively impacted by the use of the packed adsorption columns and that cosmetic-grade C-PC could still be produced at the end of the process if the crude extract had its concentration of C-PC reduced. This was found to be true when using slightly different particle sizes of activated charcoal in the columns, as well as when varying the feed flowrates. This meant that the purification steps were now able to recover the majority of the C-PC that entered the process in the crude extract. The increase in the product quantity relative to the feed would be expected to lead to a more economically viable process, assuming that the columns would not be significantly more expensive to run than a suspension.

These results all demonstrated that this research project has been able to fulfil the objectives which were specified at its outset. The adsorption, by using chitosan and activated charcoal, was able to increase the purity of C-PC sufficiently for cosmetic-grade C-PC to be produced when used in combination with the existing precipitation step as well as microfiltration and ultrafiltration. This encompassed all other requirements of cosmetic-grade C-PC – such as the

E-value and level of microbial contamination – and enabled the ATPS to be excluded in order for a more robust process to be developed. Additionally, by using the packed adsorption columns as opposed to powdered activated charcoal, sufficient C-PC recovery could be achieved over the whole process, making it more suitable to be implemented on a larger scale.

9.2 Recommendations

Ultimately, there seems to be a great deal of potential in using the proposed process – where chitosan and activated charcoal adsorption form a crucial part – to purify C-PC to be used in cosmetic products. However, there are certain aspects of this process which potentially require further consideration and investigation in order to improve them and be more certain of its ability to be effective on the commercial scale.

The first set of these recommendations concerns the initial stages of the process – namely the leaching and cell debris removal. The way the process has been conducted thus far has leaching taking place overnight without stirring at room temperature. Aspects of this leaching could be investigated further, such as the potential for stirring to improve the C-PC purity and recovery achieved, as well as reducing the leaching time required. As discussed, using centrifugation to remove the unwanted cell debris results in much of the desired liquid being held within the green biomass pellet. In theory, a rinse and secondary centrifugation of this pellet would enable more C-PC to be recovered and enable the crude extract to be diluted – a necessary step to produce the cosmetic-grade C-PC. However, it would be beneficial to have this step actually tested through experimental work to confirm its effectiveness.

Although the adsorption step has been tested in great detail, there are still a couple of aspects that would benefit from further research. This would predominantly involve the packed adsorption column and a better understanding of the full range of its performance. As mentioned, it was not possible to incorporate the chitosan into the packed columns and it had to be added as a separate purification step. This meant that there was no opportunity for activated charcoal and chitosan to interact with one another in the solution and an additional centrifugation step was required. The chitosan could potentially be included in the columns, either in the form of pellets or other larger particles, or by coating the powder onto e.g. glass beads. The exact form of the chitosan used should be tested, as well as the quantities in which it is added in order for the columns to operate as effectively as possible. Following on from this, another aspect worth investigating is to run the columns for longer periods of time before they are flushed with buffer and the adsorbents are regenerated. In this manner, the effectiveness of both activated charcoal and chitosan over time and multiple uses can be understood and it will be known how often these particles need to be replaced. These experiments should also consider how long a column can be run before a decrease in its performance occurs. Adsorbents purchased from local suppliers should be tested in place of the more expensive, analytical-grade products available from Sigma-Aldrich (and used in this project). These local products are likely what would be purchased for a commercial process based in South Africa and so it would be useful to confirm that there is no significant impact on performance when they are used. In addition to this, it would be beneficial for the important properties of the activated charcoal samples from the different suppliers to be fully characterised so that their performances can be better understood, and any differences can be explained mechanistically. This would include the BET surface area, pore size distribution and any functional groups present. Finally, conducting kinetic studies on the adsorptions and attempting to understand their mechanisms in greater detail will benefit any future work conducted on the adsorption columns. Importantly, it can be better understood where the adsorption equilibrium lies and this will guide the decisions made in any future column designs.

Another recommendation based on the results presented in this research project involves further testing of the microbial contamination. Although this was done using nutrient agar plates for the crude extract, and after adsorption had taken place, it would be beneficial to test the contamination level at more points in the process. This would firstly provide an indication of how effective precipitation is at removing microorganisms and it would confirm that there are no unwanted contaminants in the final product and that the microfiltration step is operating as intended. Additionally, it would be worth repeating the contamination tests on the adsorption stage to understand what impact the column has on removing unwanted microbes, as well as improving the degree of certainty of the results. Lastly, the spread plating aspect of these tests can be done using various types of media, as this will enable different microorganisms to grow and provide a better understanding of what might be present in the process liquid.

Finally, it would be beneficial to perform a cost evaluation on the entire process as it has been proposed. According to what was presented in literature, none of the steps included in the process should be too expensive to prevent the process from operating in an economically efficient manner. However, this needs to be confirmed by determining what the full cost of running the purification would be, and if the overall recovery of C-PC throughout the process is sufficient to generate a profit.

By following these recommendations, a full appreciation of all aspects of the C-PC purification process can be obtained and hopefully enable cosmetic-grade C-PC to be produced more efficiently. This is important, because natural pigments like C-PC are becoming more sought after, and so there is the need to continually find cheaper and easier methods to produce it.

References

Antonino, R.S.C.M.D.Q., Fook, B.R.P.L., Lima, V.A.D.O., Rached, R.Í.D.F., Lima, E.P.N., Lima, R.J.D.S., Covas, C.A.P. & Fook, M.V.L. 2017. Preparation and characterization of chitosan obtained from shells of shrimp (Litopenaeus vannamei Boone). *Marine Drugs*. 15(5):1–12. DOI: 10.3390/md15050141.

Arnold, N.D., Brück, W.M., Garbe, D. & Brück, T.B. 2020. Enzymatic modification of native chitin and conversion to specialty chemical products. *Marine Drugs*. 18(2):1–26. DOI: 10.3390/md18020093.

Barikani, M., Oliaei, E., Seddiqi, H. & Honarkar, H. 2014. Preparation and application of chitin and its derivatives: a review. *Iranian Polymer Journal (English Edition)*. 23(4):307–326. DOI: 10.1007/s13726-014-0225-z.

Beaney, P.D., Gan, Q., Magee, T.R.A., Healy, M. & Lizardi-Mendoza, J. 2007. Modification of chitin properties for enzymatic deacetylation. *Journal of Chemical Technology & Biotechnology*. 82:165–173. DOI: 10.1002/jctb.

Beer, S. & Eshel, A. 1985. Determining phycoerythrin and phycocyanin concentrations in aqueous crude extracts of red algae. *Marine and Freshwater Research*. 36(6):785–792. DOI: 10.1071/MF9850785.

Begum, H., Yusoff, F.M.D., Banerjee, S., Khatoon, H. & Shariff, M. 2016. Availability and utilization of pigments from microalgae. *Critical Reviews in Food Science and Nutrition*. 56(13):2209–2222. DOI: 10.1080/10408398.2013.764841.

Belhachemi, M. 2021. Adsorption of organic compounds on activated carbons. In *Sorbents Materials for Controlling Environmental Pollution*. A. Núñez-Delgado, Ed. Elsevier. 355–385.

Bennett, A. & Bogorad, L. 1973. Complementary chromatic adaption in a filamentous blue-green alga. *Journal of Cell Biology*. 58(2):419–435. DOI: 10.1083/jcb.58.2.419.

Bryant, D.A., Glazer, A.N. & Eiserling, F.A. 1976. Characterization and structural properties of the major biliproteins of Anabaena sp. *Archives of Microbiology*. 110(1):61–75. DOI: 10.1007/BF00416970.

Bryant, D.A., Guglielmi, G., de Marsac, N.T., Castets, A.M. & Cohen-Bazire, G. 1979. The structure of cyanobacterial phycobilisomes: a model. *Archives of Microbiology*. 123(2):113–127. DOI: 10.1007/BF00446810.

Chaiklahan, R., Chirasuwan, N., Loha, V., Tia, S. & Bunnag, B. 2011. Separation and purification of phycocyanin from Spirulina sp. using a membrane process. *Bioresource Technology*. 102(14):7159–7164. DOI: 10.1016/j.biortech.2011.04.067.

Chaiklahan, R., Chirasuwan, N. & Bunnag, B. 2012. Stability of phycocyanin extracted from Spirulina sp.: influence of temperature, pH and preservatives. *Process Biochemistry*. 47(4):659–664. DOI: 10.1016/j.procbio.2012.01.010.

Chethana, S., Nayak, C.A., Madhusudhan, M.C. & Raghavarao, K.S.M.S. 2015. Single step aqueous two-phase extraction for downstream processing of C-phycocyanin from Spirulina platensis. *Journal of Food Science and Technology*. 52(4):2415–2421. DOI: 10.1007/s13197-014-1287-9.

Chiou, C.T. 2002. Fundamentals of the Adsorption Theory. In *Partition and Adsorption of Organic Contaminants in Environmental Systems*. 39–52. DOI: 10.1002/0471264326.ch4.

Cohen-Bazire, G., Béguin, S., Rimon, S., Glazer, A.N. & Brown, D.M. 1977. Physico-chemical

and immunological properties of allophycocyanins. *Archives of Microbiology*. 111(3):225–238. DOI: 10.1007/BF00549359.

Demirbas, A. 2009. Agricultural based activated carbons for the removal of dyes from aqueous solutions: a review. *Journal of Hazardous Materials*. 167(1–3):1–9. DOI: 10.1016/j.jhazmat.2008.12.114.

Deniz, F. 2013. Adsorption properties of low-cost biomaterial derived from Prunus amygdalus L. for dye removal from water. *The Scientific World Journal*. 2013(July 2013). DOI: 10.1155/2013/961671.

Doran, P.M. 2013. Unit Operations. In *Bioprocess Engineering Principles*. Second ed. Academic Press. 445–595.

Dutta, P.K., Ravikumar, M.N.V. & Dutta, J. 2002. Chitin and chitosan for versatile applications. *Journal of Macromolecular Science - Polymer Reviews*. 42(3):307–354. DOI: 10.1081/MC-120006451.

Eriksen, N.T. 2008. Production of phycocyanin - a pigment with applications in biology, biotechnology, foods and medicine. *Applied Microbiology and Biotechnology*. 80(1):1–14. DOI: 10.1007/s00253-008-1542-y.

Fekrat, F., Nami, B., Ghanavati, H., Ghaffari, A. & Shahbazi, M. 2019. Optimization of chitosan/activated charcoal-based purification of Arthrospira platensis phycocyanin using response surface methodology. *Journal of Applied Phycology*. 31(2):1095–1105. DOI: 10.1007/s10811-018-1626-8.

Focher, B., Beltrame, P.L., Naggi, A. & Torri, G. 1990. Alkaline N-deacetylation of chitin enhanced by flash treatments. Reaction kinetics and structure modifications. *Carbohydrate Polymers*. 12(4):405–418. DOI: 10.1016/0144-8617(90)90090-F.

Glazer, A.N. & Hixson, C.S. 1975. Characterization of R-phycocyanin. Chromophore content of R-phycocyanin and C-phycoerythrin. *Journal of Biological Chemistry*. 250(14):5387–5495. DOI: 10.1016/s0021-9258(19)41208-8.

Griffiths, M., Harrison, S.T.L., Smit, M. & Maharajh, D. 2016. Major commercial products from micro- and macroalgae. In *Algae Biotechnology*. F. Bux & Y. Chisti, Eds. Springer, Cham. 269–300.

Guedes, A.C., Amaro, H.M. & Malcata, F.X. 2011. Microalgae as sources of carotenoids. *Marine Drugs*. 9(4):625–644. DOI: 10.3390/md9040625.

Guibal, E. 2004. Interactions of metal ions with chitosan-based sorbents: A review. *Separation and Purification Technology*. 38(1):43–74. DOI: 10.1016/j.seppur.2003.10.004.

Gyliene, O., Rekertas, R. & Šalkauskas, M. 2002. Removal of free and complexed heavy-metal ions by sorbents produced from fly (Musca domestica) larva shells. *Water Research*. 36(16):4128–4136. DOI: 10.1016/S0043-1354(02)00105-7.

Harrison, S.T.L., Burke, M.A., Pott, R.W.M. & Fagan-Endres, M.A. 2020. *Patent No. US 2020/0255473 A1*. United States.

Henning, K.D. & Schäfer, S. 1993. Impregnated activated carbon for environmental protection. *Gas Separation and Purification*. 7(4):235–240. DOI: 10.1016/0950-4214(93)80023-P.

Hockey, J.T. 2022. Improving a process using aqueous two-phase systems for C-phycocyanin extraction from Spirulina. University of Cape Town.

Honarkar, H. & Barikani, M. 2009. Applications of biopolymers I: chitosan. *Monatshefte fur Chemie*. 140(12):1403–1420. DOI: 10.1007/s00706-009-0197-4.

İlter, I., Akyıl, S., Demirel, Z., Koç, M., Conk-Dalay, M. & Kaymak-Ertekin, F. 2018. Optimization of phycocyanin extraction from Spirulina platensis using different techniques. *Journal of Food Composition and Analysis*. 70(April):78–88. DOI: 10.1016/j.jfca.2018.04.007.

Islam, S., Bhuiyan, M.A.R. & Islam, M.N. 2017. Chitin and chitosan: structure, properties and applications in biomedical engineering. *Journal of Polymers and the Environment*. 25(3):854–866. DOI: 10.1007/s10924-016-0865-5.

Jafari, M., Rahimi, M.R., Ghaedi, M. & Dashtian, K. 2017. ZnO nanoparticles loaded different mesh size of porous activated carbon prepared from Pinus eldarica and its effects on simultaneous removal of dyes: multivariate optimization. *Chemical Engineering Research and Design*. 125:408–421. DOI: 10.1016/j.cherd.2017.07.011.

Jayakumar, R., Menon, D., Manzoor, K., Nair, S. V. & Tamura, H. 2010. Biomedical applications of chitin and chitosan based nanomaterials - a short review. *Carbohydrate Polymers*. 82(2):227–232. DOI: 10.1016/j.carbpol.2010.04.074.

Jayakumar, R., Prabaharan, M., Nair, S. V. & Tamura, H. 2010. Novel chitin and chitosan nanofibers in biomedical applications. *Biotechnology Advances*. 28(1):142–150. DOI: 10.1016/j.biotechadv.2009.11.001.

Kamble, S.P., Gaikar, R.B., Padalia, R.B. & Shinde, K.D. 2013. Extraction and purification of C-phycocyanin from dry Spirulina powder and evaluating its antioxidant, anticoagulation and prevention of DNA damage activity. *Journal of Applied Pharmaceutical Science*. 3(8):149–153. DOI: 10.7324/JAPS.2013.3826.

Kaur, G., Khattar, J.I.S., Singh, D.P., Singh, Y. & Nadda, J. 2009. Microalgae: a source of natural colours. *Algal Biology and Biotechnology*. (July 2016):129–149.

Kuddus, M., Singh, P., Thomas, G. & Al-Hazimi, A. 2013. Recent developments in production and biotechnological applications of C-phycocyanin. *BioMed Research International*. 2013. DOI: 10.1155/2013/742859.

Kumar, D., Dhar, D.W., Pabbi, S., Kumar, N. & Walia, S. 2014. Extraction and purification of C-phycocyanin from Spirulina platensis (CCC540). *Indian Journal of Plant Physiology*. 19(2):184–188. DOI: 10.1007/s40502-014-0094-7.

Kursar, T.A., van der Meer, J. & Alberte, R.S. 1983. Light-harvesting system of the red alga Gracilaria tikvahiae. *Plant Physiology*. 73(2):361–369. DOI: 10.1104/pp.73.2.361.

Lauceri, R., Bresciani, M., Lami, A. & Morabito, G. 2018. Chlorophyll a interference in phycocyanin and allophycocyanin spectrophotometric quantification. *Journal of Limnology*. 77(1):169–177. DOI: 10.4081/jlimnol.2017.1691.

Lee, S.H., Lee, J.E., Kim, Y. & Lee, S.Y. 2016. The production of high purity phycocyanin by Spirulina platensis using light-emitting diodes based two-stage cultivation. *Applied Biochemistry and Biotechnology*. 178(2):382–395. DOI: 10.1007/s12010-015-1879-5.

Liao, X., Zhang, B., Wang, X., Yan, H. & Zhang, X. 2011. Purification of C-phycocyanin from spirulina platensis by single-step ion-exchange chromatography. *Chromatographia*. 73(3–4):291–296. DOI: 10.1007/s10337-010-1874-5.

Mansour, F., Al-Hindi, M., Yahfoufi, R., Ayoub, G.M. & Ahmad, M.N. 2018. The use of activated carbon for the removal of pharmaceuticals from aqueous solutions: a review. *Reviews in Environmental Science and Biotechnology*. 17(1):109–145. DOI: 10.1007/s11157-017-9456-8.

Martinou, A., Kafetzopoulos, D. & Bouriotis, V. 1995. Chitin deacetylation by enzymatic means: monitoring of deacetylation processes. *Carbohydrate Research*. 273(2):235–242. DOI: 10.1016/0008-6215(95)00111-6.

Menéndez-Díaz, J.A. & Martín-Gullón, I. 2006. Types of carbon adsorbents and their production. In *Activated carbon surfaces in environmental remediation*. V. 7. 1–47. DOI: 10.1016/S1573-4285(06)80010-4.

Min, B.M., Lee, S.W., Lim, J.N., You, Y., Lee, T.S., Kang, P.H. & Park, W.H. 2004. Chitin and chitosan nanofibers: electrospinning of chitin and deacetylation of chitin nanofibers. *Polymer*. 45(21):7137–7142. DOI: 10.1016/j.polymer.2004.08.048.

Miretzky, P. & Cirelli, A.F. 2009. Hg(II) removal from water by chitosan and chitosan derivatives: a review. *Journal of Hazardous Materials*. 167(1–3):10–23. DOI: 10.1016/j.jhazmat.2009.01.060.

Mohamed, R.R. 2021. *Chitin and chitosan as adsorbents*. INC. DOI: 10.1016/b978-0-12-820541-9.00004-1.

Montgomery, D.C. 2017. *Design and analysis of experiments*. 9th ed. Available: www.wiley.com/go/permissions.%0Ahttps://lccn.loc.gov/2017002355.

Moraes, C.C., Sala, L., Cerveira, G.P. & Kalil, S.J. 2011. C-Phycocyanin extraction from Spirulina platensis wet biomass. *Brazilian Journal of Chemical Engineering*. 28(1):45–49. DOI: 10.1590/S0104-66322011000100006.

Moura, J.M., Gründmann, D.D.R., Cadaval, T.R.S., Dotto, G.L. & Pinto, L.A.A. 2016. Comparison of chitosan with different physical forms to remove Reactive Black 5 from aqueous solutions. *Journal of Environmental Chemical Engineering*. 4(2):2259–2267. DOI: 10.1016/j.jece.2016.04.003.

Ng, I.S., Tang, M.S.Y., Show, P.L., Chiou, Z.M., Tsai, J.C. & Chang, Y.K. 2019. Enhancement of C-phycocyanin purity using negative chromatography with chitosan-modified nanofiber membrane. *International Journal of Biological Macromolecules*. 132:615–628. DOI: 10.1016/j.ijbiomac.2019.03.235.

Nisticò, D.M., Piro, A., Oliva, D., Osso, V., Mazzuca, S., Fagà, F.A., Morelli, R., Conidi, C., et al. 2022. A combination of aqueous extraction and ultrafiltration for the purification of phycocyanin from Arthrospira maxima. *Microorganisms*. 10(2). DOI: 10.3390/microorganisms10020308.

O Carra, P. 1965. Purification and N-terminal analyses of algal biliproteins. *The Biochemical journal*. 94:171–174. DOI: 10.1042/bj0940171.

O Carra, P., O hEocha, C. & Carrol, D.M. 1964. Spectral properties of the phycobilins. I. phycoerythrobilin. *Biochemistry*. 3(9):1343–1350. DOI: 10.1021/bi00897a026.

Papadaki, S., Kyriakopoulou, K., Tzovenis, I. & Krokida, M. 2017. Environmental impact of phycocyanin recovery from Spirulina platensis cyanobacterium. *Innovative Food Science and Emerging Technologies*. 44:217–223. DOI: 10.1016/j.ifset.2017.02.014.

Park, J., Lee, H., Dinh, T.B., Choi, S., De Saeger, J., Depuydt, S., Brown, M.T. & Han, T. 2022. Commercial potential of the cyanobacterium Arthrospira maxima: physiological and biochemical traits and the purification of phycocyanin. *Biology*. 11(5):1–18. DOI: 10.3390/biology11050628.

Patel, S. & Goyal, A. 2013. Current and prospective insights on food and pharmaceutical applications of spirulina. *Current Trends in Biotechnology and Pharmacy*. 7(2):681–695.

Patil, G. & Raghavarao, K.S.M.S. 2007. Aqueous two phase extraction for purification of C-phycocyanin. *Biochemical Engineering Journal*. 34(2):156–164. DOI: 10.1016/j.bej.2006.11.026.

Patil, G., Chethana, S., Sridevi, A.S. & Raghavarao, K.S.M.S. 2006. Method to obtain C-

phycocyanin of high purity. *Journal of Chromatography A*. 1127(1–2):76–81. DOI: 10.1016/j.chroma.2006.05.073.

Potwora, R.J. 2016. *Activated carbon particle size: balance between kinetics and capacity*. Available: https://agualatinoamerica.com/2016/06/15/activated-carbon-particle-size-balance-kinetics-capacity/ [2023, January 25].

Quesada, H.B., de Araújo, T.P., Vareschini, D.T., de Barros, M.A.S.D., Gomes, R.G. & Bergamasco, R. 2020. Chitosan, alginate and other macromolecules as activated carbon immobilizing agents: a review on composite adsorbents for the removal of water contaminants. *International Journal of Biological Macromolecules*. 164:2535–2549. DOI: 10.1016/j.ijbiomac.2020.08.118.

Ragusa, I., Nardone, G.N., Zanatta, S., Bertin, W. & Amadio, E. 2021. Spirulina for skin care: A bright blue future. *Cosmetics*. 8(1):1–19. DOI: 10.3390/cosmetics8010007.

Rito-Palomares, M., Nuez, L. & Amador, D. 2001. Practical application of aqueous two-phase systems for the development of a prototype process for C-phycocyanin recovery from Spirulina maxima. *Journal of Chemical Technology and Biotechnology*. 76(12):1273–1280. DOI: 10.1002/jctb.507.

Safaei, M., Maleki, H., Soleimanpour, H., Norouzy, A., Zahiri, H.S., Vali, H. & Noghabi, K.A. 2019. Development of a novel method for the purification of C-phycocyanin pigment from a local cyanobacterial strain Limnothrix sp. NS01 and evaluation of its anticancer properties. *Scientific Reports*. 9(1):1–16. DOI: 10.1038/s41598-019-45905-6.

Saini, V.K. & Shankar, A. 2019. *How to Improve Selectivity of a Material for Adsorptive Separation Applications*. DOI: 10.1007/978-3-319-73645-7_43.

Schobert, H.H. 2013. Carbon products from fossil and biofuels. In *Chemistry of Fossil Fuels and Biofuels*. Cambridge University Press. 435–452.

Schwartz, L. 2003. Diafiltration: a fast, efficient method for desalting or buffer exchange of biological samples. *Pall Scientific & Technical Report*. 6. Available: http://www4.pall.com/pdf/02.0629_Buffer_Exchange_STR.pdf.

Sensient. 2021. *Spirulina P-WS*.

Silva, S.C., Ferreira, I.C.F.R., Dias, M.M. & Barreiro, M.F. 2020. Microalgae-derived pigments: a 10-year bibliometric review and industry and market trend analysis. *Molecules*. 25(3406):1–23. DOI: 10.3390/molecules25153406.

Sivashankari, P.R. & Prabaharan, M. 2017. Chemical and physical modification of chitosan-based biomaterials. *Chitosan Based Biomaterials, volume 1*. 116–133.

Soni, R.A., Sudhakar, K. & Rana, R.S. 2017. Spirulina – from growth to nutritional product: a review. *Trends in Food Science and Technology*. 69:157–171. DOI: 10.1016/j.tifs.2017.09.010.

Sørensen, L., Hantke, A. & Eriksen, N.T. 2013. Purification of the photosynthetic pigment C-phycocyanin from heterotrophic Galdieria sulphuraria. *Journal of the Science of Food and Agriculture*. 93(12):2933–2938. DOI: 10.1002/jsfa.6116.

Tadda, M.A., Ahsan, A., Shifu, A., ElSergany, M., Arunkumar, T., Jose, B., Abdur Razzaque, M. & Nik Daud, N.N. 2018. A review on activated carbon from biowaste: process, application and prospects. *Journal of Advanced Civil Engineering Practice and Research*. 5(3):82–83.

Tandeau de Marsac, N. & Houmard, J. 1988. Complementary chromatic adaptation: physiological conditions and action spectra. *Methods in Enzymology*. 167(1983):318–328.

Telegina, T.A., Biryukov, M. V., Terekhova, I. V., Vechtomova, Y.L. & Kritsky, M.S. 2018.

Isolation and characterization of water-soluble chromoproteins from Arthrospira platensis cyanobacteria: C-phycocyanin, allophycocyanin, and carotenoid- and chlorophyll-binding proteins. *Applied Biochemistry and Microbiology*. 54(6):631–638. DOI: 10.1134/S0003683818060145.

Tsai, M.L. & Chen, R.H. 2017. Modifying the molecular weight of chitosan. *Chitosan Based Biomaterials*. 1:135–158. DOI: 10.1016/B978-0-08-100230-8.00006-6.

Vunain, E., Mishra, A.K. & Mamba, B.B. 2017. Fundamentals of chitosan for biomedical applications. In *Chitosan Based Biomaterials Volume 1*. Woodhead Publishing Series. 3–30.

Wan, M., Zhao, H., Guo, J., Yan, L., Zhang, D., Bai, W. & Li, Y. 2021. Comparison of C-phycocyanin from extremophilic Galdieria sulphuraria and Spirulina platensis on stability and antioxidant capacity. *Algal Research*. 58(February):102391. DOI: 10.1016/j.algal.2021.102391.

Wang, W., Zhang, X., Xu, C. & Cheng, H. 2012. Purification and concentration of C-phycocyanin from Spirulina platensis using aqueous two-phase system. *Applied Mechanics and Materials*. 138–139:995–1001. DOI: 10.4028/www.scientific.net/AMM.138-139.995.

Wang, X.Q., Li, L.N., Chang, W.R., Zhang, J.P., Gui, L.L., Guo, B.J. & Liang, D.C. 2001. Structure of C-phycocyanin from Spirulina platensis at 2.2 Å resolution: a novel monoclinic crystal form for phycobiliproteins in phycobilisomes. *Acta Crystallographica Section D: Biological Crystallography*. 57(6):784–792. DOI: 10.1107/S0907444901004528.

Web of Science. 2023. *Citation Report*.

Wingfield, P. (in press). Protein precipitation using ammonium sulfate. *Current Protocols in Protein Science*. A.3F.1-A.3F.8. DOI: 10.1002/0471140864.psa03fs13.

Yacobi, Y.Z., Köhler, J., Leunert, F. & Gitelson, A. 2015. Phycocyanin-specific absorption coefficient: eliminating the effect of chlorophylls absorption. *Limnology and Oceanography: Methods*. 13(4):157–168. DOI: 10.1002/lom3.10015.

Yahyaei, M., Mehrnejad, F., Naderi-manesh, H. & Rezayan, A.H. 2018. Protein adsorption onto polysaccharides: comparison of chitosan and chitin polymers. *Carbohydrate Polymers*. 191(December 2017):191–197. DOI: 10.1016/j.carbpol.2018.03.034.

Yan, S.G., Zhu, L.P., Su, H.N., Zhang, X.Y., Chen, X.L., Zhou, B.C. & Zhang, Y.Z. 2011. Single-step chromatography for simultaneous purification of C-phycocyanin and allophycocyanin with high purity and recovery from Spirulina (Arthrospira) platensis. *Journal of Applied Phycology*. 23(1):1–6. DOI: 10.1007/s10811-010-9525-7.

Yin, C.Y., Aroua, M.K. & Daud, W.M.A.W. 2007. Review of modifications of activated carbon for enhancing contaminant uptakes from aqueous solutions. *Separation and Purification Technology*. 52(3):403–415. DOI: 10.1016/j.seppur.2006.06.009.

Yoshikawa, N. & Belay, A. 2008. Single-laboratory validation of a method for the determination of C-phycocyanin and allophycocyanin in Spirulina (Arthrospira) supplements and raw materials by spectrophotometry. *Journal of AOAC International*. 91(3):524–529. DOI: 10.1093/jaoac/91.3.524.

Zabi, N.Z., Ibrahim, W.N.W., Hanapi, N.S.M. & Hadzir, N.M. 2021. Removal of various contaminants by highly porous activated carbon sorbent derived from agricultural waste produced in Malaysia - a review. *Nature Environment and Pollution Technology*. 20(3):1173–1183. DOI: 10.46488/NEPT.2021.V20I03.025.

Zhang, G.H., Xi, J.B., Chen, W. & Bai, Z.W. 2020. Comparison in enantioseparation performance of chiral stationary phases prepared from chitosans of different sources and molecular weights. *Journal of Chromatography A*. 1621. DOI: 10.1016/j.chroma.2020.461029.

Zhang, M., Haga, A., Sekiguchi, H. & Hirano, S. 2000. Structure of insect chitin isolated from beetle larva cuticle and silkworm (Bombyx mori) pupa exuvia. *International Journal of Biological Macromolecules*. 27(1):99–105. DOI: 10.1016/S0141-8130(99)00123-3.

Appendix A: Additional Data

A1: Absorbance Standard Curves for 280 nm, 620 nm and 650 nm

In order to accurately measure the optical density, or absorbance, of a solution, it often needed to be diluted to within a linear range. The calibration curves used to determine the linear ranges for the necessary wavelengths can be seen in Figures 49 to 51.

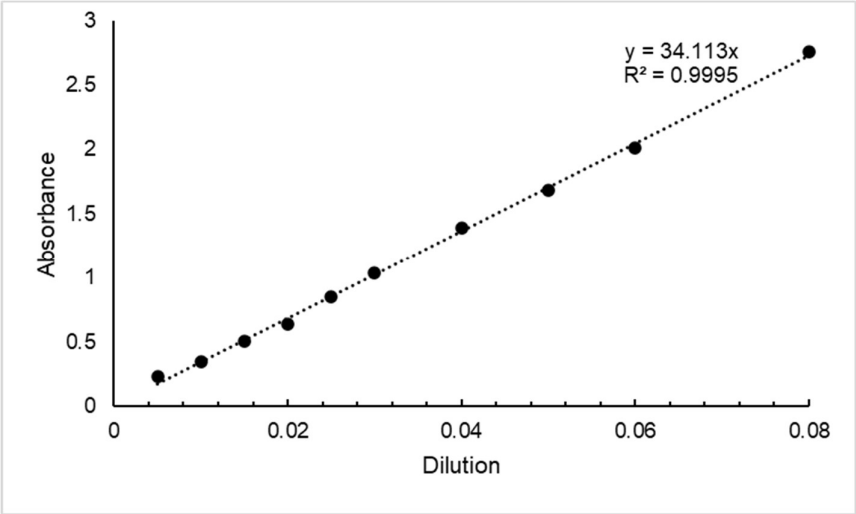

Figure 49: Absorbance standard curve for wavelength of 280 nm.

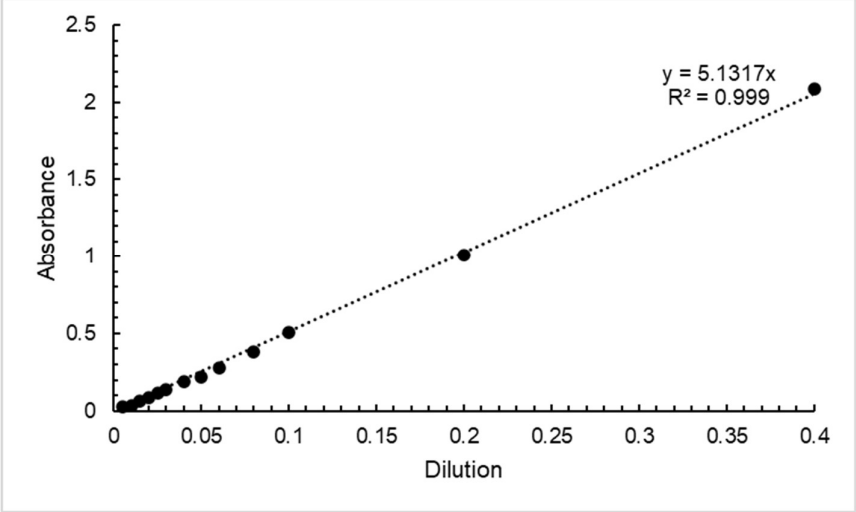

Figure 50: Absorbance standard curve for wavelength of 620 nm.

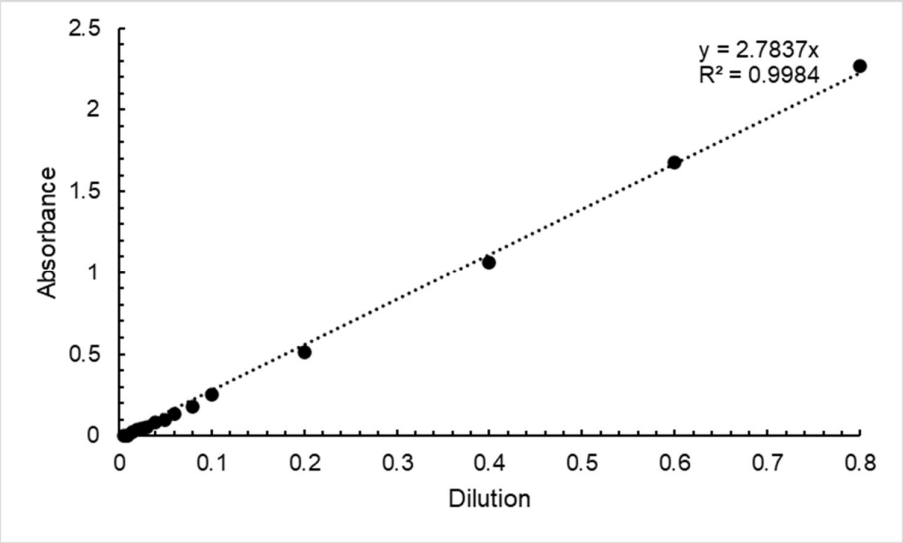

Figure 51: Absorbance standard curve for wavelength of 650 nm.

A2: pH Calibration Curve

When adjusting the leaching and adsorption pH as part of the central composite design, the overall concentration of citrate was maintained at 5 $g.L^{-1}$. However, the relative amounts within this 5 $g.L^{-1}$ of sodium citrate dihydrate and citric acid monohydrate were varied to change the pH to the desired value. The calibration curve used for this can be seen in Figure 52.

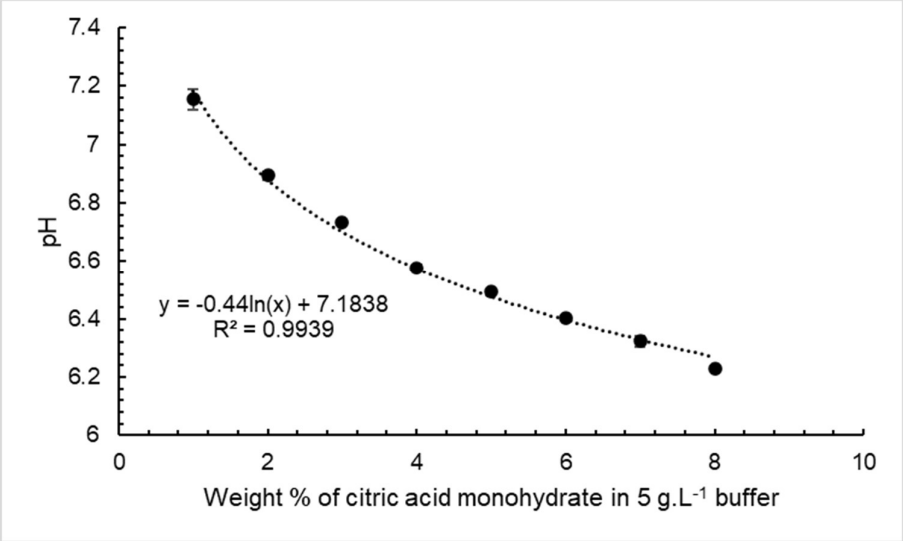

Figure 52: Impact on solution pH of varying the relative amount of citric acid monohydrate in a 5 $g.L^{-1}$ citrate buffer.

A3: Summary of Process Runs for Freeze Dried Samples

The results of sending several samples through a freeze drying step were presented in Chapter 8.5. Table 18 provides a summary of the purification process followed for each sample which was freeze dried and measured.

Table 18: Summary of full process used to prepare samples which underwent freeze drying. All adsorption steps took place using chitosan at 0.2% weight per total initial volume and activated charcoal at 8% weight per total initial volume for high concentration C-PC samples and at 4% weight per total initial volume for low concentration C-PC samples. Precipitation concentrations are based on total initial volume of liquid.

Run No.	Description of purification process used
Run A	leaching → adsorption → precipitation at 0.11 $g.mL^{-1}$ → precipitation at 0.27 $g.mL^{-1}$ → precipitation at 0.32 $g.mL^{-1}$ → microfiltration → ultrafiltration
Run B	leaching → adsorption → precipitation at 0.32 $g.mL^{-1}$ → microfiltration → ultrafiltration
Run C	leaching → adsorption → precipitation at 0.36 $g.mL^{-1}$ → microfiltration → ultrafiltration
Run D	leaching → precipitation at 0.36 $g.mL^{-1}$ → adsorption → microfiltration → ultrafiltration
Run E	leaching → adsorption → precipitation at 0.36 $g.mL^{-1}$ → adsorption → microfiltration → ultrafiltration

A4: Summary of Process Unit Operations

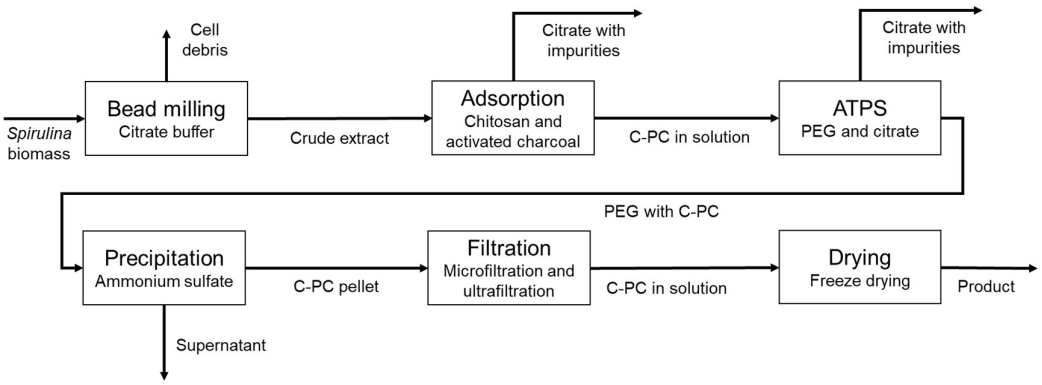

Figure 53: Block flow diagram of general purification process to generate C-PC from *Spirulina*.

Appendix B: Link to Data Files

10.25375/uct.22068836